Title
Molecular determinants of flavivirus non-structural protein 1

Author
Lo, Nicholas Tzuning

Publication Date
2022

Peer reviewed|Thesis/dissertation

Molecular determinants of flavivirus non-structural protein 1

by

Nicholas Lo Tzu Ning

A dissertation submitted in partial fulfillment of

the requirements for the degree of

Doctor of Philosophy

in

Infectious Diseases and Immunity

in the

Graduate Division

of the

University of California, Berkeley

Committee in charge:

Professor Eva Harris, Chair
Professor Laurent Coscoy
Professor Britt Glaunsinger
Professor James Hurley

Summer 2022

Abstract

Molecular determinants of flavivirus non-structural protein 1

by

Nicholas Lo Tzu Ning

Doctor of Philosophy in Infectious Diseases and Immunity

University of California, Berkeley

Professor Eva Harris, Chair

Flaviviruses are arthropod-borne, positive-sense RNA viruses of significant medical and public health importance. While safe and effective vaccines have been developed against some members of the *Flavivirus* genus, limited progress has been made against others, such as dengue (DENV), West Nile (WNV), and Zika (ZIKV) viruses – which cause distinct human diseases and affect different tissues. Importantly, there are currently no flavivirus-specific therapeutics. Flaviviruses encode a secreted non-structural protein 1 (NS1) that directly interacts with endothelial cells, resulting in barrier dysfunction. The clinical manifestations of these interactions are thought to include DENV NS1-induced vascular leak in the lungs, WNV NS1 enhancing viral infection of the brain, and ZIKV NS1 causing hyperpermeability in placental tissues. We previously found that flavivirus NS1 binds to endothelial cells and disrupts barrier functions in a tissue-specific manner consistent with the disease tropism of the respective viruses. Understanding the underlying molecular mechanism of tissue-specific NS1-endothelial cell interactions will help guide better interventions to prevent and control flaviviral diseases. To elucidate the distinct role(s) that the domains of NS1 (β-roll, wing, and β-ladder) play in NS1 interactions with endothelial cells, we constructed flavivirus NS1 chimeras that exchanged the wing and β-ladder domains in a pair-wise manner between DENV, WNV, and ZIKV NS1. We found that both the NS1 wing and β-ladder domains conferred NS1 tissue-specific endothelial dysfunction, with the wing conferring cell binding and the β-ladder involved in inducing endothelial hyperpermeability as measured by trans-endothelial electrical resistance assay. Then, we utilized the DENV-WNV NS1 chimera and identified residues 91 to 93 (GDI) of DENV NS1 as a molecular motif determining binding specificity. Using a mouse model of localized leak, we corroborated that the NS1 wing domain and GDI molecular determinant motif triggered NS1-induced vascular leak *in vivo*. Further, we report other molecular determinants of interest, including a highly conserved motif in the NS1 wing domain that mediates pan-flavivirus NS1 binding to pulmonary endothelial cells and identified the wing domain to mediate interactions with endothelial cell surface glycans. Finally, we explored the protective effects of the iminosugar UV-4B against DENV NS1-induced endothelial dysfunctions by inhibiting proper host-dependent glycosylation processing of NS1. Taken together, these findings contribute to improved understanding of flavivirus NS1 and the molecular details conferring its tissue-specific functional patterns, that could help guide future vaccine design and therapeutic developments.

Table of Contents

Acknowledgements

They say it takes a village to raise a child – this is especially true in the training of a scientist. This year marks my 10th year in the United States, and I wouldn't have gotten here today without the tremendous support of so many people at various stages of my career. The COVID19 pandemic made a significant mark in the third year of my PhD, as it did in everyone's life. It reminded me of a defining motivation to pursue infectious disease research, the SARS pandemic in 2003, when I was in primary two in Taipei. Seventeen years later, I had the privilege to be in the Harris lab during the pandemic to contribute to our East Bay serosurveillance study, which was a timely reminder of why we do what we do.

I would first like to thank my advisor, Dr. Eva Harris, for giving me the opportunity to grow as a scientist in such a dynamic lab and for the guidance and push through my projects. I want to acknowledge and sincerely thank every member of the Harris Lab, who are some of the most amazing scientists I've worked with for the past five years. Thank you to Chunling Wang, Dustin Glasner, Sandra Bos, Felix Pahmeier, Elias Duarte, Aaron Graber, Reinaldo Mercado, Henry Puerta-Guardo, Diego Espinosa, and Gregorio Dias. I'm especially grateful to Scott Biering, who I worked with closely throughout my PhD; thank you for all the technical help, friendly banters, discussions about science and non-science, and challenging me to grow scientifically and professionally. I would also like to thank all the past and present undergrads for always keeping the lab joyful and full of energy, and especially to Susan Roodsari – whose help during my last year of PhD was pivotal to pushing the projects through the finish line.

Thank you to the past and present members of the Infectious Diseases and Immunity graduate program for all the fun, navigating academia, and figuring out research. Thank you especially to Derek Bangs, Perri Callaway, Gina Borgo, Joseph Tran, Abigail Kane, and Claire Mastrangelo.

To my pusheen friends who keep me grounded from the ivory tower: Sean Carim, Kartikye Mittal, Vanessa Ng, Luke Wang, Chew Keng Chee, Katherine Sham, Ng Jun Jie, Emmanuel Lee, and more – thank you for keeping my life in perspective and taking me into the worlds of tech and start-up ever so often, and for the many trips, food adventures, and rabak nights.

Thank you to my pandemic bubble Marcus Wong, Joel Reyes, and Nick Dolan for the endless pies, boardgames, Westworld, outdoor climbing, and hiking during the height of the pandemic that kept me sane. Thank you also to my Bay Area friends who kept me socially engaged, physically and mentally active with skiing, camping, bike rides, and adventures that rekindled my love for the outdoors this past five years.

To my friends afar in Singapore, Seattle, New York, and beyond: thanks for picking up my 1am calls and entertaining my getaways, skiing, camping, and other adventures: Zack Chua, Genevieve Tan, Koh Liang Wei, Chin Zhong Wei, Jerald Han, Natalie Sombuntham, Josh Wang, Matthew Mikrut, Peter Soewardiman, Kate Tan, Liau Wen Rui, Jamie Lo, Christine Song, Justin Goh, Clarissa Tan, Nicole Aw, and many more – thank you for cheering me on from afar.

Additionally to Marcus Wong: thank you for entertaining my countless rants, experiment ideas, wild propositions and more, both in lab and at home, and for this past four years. Be it on the rock

wall, at the tissue culture hood, or with my incessant questions about becoming Asian-*American*, thank you for patiently putting up with me.

To mum, dad, and Tzu Heng: thank you for the opportunity to America and continual support in me. It is a privilege and an honour to be the first doctor in the family.

Chapter 1

Introduction

Flaviviruses

Flaviviruses are vector-borne, positive-stranded RNA viruses that cause human diseases of public health significance, collectively causing approximately 400 million annual infections globally with half of the global population at risk [1,2]. Most flaviviruses are transmitted to humans via mosquitoes. Consequently, most of the diseases occur in low- and middle-income countries within the tropical and sub-tropical regions, where the human and economic costs are significant. While safe and effective human vaccines have been developed against some of these viruses such as yellow fever (YFV) and Japanese encephalitis (JEV) viruses, less progress has been made against others such as dengue (DENV) and West Nile (WNV) viruses [3] . With climate change, increased global movement of people and goods, and changing land usage as countries develop [4–6], flaviviruses remain a major public health concern that warrant greater research and understanding for effective mitigation strategies.

Flaviviral diseases are clinically diverse. Zika (ZIKV), WNV, JEV, and tick-borne encephalitis (TBEV) viruses cause neurological pathologies such as encephalitis and meningitis, which can lead to cognitive impairment, seizures, and paralysis [7]. ZIKV also causes Guillain-Barré syndrome in adults and congenital Zika syndrome in infants, the best known of which is microcephaly [8]. In contrast, YFV causes the prototypical haemorrhagic fever with symptoms such as fever, nausea, and haemorrhage that share pathophysiological features with other unrelated haemorrhagic fevers, but with increased severity in hepatic dysfunctions [9]. DENV, the most widespread flavivirus, causes the eponymous systemic disease, dengue fever, where patients present with myalgia, arthralgia, retroorbital and abdominal pain, rash, and in severe cases haemorrhagic fever and shock with pronounced pathologies in the lungs [10].

Flavivirus virology

As an enveloped, positive-stranded RNA virus, flaviviruses have a ~10.7kb genome which encodes 3 structural proteins (capsid, C; (pre-)membrane, pr/M; envelope, E) and 7 non-structural (NS) proteins (NS1, NS2a, NS2b, NS3, NS4A, NS4B, NS5) [11,12]. The spherical virion surface consists of E and pr/M proteins arranged in icosahedral-like symmetry. While the structural proteins provide the scaffold of the virus, the non-structural proteins play critical roles in supporting the viral life cycle. Briefly, NS1 is involved broadly in viral replication and viral pathogenesis; NS2A orchestrates virion assembly and maturation [13,14]; NS2B and NS3 form a viral protease complex responsible for the proteolytic processing of the translated flavivirus polyprotein [15–17]; NS3 additionally has helicase activity [18,19]; NS4A/4B are involved in membrane remodeling [20] and interact with NS1 to form the replication complex at the ER [21–24]; and NS5 acts as the RNA-dependent RNA polymerase and is essential for capping of the nascent RNA genome [25,26]. Additionally, NS1 [27–30], NS2B/3 [31–33], NS4B [34], and NS5 [35,36] all contribute to flavivirus immune evasion by subverting various innate immune responses such as RIG-I, MDA-5, complement, JAK-STAT, and cGAS-STING pathways. Two fascinating discoveries regarding DENV immune evasion are that DENV NS2B/3 could only cleave human but not murine or other primate STING proteins [37], and that DENV and ZIKV NS5 can only cleave human but not murine STAT2 [38,39], in part explaining why modeling DENV and flaviviral infections in animal models has been difficult.

Flaviviruses bind to a variety of mammalian cell types through interactions with cell surface-bound glycosaminoglycans (GAGs) and the cognate receptor(s) of each virus, as well as certain attachment factors such as C-type lectins (e.g., dendritic-cell-specific intracellular adhesion molecule-3-grabbing non-integrin [DC-SIGN]) [40–42]. Notably, DENV primarily infects

immune cells of myeloid lineage in humans, including monocytes, macrophages, and dendritic cells [43–45]. Upon receptor-mediated entry into host cells, a conformational change in the flavivirus E protein is triggered by decrease in pH in the endosome, catalyzing the membrane fusion that releases the viral capsid into the cytoplasm, allowing for genome uncoating. The viral genome is then translated directly in the endoplasmic reticulum (ER) as a single polyprotein, which then gets cleaved into individual proteins by both viral and host proteases [46]. Following the synthesis of NS3 helicase and NS5 RNA-dependent RNA polymerase, RNA replicates in vesicle packets where the initial viral assembly also occurs [47]. The nascent viral particles are then transported through the Golgi apparatus where viral maturation and post-translational modifications such as glycosylation occur, before being secreted from the host cell into the bloodstream [1,11,12].

Dengue and dengue virus

Among flaviviruses, the four dengue virus serotypes (DENV1-4) are among the most well-known and well-studied, understandably so in part due to two main reasons: 1) DENV is the most widely-transmitted mosquito-borne virus, and 2) antibody-dependent enhancement of disease can occur in heterologous secondary infections (secondary infection with a distinct serotype from the first infection).

While around 75% of DENV infections are asymptomatic [2], symptomatic DENV infections can result in classic dengue fever (DF), which presents with debilitating but self-limiting symptoms characterized by high fever, rash, retro-orbital pain, myalgia, and arthralgia [2,48]. Some symptomatic DENV infections can progress to the more severe dengue haemorrhagic fever (DHF) and dengue shock syndrome (DSS) [49], which were re-classified by the World Health Organization (WHO) in 2009 as “severe dengue” [50].

Some of the clinical hallmarks of severe dengue (DHF/DSS) include thrombocytopaenia and vascular leak [51]. Thrombocytopenia is defined as low platelet count (<100,000 in the case of DHF/DSS), as a result of platelet destruction or reduced platelet production in the bone marrow [52–54]. This, together with other coagulopathies, leads to haemorrhagic manifestations characteristic of DHF/DSS.

In vascular leak, the vascular endothelium becomes hyperpermeable and fluids extravasate into tissues. One such presentation is pleural effusion, leading to pulmonary oedema, which can progress to respiratory distress. Leakage of fluid from the circulatory system into the interstitial space results in hypotension (low blood pressure) and/or narrow pulse pressure, which can lead to hypovolaemic shock and death [55,56].

Vascular leak occurs as a result of endothelial hyperpermeability and dysfunction, which has traditionally been attributed to a hyperactivated and misdirected immune response to the prior rather than the current infecting serotypes, leading to uncontrolled viral infection and immune cell activation [57,58]. However, over the past few years, our laboratory and others have demonstrated that the secreted NS1 protein of DENV directly contributes to endothelial dysfunction and vascular leak through interactions with endothelial and immune cells that result in the breakdown of endothelial barrier components such as the glycocalyx and intercellular junctional proteins [59–67]. As I further elaborate in the following sections, the observation that NS1 directly causes endothelial dysfunction sets the foundation for my projects in the Harris laboratory and in this dissertation.

Vascular leak and endothelial hyperpermeability

During a viral infection, the immune system responds by producing pro-inflammatory cytokines such as interferon (IFN)-γ, tumor necrosis factor (TNF)-α, interleukin (IL)-6, and IL-8. These cytokines can increase vascular permeability to allow innate immune cells and humoral effector molecules to extravasate from the blood into the tissue to control and eliminate the pathogens [68,69]. A hyperactivated, dysregulated immune activation can result in disruption of the endothelial barrier that lines the vasculature, making the endothelium *hyper*permeable to allow fluids and solutes to extravasate into tissues and accumulate there [57,70,71]. Clinically, the rapid loss of fluids from the blood can lead to sudden loss of blood pressure resulting in hypovolemic shock, which can be fatal, while the fluid accumulation can be observed as pulmonary edema that makes breathing challenging, one of the clinical presentations of severe dengue [72,73].

One of the primary hypotheses for the causation of severe dengue is immunopathogenesis, when immune activation becomes dysregulated, often referred to as a "cytokine storm" [74]. This is thought to occur during a secondary heterologous DENV infection, where the infecting DENV serotype differs from the serotype of a previous DENV infection, leading to antibody-dependent enhancement (ADE). During ADE, cross-reactive but sub-neutralizing antibodies facilitate viral uptake by Fcγ-receptor bearing cells, leading to increased viraemia, infection, and activation of the target monocytes that result in a cytokine storm. The ADE phenomenon has been shown *in vitro* [75–78], as well as through a well-characterized human cohort study in Nicaragua [79–81]. In addition to the immune system gone awry, other inflammation modulators such as platelet activating factors, macrophage migration inhibitory factors, and endopeptidases, have also been shown to mediate vascular leak [53,55,82].

Determinants of endothelial barrier function

The two barrier determinants of endothelial cells in the vasculature are the intercellular junctional complexes and the endothelial glycocalyx. When the endothelial barrier is disrupted, either as a result of immune activation or endothelial-intrinsic factors, the endothelium becomes hyperpermeable [83–85], allowing leakage of fluid out of the circulatory system, which could result in shock and fluid build-up in tissues.

Intercellular junctional complexes form the physical contact sites between two cells and are involved in cell-cell adhesion, communication, and barrier function [84,86]. Specifically, tight (TJ) and adherens (AJ) junctions mediate the inter-cellular permeability [87]. The occludin, claudin (of TJ), and cadherin proteins (of AJ) connect neighbouring endothelial cells and physically regulate fluid passage into the underlying tissues in a semi-permeable manner [86,88].

The glycocalyx is a complex network of membrane-bound glycoproteins and proteoglycans that coat the luminal surface of endothelial cells [57,83,89,90]. The glycocalyx is a dense, kelp forest-like matrix that protects the underlying endothelial cells from the shear force generated by blood flow, forming a physical barrier that prevents bloodstream molecules from reaching the endothelium [83,89]. Sialic acid (Sia) molecules and glycosaminoglycans (GAGs) such as heparan sulfate, chondroitin sulfate, and hyaluronic acid are major components of the glycocalyx and contribute to the maintenance of its barrier function by mediating homeostasis, signaling, and interactions with blood cells. In severe dengue patients, elevated levels of Sia and various GAG components have been observed in circulation [91–95], which is recapitulated in a murine model of severe dengue [96].

Disruptions of both the glycocalyx and the intercellular junctional complexes have been observed clinically and strongly associate with plasma leakage, a hallmark of severe dengue [94,95].

Flavivirus and DENV NS1

When a patient presents with dengue-like symptoms at a clinic or hospital, various laboratory diagnostic tests are available to confirm a positive DENV infection. These tests utilize different molecular and serological approaches such as reverse transcription-polymerase chain reaction (RT-PCR), virus isolation, detection of IgM and IgG antibodies, and detection of the secreted DENV NS1 protein. Detection of DENV NS1 in blood samples is one of the most widely used approaches in clinical diagnosis, as NS1 antigenemia in DENV-infected individuals correlates with both viraemia and disease severity [97–99]. Circulating levels of NS1 have been reported to vary from 0.1 to 10 μg/mL, with concentrations up to 200 ng/mL in dengue fever and levels >600 ng/ml in severe dengue patients [98,100].

NS1 is a ~55-kDa glycoprotein secreted by flavivirus-infected cells that is highly conserved across the flaviviruses [101–103]. DENV NS1 dimerizes in the ER and is displayed as a dimer on intracellular membranes. It plays key roles in viral replication [104], interacting with NS2B and NS4B to contribute to the formation of the viral replication complex [22,24,47,105]. The NS1 dimers can trimerize to form hexamers that are secreted by DENV-infected cells into the bloodstream as a soluble lipoprotein that contains non-specific, size-restricted lipid cargo [102,106–109]. Secreted NS1 aids in viral particle production and interacts with lipids [110,111]. Secreted NS1 also helps DENV evade immune detection by binding to components of the complement pathway, protecting the virus from complement-mediated neutralization and preventing the killing of infected cells [27–29,112,113]. NS1 is also intimately involved in DENV pathogenesis, which will be further reviewed in dedicated sections. Of particular note is that NS1 is the only secreted protein of DENV and other flaviviruses [107], which is interesting as it is atypical for viral proteins to be secreted by infected cells – most viruses typically retain the viral proteins intracellularly to promote viral replication and to evade immune detection.

DENV NS1 causes vascular leak *in vivo* and endothelial hyperpermeability *in vitro*

As the level of NS1 in DENV-infected individuals correlates with disease severity, we initially hypothesized that NS1 may play a direct role in DENV pathogenesis. It was first reported by our laboratory that NS1-vaccinated mice were protected against lethal DENV challenge compared to ovalbumin (OVA) control-vaccinated mice, and that the protection was against lethal vascular leak syndrome [64]. Passive transfer of serum from NS1-vaccinated mice also protected against lethal DENV2 challenge and inhibited NS1-induced endothelial hyperpermeability *in vitro* compared to serum from OVA-vaccinated mice [64]. In the same study, it was also shown that the addition of exogenous NS1 to an otherwise sub-lethal DENV infection rendered the infection lethal, suggesting that NS1 indeed plays a role in DENV pathogenesis.

Subsequently, several studies explored the mechanisms by which DENV NS1 may contribute to vascular leak, which I describe in the following paragraphs as their relative direct or indirect effects on endothelial cells.

Endothelial cell-intrinsic mechanism

To investigate whether DENV NS1 directly mediates the barrier functions of endothelial cells, the Harris laboratory modelled vascular leak *in vitro* using a trans-endothelial electrical resistance (TEER) assay that measures the electrical resistance differential between endothelial cell

monolayer seeded in the apical chamber of a transwell versus the basal chamber, following treatment of NS1 on the endothelial cell monolayer. We found that NS1 disrupts the endothelial glycocalyx layer (EGL) on pulmonary endothelial cells in a dose-dependent manner by inducing degradation of sialic acid and cleavage of heparan sulfate proteoglycans, resulting in TEER reduction, which is a proxy for increased endothelial hyperpermeability [59]. A follow-up study revealed that NS1-induced EGL disruption is independent of cytokines and other inflammatory mediators [65].

Numerous pathways that link NS1 to disruption of EGL components have been proposed. NS1 can stimulate leukocytes to produce matrix metalloproteinases (MMPs) through the NF-κB signaling pathway, leading to degradation of tight and adherens junction proteins and increasing vascular permeability *in vitro* and *in vivo* [114]. Separately, NS1 can also stimulate endothelial cells to secrete macrophage migration inhibitory factor (MIF), resulting in EGL degradation [82,115]. The observation that NS1 leads to EGL degradation resulting in enhanced vascular permeability is corroborated by clinical data. Alongside NS1 levels, the levels of EGL components such as syndecan-1, MMP-9, MIF, heparan sulfate, and chondroitin sulfate have been observed to be elevated in dengue patient sera in a manner that that correlated with disease severity [91,92,94].

In addition to EGL disruption, NS1 has also been implicated in compromising the adherens (AJ) and tight junction (TJ) proteins that mediate cell-cell barriers. DENV NS1 has been shown to modulate the permeability and TJ/AJ proteins of skin [82] and umbilical vein endothelial cells [114,116]. Further studies showed that DENV NS1, along with NS1 from ZIKV, WNV, JEV, and YFV triggered internalization of vascular endothelial (VE)-cadherin and phosphorylation of β-catenin, both components of the interjunctional complex, through the canonical interjunctional protein remodeling pathway that occurs during endothelial barrier breakdown [67]. Ongoing studies in our laboratory and others aim to better define the various endothelial-intrinsic mechanisms through which DENV and other flavivirus NS1 proteins could be causing endothelial hyperpermeability.

Non-endothelial cell-intrinsic mechanism

Vascular leak during severe dengue is usually attributed to an aberrant immune reaction, such as cytokine storm, in response to the viral infection. However, several groups were curious as to whether DENV NS1 could independently trigger an immune reaction to cause vascular leak and endothelial hyperpermeability. NS1 was found to activate both human peripheral blood mononuclear cells (PBMCs) and murine bone marrow-derived macrophages (BMDMs) potentially via Toll-like receptor (TLR) 4, resulting in the production of inflammatory cytokine IL-6 and the transcription of TNF-α, IL-1β, and IL-8 genes [66]. However, the specific TLRs and pathways involved in NS1 activation of immune cells remain contested, where conflicting data regarding the contributions of TLR2 and TLR6 exist [117,118]. NS1 has also been demonstrated to activate vascular growth factors such as angiopoietin-2 [63] and lipid mediators such as phospholipase A_2 [119]. These associations collectively are likely to cause damage to the endothelial glycocalyx and intercellular junctional complexes, leading to vasculopathy.

Thrombocytopaenia as a result of severe dengue has been associated with activated platelets, which along with its released extracellular vesicles can stimulate pro-inflammatory cytokine secretion that leads to vascular dysfunction [120]. Platelets are anucleated blood cells responsible for clotting and are critical for maintaining vascular homeostasis. Activated platelets undergo enhanced coagulation and desialytion, accelerating their clearance, which contributes to thrombocytopenia and vascular leak [53,121]. DENV NS1 has been directly linked to triggering

platelet activation by binding to surface-expressed TLR4, resulting in platelet aggregation and adhesion to monocytes [53]. Increased levels of platelet-monocyte aggregates have been observed in dengue patients exhibiting thrombocytopaenia, and these aggregates triggered the release of pro-inflammatory cytokines such as IL-1β and IL-8 in the corresponding *ex vivo* observations [122]. While NS1 can activate platelets, whether activated platelets directly contribute to vascular dysfunction remains undetermined. Nonetheless, a growing body of evidence suggest that platelets are involved in complex interactions with neutrophils and monocytes to promote inflammation-associated vascular dysfunction and hyperpermeability.

In the same vein, NS1 has been reported to induce auto-antibodies that interfere with the blood clotting cascade. Together with platelets, fibrin, when converted from its inactive form fibrinogen, forms a physical mesh that contributes to clotting and hemostasis. Its counterpart, the anti-clotting mechanism, involves the plasma constituent plasminogen, which when converted to its active form of plasmin can cleave fibrin clots to promote blood flow. DENV NS1 has been shown to induce plasminogen cross-reactive autoantibodies through molecular mimicry of anti-NS1 antibodies, which can contribute to haemorrhage in severe dengue [123]. Similar molecular mimicry of anti-NS1 autoantibodies have been reported for the cross-species conserved lysine-rich CEACAM1 co-isolated (LYRIC) protein [124,125], which is expressed on endothelial cells but whose functions are otherwise unknown; these autoantibody epitopes concentrate towards the C-terminus of DENV NS1.

NS1 is thought to circulate as a hexameric protein, which carries a lipid cargo within the hexamer barrel [101,107]. Recently, the link between the NS1 lipid cargo and vascular hyperpermeability has been explored. NS1 has been reported to interact with high-density lipoprotein (HDL), which are lipoprotein complexes comprised of large lipid units surrounded by apolipoproteins (ApoA1) [110,126]. It has been reported that lipoprotein particles circulating in the blood can mediate vascular homeostasis and regulate inflammation and innate immune responses that impact endothelial and vascular integrity [127,128]. While NS1 and HDL each independently does not stimulate cytokine production from macrophages, HDL component ApoA1 neutralized NS1-induced activation of primary murine macrophages in a dose-dependent manner [126]. Conversely, in primary human macrophages, NS1-HDL complex stimulated production of inflammatory cytokines TNF-α, IL-6, and IL-1β [110], which can increase vascular hyperpermeability and contribute to viral dissemination into tissues. The NS1-HDL association may indeed play greater roles in DENV pathogenesis, as NS1 can use the HDL scavenger receptor SRB1 to internalize into cultured cells [129].

NS1 interacts with endothelial cells in a tissue-specific manner consistent with viral tropism

NS1 is a highly conserved protein across the *Flavivirus* genus, exhibiting up to 60% similarity among different viruses [130,131]. While the characteristics of NS1 from other flavivirus infections in humans remain to be explored, NS1 has been detected in sera from mice infected with WNV, ZIKV, JEV, and YFV [132–134]. In particular, the contribution of NS1 to vascular hyperpermeability in other flavivirus infections has been explored in various studies. ZIKV NS1 was found in ZIKV-infected human placental tissues [135], and ZIKV NS1 caused hyperpermeability in human placental explants by inducing the shedding of GAG components such as heparan sulfate and hyaluronic acid [62]. ZIKV NS1 induced vascular degeneration in retinal cells [136], and also disrupted junctional proteins in brain endothelial cells, resulting in their barrier dysfunction [60,137]. WNV NS1 can remodel the actin cytoskeleton of cultured cells, leading to formation of tunneling nanotubules that WNV could use to infect neighbouring cells

[138]. WNV NS1 also facilitates WNV dissemination across the blood-brain barrier in a murine model of WNV infection [139].

Flaviviruses infect different tissues and cause clinical pathologies in the specific tissues they infect. Interestingly, the Harris laboratory found that the NS1 proteins from multiple flaviviruses interact with the endothelial cells of distinct tissue origin in a manner consistent with the tropism of their respective flaviviruses [140]. For example, DENV NS1 binds multiple cell lines including human pulmonary microvascular endothelial cells (HPMEC), which correlates with the systemic nature of DENV infection that can be observed in the lungs [141]. In contrast, WNV NS1 binds human brain microvascular endothelial cells (HBMEC) but interacts minimally with HPMEC, as WNV causes neurological pathologies such as encephalitis and meningitis but not pulmonary pathologies [7]. Similarly, ZIKV NS1 binds strongly to both HBMEC and human umbilical vein endothelial cells (HUVEC), but minimally with HPMEC, as ZIKV causes neurological and congenital pathologies transmitted *in utero* but not pulmonary pathologies.

Following NS1 binding to human endothelial cells, it enters the cell via clathrin-mediated endocytosis [142]. NS1 induces the production of enzymes such as cathepsin-L and sialidases that cleave EGL components heparan sulfate and syndecan-1 [59,65], as well as disrupt the adherens and tight junction protein complexes that form the physical endothelial cell-cell barrier [67] – collectively resulting in a hyperpermeable endothelium. Interestingly, NS1-induced disruption of EGL and intercellular junctional complexes, leading to endothelial hyperpermeability, also occur with the same tissue-specificity as NS1-endothelial cell binding, which again is concomitant with the tropism of the respective "parent" flaviviruses. The same NS1-host tissue specificity was also observed in both localized and systemic *in vivo* murine models [65,140,143]. One notable outlier was the YFV NS1, which binds endothelial cells of every major tissue, and exhibits liver tissue specificity only in relation to endothelial disruption and hyperpermeability as well as *in vivo*. It was found that while YFV NS1 was able to bind to multiple human endothelial cells of different tissue origins, it was only internalized into human liver sinusoidal endothelial cells (HLSECs), subsequently triggering downstream pathogenic processes. How and why different flavivirus NS1 proteins exhibit differential tissue-specific interactions is where the projects in this dissertation begin.

NS1 receptor(s) identity remains elusive

While NS1 has many associated binding factors and interacts with surface glycans of endothelial cells, attempts to identify the definitive receptor remains a major question within the field.

NS1 initiates its binding to endothelial cells via surface-bound glycan components. This interaction is thought to be mediated by the positively charged residues that form the exposed surface of NS1 hexamer, which initiate a non-specific interaction with the largely negatively charged sulfated glycans on endothelial cell surfaces [144]. Endothelial cells have been shown to harbour distinct tissue-specific GAGs that contribute to NS1 tissue-specific binding to endothelial cells [145]. This initial interaction is thought to facilitate NS1 binding to a proteinaceous receptor(s), enter cells through clathrin-mediated endocytosis [142], and cause downstream endothelial dysfunctions.

Several receptors have been proposed over the years, including TLR4, and more recently SRB1. NS1 activates platelets, resulting in thrombocytopaenia via binding with TLR4 [53]. NS1 has also been reported to bind TLR4 on both endothelial and immune cells, resulting in endothelial-intrinsic and immune-mediated endothelial dysfunction [66,117]. NS1 also induces endocan production by

endothelial cells that contributes to lymphopenia in a TLR4-dependent manner [146]. Since NS1 is a lipoprotein that associates with HDL [107,110], it was thought that NS1 could hijack the lipid metabolism pathway to gain cell entry, using HDL scavenger receptor B1 (SRB1). NS1 entry into C6/36 and Huh7 cells were blocked by anti-SRB1 antibodies, and NS1-SRB1 interaction was demonstrated *in situ* by proximity ligation and *in vitro* by surface plasmon resonance (SPR) [129].

Recent projects in the Harris laboratory have identified a G-protein coupled receptor, beta-2 adrenergic receptor (β2AR), as well as a receptor tyrosine kinase, epidermal growth factor receptor (EGFR) as putative NS1 receptors. β2AR and EGFR are vital membrane proteins implicated in phosphatidylinositol 3-kinase (PI3K) signaling, which is required for NS1-mediated endothelial dysfunction [67]. NS1-induced β2AR can transactivate EGFR via matrix metalloproteinase (MMP) intermediates, and can also mediate clathrin-mediated endocytosis. The identification of these NS1 receptors were corroborated by RNA-seq analyses that compared the transcriptome of endothelial cells that were treated with either wild-type NS1 or endocytosis-deficient NS1-N207Q mutant [142]. siRNA knockdown, CRIPSR-Cas9 knock-out, and inhibitor studies, as well as functional data, all unequivocally support β2AR as a major receptor for NS1 on endothelial and other cells. Ongoing studies are underway to further validate β2AR and EGFR as NS1 receptors and to examine the implications for designing NS1-centric dengue vaccines and therapeutics.

NS1 structure

Flavivirus NS1 is 352 amino acids (aa) in length, with a molecular mass between 40–50 kDa depending on its glycosylation states at asparagine (N) residues 130 and 207 for most of the flaviviruses, and an additional N-linked glycosylation site at residue 175 for some neurotropic flaviviruses such as WNV, St. Louis encephalitis (SLEV) and Murray Valley encephalitis (MVEV) viruses [147].

NS1 monomer contains three highly conserved domains – the β-roll (residues 1–29), wing (38–151), and β-ladder (181–352) domains [131,148,149] (Fig. 1A). The two connecting regions between β-roll/wing and wing/β-ladder domains (residues 30–37 and 152–180) form one 3-stranded β-sheet in the tertiary NS1 structure. In the membrane-binding dimer form [101,109], the β-ladder domain makes up the central dimer structure with extensive β-sheets on the external-facing side termed “spaghetti loop” (Fig. 1B). The wing domain of each monomer extends out of the central structure in both directions; it encompasses a flexible loop at residues 108–129, which have not been successfully resolved except for ZIKV NS1 [148,149]. The β-roll is positioned at the membrane-facing side accompanied by the two connecting regions and the wing flexible loop, together forming the hydrophobic inner surface of the flavivirus NS1 dimer, which also faces in towards the lipid-filled center of the barrel formed by the NS1 hexamer. The N-linked glycosylation at N130 and N207 are essential for stabilizing the secreted hexamer for secretion and extracellular stability [150], as well as internalization into endothelial cells [142].

Secreted NS1 is thought to exist as a hexamer in circulation but is found as a dimer in the membrane-bound state, although high-resolution structural evidence has been lacking, and secreted NS1 has increasingly been shown to exist as a heterologous mixture of oligomerization states [151]. Nonetheless, how the hexamer-dimer switch occurs and its significance towards NS1-mediated flavivirus pathogenesis remains elusive and is a bourgeoning question. It has been shown recently that NS1 interacts with the ApoA1 of HDL either directly or through hydrophobic protein-lipid interactions [110,152], and can exist in various forms of dimers, tetramers, and hexamers depending on the dynamic equilibrium between the amount of circulating HDL and free NS1 [151,152]. Dimeric NS1 is also found to have a higher thermal dissociation requirement from HDL

particles than from the NS1 hexamer itself [110], further supporting the idea that NS1 dimers could be drawn away from circulating hexamers/ oligomers to the lipids and glycoproteins on the surface of endothelial cells to initiate the interactions with their various association factors and cognate receptor(s).

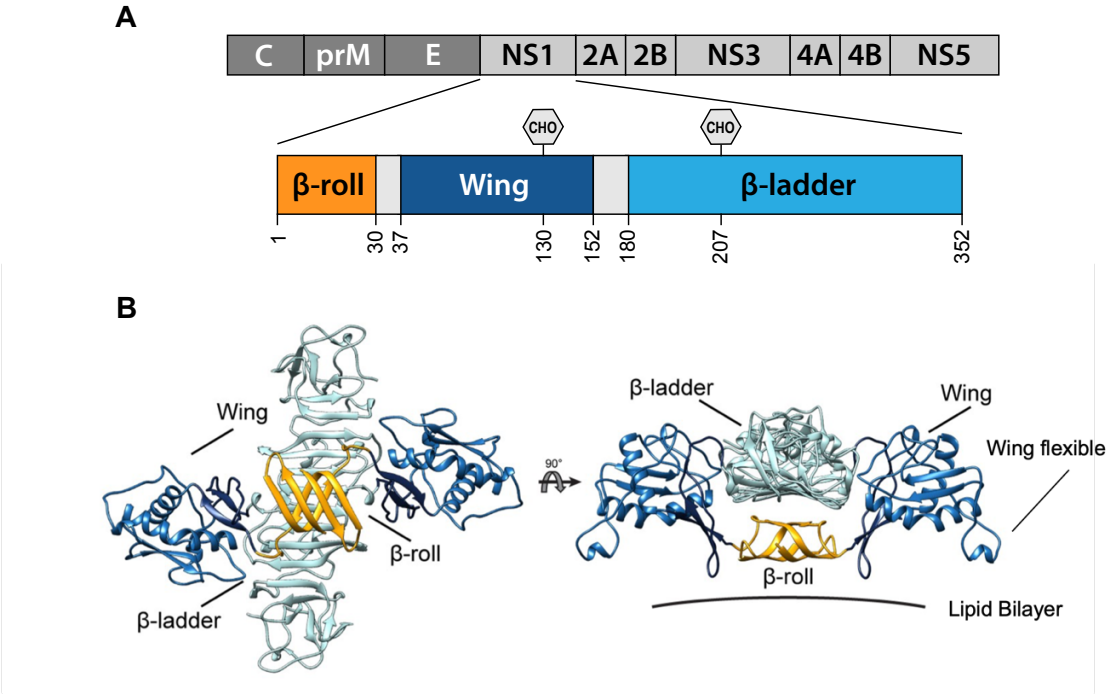

Figure 1. Structure of flavivirus non-structural protein 1 (NS1).
(A) NS1 is one of the seven non-structural proteins of flaviviruses and contains three domains – β-roll, wing, and β-ladder – with two glycosylation sites at residues Asn-130 and Asn-207 (three for WNV and several other NS1). **(B)** Crystal structure of NS1 dimers with the corresponding domains labelled and color-coded, adapted from [104].

The NS1 β-roll and wing domains contain many hydrophobic residues that are predicted to interact with the plasma membrane of cells [131,149]. Previous immunization studies by our group that vaccinated mice with DENV NS1 found the wing domain to be highly immunodominant, where a majority of the antibodies in sera were made against the wing domain. This observation was corroborated by human clinical samples, where we found a majority of NS1 antibodies to be targeting the wing domain [153]. Moreover, anti-wing antibodies were found to be protective against lethal DENV challenge in mice [64,125], suggesting that the wing domain might play a major role in mediating NS1-induced pathogenesis.

The surface-exposed residues in the wing and β-roll domains are conserved among DENV serotypes but divergent across the *Flavivirus* genus (e.g., between DENV and WNV), supporting their possible roles in mediating NS1 tissue-specific interactions. Several studies have examined the relative contributions of various residues across the entire NS1 protein. Conserved, hydrophobic residues in the flexible loop within the wing domain (Trp-115, Trp-118, Gly-119) have been identified to partially contribute to DENV NS1 binding to HPMEC [131,142,143]. Interestingly, NS1 dimer interactions with ApoA1 have been mapped also to residues in the wing domain and hydrophobic parts of the β-roll domains of DENV NS1 [152], highlighting the importance of NS1 wing domain and hydrophobic residues. In contrast, select residues in the β-

ladder domain have been implicated as important for NS1-induced endothelial hyperpermeability [154,155], while being dispensable for binding endothelial cells [142,143].

While these data offer clues about NS1 molecular determinants of tissue-specific interactions with endothelial cells, open questions remain – such as which domains and residues play what roles in NS1-induced pathogenesis and tissue-specificity, what host factors are involved, and what potential implications these results would have on DENV and broader flavivirus vaccines and therapeutics.

Potential of DENV NS1 as a vaccine or therapeutic target

Vaccine target

Dengue remains a major health issue in part due to the lack of effective therapeutics and the limited efficacy of the only licensed vaccine (as of June 2022), Dengvaxia. Dengvaxia is a live-attenuated tetravalent chimeric vaccine based on the existing YFV vaccine, using YFV-17D vaccine strain as the backbone and contains the prM and E proteins from all four DENV strains [156]. Counter-intuitively, Dengvaxia is indicated only for people with prior DENV infection, for fear of antibody-dependent enhancement (ADE), which may exacerbate subsequent DENV infection in DENV-naïve (i.e., seronegative) individuals. ADE has been demonstrated only for structural proteins, predominantly the E protein [79,157], but not for non-structural proteins. As a secreted protein that does not induce antibodies (Abs) against the virion, NS1 thus serves as an attractive vaccine target without the fear of ADE.

Since NS1 antigenaemia in infected individuals correlates with DENV viraemia, its presence early in infection can elicit a robust humoral and cell-mediated immune response. The immunodominant wing domain and the C-terminus of β-ladder domain provide many B cell epitopes, and the resulting anti-NS1 Abs can limit NS1-mediated dengue pathogenesis to protect against severe dengue. In T-cell-mediated immunity, PBMCs recognize NS1 via pattern recognition receptors such as TLR4, which will trigger the release of inflammatory cytokines such as IL-6, IL-8, and TNF-α that help resolve viral infection when produced in appropriate, non-pathogenic amounts [158].

However, anti-NS1 Abs elicited from NS1 immunization with atypical DENV strains such as D2Y98P that circulate in Southeast Asia may not be protective against disease, cautioning the approach heralding NS1 as a universal dengue vaccine candidate [159]. Moreover, NS1 is known to exhibit molecular mimicry with human self-antigens in the blood clotting system [123] and endothelial cells [124,160–162], potentially presenting anti-NS1 Abs with a threat of autoimmunity [163,164].

Nonetheless, numerous NS1-based dengue vaccines are currently under development [165]. The current vaccines based on live-attenuated viruses include the entire DENV genome, in contrast to Dengvaxia which elicits immunity only against the DENV prM and E proteins. One of the vaccines furthest along in the development pipeline is Takeda's TAK-003 tetravalent vaccine, which comprises DENV2 backbone with prM and E from all four DENV serotypes. The sera elicited from immunization contained NS1 Abs that were able to protect against NS1-induced endothelial dysfunction [166]. Thus far, the TAK-003 vaccine has demonstrated efficacy and little safety concern arising from ADE in both adults [167] and children [168], although long-term follow-up studies after the Phase 3 clinical trial are still ongoing.

Therapeutic target

On the therapeutics front, currently only supportive treatments exist for dengue, with no licensed therapeutic drugs available. As severe dengue is significantly associated with and enhanced by NS1, targeting NS1 with therapeutic antibodies or compounds to prevent severe dengue appears prudent. As NS1 is not a structural component of the virion, anti-NS1 mAbs should pose little risk of ADE. Moreover, as NS1 plays multifaceted roles in the DENV life cycle ranging from replication and immune evasion to direct pathogenesis, anti-NS1 Abs or compounds can protect via distinct therapeutic mechanisms against different NS1 functions.

Indeed, anti-NS1 Abs utilize complement-dependent cytotoxicity of infected cells to reduce viral replication in both DENV and JEV [125,169,170]. Anti-NS1 Abs can also block NS1-induced pathogenicity both *in vivo* and *in vitro*, with no demonstrated ADE activities [64,143,154,171].

Besides Abs, iminosugars have been shown to be a class of potent anti-NS1 compounds. Iminosugars are monosaccharide analogues where a nitrogen atom has replaced the oxygen atom in the ring of the saccharide structure. Iminosugars have been shown to competitively inhibit α-glucosidases I and II [172,173], which are important ER glycoprotein enzymes that process N-linked oligosaccharides attached to proteins. Improper trimming and processing of the oligosaccharides on proteins result in misfolding, mis-assembly, and reduced secretion of proteins. Iminosugars have thus been explored as antivirals against enveloped viruses, and their antiviral properties have been demonstrated against flaviviruses. One alkyl iminosugar derivative *N*N-DNJ blocked JEV and DENV infection of BHK21 cells, and reduced the secretion of E and NS1 proteins [174].

Given their antiviral and pharmaceutical potential, derivatives of one natural iminosugar product, 1-deoxynojirimycin (DNJ), commonly identified as UV-1 through UV-5, have been developed and marketed for clinical use in humans [175]. These compounds were evaluated against DENV in an *in vivo* screen, and a resulting DNJ derivative, UV-4, protected mice against lethal DENV challenge under both regular and ADE conditions, with reductions in both viraemia and immune activation [176]. The hydrochloride salt of UV-4, *N*-(9'-methoxynonyl)-1-deoxynojirimycin or M*O*N-DNJ (UV-4B), showed high genetic barrier to escape mutations [177], and was further tested against DENV in a dosage and pharmacokinetics study. UV-4B was found to reduce infectious virus production *in vitro* against all four DENV serotypes, including clinical isolates. Inhibition of the ER α-glucosidase pathway and not the glycosphingolipid pathway was found to be the underlying anti-DENV mechanism of UV-4B [178]. In the ongoing COVID-19 pandemic, UV-4B has also demonstrated *in vitro* antiviral effects against multiple strains of SARS-CoV-2, the causative viral agent of COVID-19 [179]. The pharmacokinetics study supported UV-4B's Investigational New Drug (IND) filing with the U.S. FDA, which has recently completed its Phase Ib clinical trial for safety [180].

The antiviral effects of UV-4B were attributed to its inhibition of ER α-glucosidases, which impeded proper glyco-processing of viral proteins, resulting in reduced viral secretion. One project in this dissertation explores the impact of UV-4B on DENV NS1, which is also a secreted protein. As all proteins undergo post-translational processing in the ER and Golgi apparatus, it is conceivable that UV-4B would have similar effects on NS1 as it does on the E protein, thus presenting another mechanism underlying its antiviral effects on DENV infections.

Summary and overview of dissertation

Since the discovery of the roles that DENV NS1 plays in dengue pathogenesis by the Harris laboratory and other groups in 2015, significant advances have been made across the fields of flavivirus, DENV, and NS1. Both the endothelial cell-intrinsic and immune-mediated mechanisms

of NS1-induced pathogenesis were described; the tissue-specific nature of NS1-endothelial cells interactions were reported; high-resolution crystal structures of multiple flavivirus NS1 proteins were solved, several in complex with monoclonal antibodies; the cognate receptors of NS1 are being identified; and anti-NS1 vaccines and therapeutics are being explored. Given the exciting advances in the field, this dissertation fills several existing gaps in knowledge.

In Chapter 2, I use NS1 chimeric proteins to identify the wing domain of flavivirus NS1 to contain molecular determinants of NS1 tissue-specificity and further identify residues 91 to 93 in the wing domain as molecular determinants for DENV NS1 both *in vitro* and *in vivo*. In Chapter 3, I describe the additional data that informed my path to identify the critical domains and residues described in Chapter 2, as well as some preliminary clues regarding host determinants of NS1 tissue-specificity. In Chapter 4, I test the antiviral iminosugar UV-4B with respect to its anti-NS1 effects. Taken together, this work contributes to the flavivirus and dengue fields and improves our understanding of the multifaceted NS1 in relation to its structure, propensity to bind host cells of different tissue origins, and interactions with glycans. Further, it presents new avenues for NS1-based interventions in not just dengue, but also Zika and other flaviviral diseases that have increasing needs for better vaccines and therapeutics.

References
Chapter 1

1. Pierson, T.C., and Diamond, M.S. (2020). The continued threat of emerging flaviviruses. Nat. Microbiol. *5*, 796–812.
2. Bhatt, S., Gething, P.W., Brady, O.J., Messina, J.P., Farlow, A.W., Moyes, C.L., Drake, J.M., Brownstein, J.S., Hoen, A.G., Sankoh, O., *et al.* (2013). The global distribution and burden of dengue. Nature *496*, 504–507.
3. Collins, M.H., and Metz, S.W. (2017). Progress and Works in Progress: Update on Flavivirus Vaccine Development. Clin. Ther. *39*, 1519–1536.
4. Tabachnick, W.J. (2016). Climate Change and the Arboviruses: Lessons from the Evolution of the Dengue and Yellow Fever Viruses. Annu. Rev. Virol. *3*, 125–145.
5. Chala, B., and Hamde, F. (2021). Emerging and Re-emerging Vector-Borne Infectious Diseases and the Challenges for Control: A Review. Front. Public Heal. *9*, 715759.
6. Franklinos, L.H. V, Jones, K.E., Redding, D.W., and Abubakar, I. (2019). The effect of global change on mosquito-borne disease. Lancet Infect. Dis. *19*, e302–e312.
7. Maximova, O.A., and Pletnev, A.G. (2018). Flaviviruses and the central nervous system: Revisiting neuropathological concepts. Annu. Rev. Virol. *5*, 255–272.
8. Musso, D., and Gubler, D.J. (2016). Zika Virus. Clin. Microbiol. Rev. *29*, 487–524.
9. Monath, T.P., and Vasconcelos, P.F.C. (2015). Yellow fever. J. Clin. Virol. *64*, 160–173.
10. Guzman, M., and Harris, E. (2015). Dengue. Lancet *385*, 453–65.
11. Pierson, T.C., and Diamond, M.S. (2013). Flaviviruses. In Fields Virology (Wolters Kluwer Health Adis (ESP)).
12. Chambers, T.J., Hahn, C.S., Galler, R., and Rice, C.M. (1990). Flavivirus Genome Organisation, Expression, and Replication. Annu. Rev. Microbiol. *44*, 649–688.
13. Xie, X., Zou, J., Zhang, X., Zhou, Y., Routh, A.L., Kang, C., Popov, V.L., Chen, X., Wang, Q.Y., Dong, H., *et al.* (2019). Dengue NS2A Protein Orchestrates Virus Assembly. Cell Host Microbe *26*, 606-622.e8.
14. Xie, X., Gayen, S., Kang, C., Yuan, Z., and Shi, P.-Y. (2013). Membrane Topology and Function of Dengue Virus NS2A Protein. J. Virol. *87*, 4609–4622.
15. Falgout, B., Pethel, M., Zhang, Y.M., and Lai, C.J. (1991). Both non-structural proteins NS2B and NS3 are required for the proteolytic processing of dengue virus non-structural proteins. J. Virol. *65*, 2467–2475.
16. Arias, C.F., Preugschat, F., and Strauss, J.H. (1993). Dengue 2 Virus NS2B and NS3 Form a Stable Complex That Can Cleave NS3 within the Helicase Domain. Virology *193*, 888–899.
17. Niyomrattanakit, P., Winoyanuwattikun, P., Chanprapaph, S., Angsuthanasombat, C., Panyim, S., and Katzenmeier, G. (2004). Identification of Residues in the Dengue Virus Type 2 NS2B Cofactor That Are Critical for NS3 Protease Activation. J. Virol. *78*, 13708–13716.
18. Benarroch, D., Selisko, B., Locatelli, G.A., Maga, G., Romette, J.-L., and Canard, B. (2004). The RNA helicase, nucleotide 5′-triphosphatase, and RNA 5′-triphosphatase activities of Dengue virus protein NS3 are Mg2+-dependent and require a functional Walker B motif in the helicase catalytic core. Virology *328*, 208–218.

19. Wang, C.-C., Huang, Z.-S., Chiang, P.-L., Chen, C.-T., and Wu, H.-N. (2009). Analysis of the nucleoside triphosphatase, RNA triphosphatase, and unwinding activities of the helicase domain of dengue virus NS3 protein. FEBS Lett. *583*, 691–696.

20. Miller, S., Kastner, S., Krijnse-Locker, J., Bühler, S., and Bartenschlager, R. (2007). The Non-structural Protein 4A of Dengue Virus Is an Integral Membrane Protein Inducing Membrane Alterations in a 2K-regulated Manner. J. Biol. Chem. *282*, 8873–8882.

21. Li, X.-D., Ye, H.-Q., Deng, C.-L., Liu, S.-Q., Zhang, H.-L., Shang, B.-D., Shi, P.-Y., Yuan, Z.-M., and Zhang, B. (2015). Genetic interaction between NS4A and NS4B for replication of Japanese encephalitis virus. J. Gen. Virol. *96*, 1264–1275.

22. Lindenbach, B.D., and Rice, C.M. (1999). Genetic interaction of flavivirus non-structural proteins NS1 and NS4A as a determinant of replicase function. J. Virol. *73*, 4611–21.

23. Phan, T., Kohlway, A., Dimberu, P., Pyle, A.M., and Lindenbach, B.D. (2011). The Acidic Domain of Hepatitis C Virus NS4A Contributes to RNA Replication and Virus Particle Assembly. J. Virol. *85*, 1193–1204.

24. Youn, S., Li, T., McCune, B.T., Edeling, M.A., Fremont, D.H., Cristea, I.M., and Diamond, M.S. (2012). Evidence for a Genetic and Physical Interaction between Non-structural Proteins NS1 and NS4B That Modulates Replication of West Nile Virus. J. Virol. *86*, 7360–7371.

25. Egloff, M.P., Benarroch, D., Selisko, B., Romette, J.L., and Canard, B. (2002). An RNA cap (nucleoside-2′-O-)-methyltransferase in the flavivirus RNA polymerase NS5: Crystal structure and functional characterization. EMBO J. *21*, 2757–2768.

26. TAN, B.-H., FU, J., SUGRUE, R.J., YAP, E.-H., CHAN, Y.-C., and TAN, Y.H. (1996). Recombinant Dengue Type 1 Virus NS5 Protein Expressed inEscherichia coliExhibits RNA-Dependent RNA Polymerase Activity. Virology *216*, 317–325.

27. Conde, J.N., da Silva, E.M., Allonso, D., Coelho, D.R., Andrade, I. da S., de Medeiros, L.N., Menezes, J.L., Barbosa, A.S., and Mohana-Borges, R. (2016). Inhibition of the Membrane Attack Complex by Dengue Virus NS1 through Interaction with Vitronectin and Terminal Complement Proteins. J. Virol. *90*, 9570–9581.

28. Avirutnan, P., Hauhart, R.E., Somnuke, P., Blom, A.M., Diamond, M.S., and Atkinson, J.P. (2011). Binding of Flavivirus Non-structural Protein NS1 to C4b Binding Protein Modulates Complement Activation. J. Immunol. *187*, 424–433.

29. Thiemmeca, S., Tamdet, C., Punyadee, N., Prommool, T., Songjaeng, A., Noisakran, S., Puttikhunt, C., Atkinson, J.P., Diamond, M.S., Ponlawat, A., *et al.* (2016). Secreted NS1 Protects Dengue Virus from Mannose-Binding Lectin–Mediated Neutralization. J. Immunol. *197*, 4053–4065.

30. Youn, S., Cho, H., Fremont, D.H., and Diamond, M.S. (2010). A Short N-Terminal Peptide Motif on Flavivirus Non-structural Protein NS1 Modulates Cellular Targeting and Immune Recognition. J. Virol. *84*, 9516–9532.

31. Aguirre, S., Maestre, A.M., Pagni, S., Patel, J.R., Savage, T., Gutman, D., Maringer, K., Bernal-Rubio, D., Shabman, R.S., Simon, V., *et al.* (2012). DENV Inhibits Type I IFN Production in Infected Cells by Cleaving Human STING. PLoS Pathog. *8*, e1002934.

32. Aguirre, S., Luthra, P., Sanchez-Aparicio, M.T., Maestre, A.M., Patel, J., Lamothe, F., Fredericks, A.C., Tripathi, S., Zhu, T., Pintado-Silva, J., *et al.* (2017). Dengue virus NS2B protein targets cGAS for degradation and prevents mitochondrial DNA sensing during infection. Nat. Microbiol. *2*, 1–11.

33. Riedl, W., Acharya, D., Lee, J.H., Liu, G., Serman, T., Chiang, C., Chan, Y.K., Diamond, M.S., and Gack, M.U. (2019). Zika Virus NS3 Mimics a Cellular 14-3-3-Binding Motif to Antagonize RIG-I- and MDA5-Mediated Innate Immunity. Cell Host Microbe *26*, 493-503.e6.

34. Muñoz-Jordán, J.L., Laurent-Rolle, M., Ashour, J., Martínez-Sobrido, L., Ashok, M., Lipkin, W.I., and García-Sastre, A. (2005). Inhibition of Alpha/Beta Interferon Signaling by the NS4B Protein of Flaviviruses. J. Virol. *79*, 8004–8013.

35. Ashour, J., Laurent-Rolle, M., Shi, P.-Y., and Garcia-Sastre, A. (2009). NS5 of Dengue Virus Mediates STAT2 Binding and Degradation. J. Virol. *83*, 5408–5418.

36. Roby, J.A., Esser-Nobis, K., Dewey-Verstelle, E.C., Fairgrieve, M.R., Schwerk, J., Lu, A.Y., Soveg, F.W., Hemann, E.A., Hatfield, L.D., Keller, B.C., *et al.* (2020). Flavivirus Non-structural Protein NS5 Dysregulates HSP90 to Broadly Inhibit JAK/STAT Signaling. Cells *9*, 899.

37. Stabell, A.C., Meyerson, N.R., Gullberg, R.C., Gilchrist, A.R., Webb, K.J., Old, W.M., Perera, R., and Sawyer, S.L. (2018). Dengue viruses cleave STING in humans but not in nonhuman primates, their presumed natural reservoir. Elife *7*, 1–25.

38. Ashour, J., Morrison, J., Laurent-Rolle, M., Belicha-Villanueva, A., Plumlee, C.R., Bernal-Rubio, D., Williams, K.L., Harris, E., Fernandez-Sesma, A., Schindler, C., *et al.* (2010). Mouse STAT2 Restricts Early Dengue Virus Replication. Cell Host Microbe *8*, 410–421.

39. Grant, A., Ponia, S.S., Tripathi, S., Balasubramaniam, V., Miorin, L., Sourisseau, M., Schwarz, M.C., Sánchez-Seco, M.P., Evans, M.J., Best, S.M., *et al.* (2016). Zika Virus Targets Human STAT2 to Inhibit Type i Interferon Signaling. Cell Host Microbe *19*, 882–890.

40. Davis, C.W., Nguyen, H.-Y., Hanna, S.L., Sánchez, M.D., Doms, R.W., and Pierson, T.C. (2006). West Nile Virus Discriminates between DC-SIGN and DC-SIGNR for Cellular Attachment and Infection. J. Virol. *80*, 1290–1301.

41. Perera-Lecoin, M., Meertens, L., Carnec, X., and Amara, A. (2013). Flavivirus entry receptors: An update. Viruses *6*, 69–88.

42. Chong, H.Y., Leow, C.Y., Abdul Majeed, A.B., and Leow, C.H. (2019). Flavivirus infection—A review of immunopathogenesis, immunological response, and immunodiagnosis. Virus Res. *274*, 197770.

43. Kyle, J.L., Beatty, P.R., and Harris, E. (2007). Dengue Virus Infects Macrophages and Dendritic Cells in a Mouse Model of Infection. J. Infect. Dis. *195*, 1808–1817.

44. Castillo, J.A., Naranjo, J.S., Rojas, M., Castaño, D., and Velilla, P.A. (2019). Role of Monocytes in the Pathogenesis of Dengue. Arch. Immunol. Ther. Exp. (Warsz). *67*, 27–40.

45. Flipse, J., Torres, S., Diosa-Toro, M., van der Ende-Metselaar, H., Herrera-Rodriguez, J., Urcuqui-Inchima, S., Huckriede, A., Rodenhuis-Zybert, I.A., and Smit, J.M. (2016). Dengue tropism for macrophages and dendritic cells: The host cell effect. J. Gen. Virol. *97*, 1531–1536.

46. Amberg, S.M., and Rice, C.M. (1999). Mutagenesis of the NS2B-NS3-Mediated Cleavage Site in the Flavivirus Capsid Protein Demonstrates a Requirement for Coordinated Processing. J. Virol. *73*, 8083–8094.

47. Welsch, S., Miller, S., Romero-Brey, I., Merz, A., Bleck, C.K.E., Walther, P., Fuller, S.D., Antony, C., Krijnse-Locker, J., and Bartenschlager, R. (2009). Composition and Three-Dimensional Architecture of the Dengue Virus Replication and Assembly Sites. Cell Host Microbe *5*, 365–375.

48. Stanaway, J.D., Shepard, D.S., Undurraga, E.A., Halasa, Y.A., Coffeng, L.E., Brady, O.J., Hay, S.I., Bedi, N., Bensenor, I.M., Castañeda-Orjuela, C.A., *et al.* (2016). The global burden of

dengue: an analysis from the Global Burden of Disease Study 2013. Lancet Infect. Dis. *16*, 712–723.

49. World Health Organization (1997). Dengue Hemorrhagic Fever: Diagnosis, Treatment, Prevention and Control.

50. World Health Organization (2009). Dengue: guidelines for diagnosis, treatment, prevention, and control (Geneva: World Health Organization).

51. Simmons, C.P., Farrar, J.J., van Vinh Chau, N., and Wills, B. (2012). Dengue. N. Engl. J. Med. *366*, 1423–1432.

52. Sridharan, A., Chen, Q., Tang, K.F., Ooi, E.E., Hibberd, M.L., and Chen, J. (2013). Inhibition of Megakaryocyte Development in the Bone Marrow Underlies Dengue Virus-Induced Thrombocytopenia in Humanized Mice. J. Virol. *87*, 11648–11658.

53. Chao, C.-H., Wu, W.-C., Lai, Y.-C., Tsai, P.-J., Perng, G.-C., Lin, Y.-S., and Yeh, T.-M. (2019). Dengue virus non-structural protein 1 activates platelets via Toll-like receptor 4, leading to thrombocytopenia and hemorrhage. PLoS Pathog. *15*, e1007625.

54. Hottz, E.D., Lopes, J.F., Freitas, C., Valls-De-Souza, R., Oliveira, M.F., Bozza, M.T., Da Poian, A.T., Weyrich, A.S., Zimmerman, G.A., Bozza, F.A., *et al.* (2013). Platelets mediate increased endothelium permeability in dengue through NLRP3-inflammasome activation. Blood *122*, 3405–3414.

55. Malavige, G.N., and Ogg, G.S. (2017). Pathogenesis of vascular leak in dengue virus infection. Immunology *151*, 261–269.

56. Srikiatkhachorn, A. (2009). Plasma leakage in dengue haemorrhagic fever. Thromb. Haemost. *102*, 1042–1049.

57. Srikiatkhachorn, A., Mathew, A., and Rothman, A.L. (2017). Immune-mediated cytokine storm and its role in severe dengue. Semin. Immunopathol. *39*, 563–574.

58. Malavige, G.N., Jeewandara, C., and Ogg, G.S. (2020). Dysfunctional Innate Immune Responses and Severe Dengue. Front. Cell. Infect. Microbiol. *10:590004*.

59. Puerta-Guardo, H., Glasner, D.R., and Harris, E. (2016). Dengue Virus NS1 Disrupts the Endothelial Glycocalyx, Leading to Hyperpermeability. PLoS Pathog. *12*, e1005738.

60. Rastogi, M., and Singh, S.K. (2020). Zika virus NS1 affects the junctional integrity of human brain microvascular endothelial cells. Biochimie *176*, 52–61.

61. Hui, L., Nie, Y., Li, S., Guo, M., Yang, W., Huang, R., Chen, J., Liu, Y., Lu, X., Chen, Z., *et al.* (2020). Matrix metalloproteinase 9 facilitates Zika virus invasion of the testis by modulating the integrity of the blood-testis barrier. PLoS Pathog. *16*, e1008509.

62. Puerta-Guardo, H., Tabata, T., Petitt, M., Dimitrova, M., Glasner, D.R., Pereira, L., and Harris, E. (2020). Zika Virus Non-structural Protein 1 Disrupts Glycosaminoglycans and Causes Permeability in Developing Human Placentas. J. Infect. Dis. *221*, 313–324.

63. Singh, S., Anupriya, M.G., Modak, A., and Sreekumar, E. (2018). Dengue virus or NS1 protein induces trans-endothelial cell permeability associated with VE-Cadherin and RhoA phosphorylation in HMEC-1 cells preventable by Angiopoietin-1. J. Gen. Virol. *99*, 1658–70.

64. Beatty, P.R., Puerta-Guardo, H., Killingbeck, S.S., Glasner, D.R., Hopkins, K., and Harris, E. (2015). Dengue virus NS1 triggers endothelial permeability and vascular leak that is prevented by NS1 vaccination. Sci. Transl. Med. *7*, 304ra141.

65. Glasner, D.R., Ratnasiri, K., Puerta-Guardo, H., Espinosa, D.A., Beatty, P.R., and Harris, E.

(2017). Dengue virus NS1 cytokine-independent vascular leak is dependent on endothelial glycocalyx components. PLoS Pathog. *13*, e1006673.

66. Modhiran, N., Watterson, D., Muller, D.A., Panetta, A.K., Sester, D.P., Liu, L., Hume, D.A., Stacey, K.J., and Young, P.R. (2015). Dengue virus NS1 protein activates cells via Toll-like receptor 4 and disrupts endothelial cell monolayer integrity. Sci. Transl. Med. *7*, 304ra142.

67. Puerta-Guardo, H., Biering, S.B., de Sousa, F.T.G., Shu, J., Glasner, D.R., Li, J., Blanc, S.F., Beatty, P.R., and Harris, E. (2022). Flavivirus NS1 Triggers Tissue-Specific Disassembly of Intercellular Junctions Leading to Barrier Dysfunction and Vascular Leak in a GSK-3β-Dependent Manner. Pathogens *11*, 615.

68. Kurane, I., Rothman, A.L., Livingston, P.G., Green, S., Gagnon, S.J., Janus, J., Innis, B.L., Nimmannitya, S., Nisalak, A., and Ennis, F.A. (1994). Immunopathologic mechanisms of dengue hemorrhagic fever and dengue shock syndrome. In Positive-Strand RNA Viruses (Vienna: Springer Vienna), pp. 59–64.

69. Hatch, S., Endy, T.P., Thomas, S., Mathew, A., Potts, J., Pazoles, P., Libraty, D.H., Gibbons, R., and Rothman, A.L. (2011). Intracellular Cytokine Production by Dengue Virus–specific T cells Correlates with Subclinical Secondary Infection. J. Infect. Dis. *203*, 1282–1291.

70. Vial, T., and Descostes, J. (1995). Immune-mediated side-effects of cytokines in humans. Toxicology *105*, 31–57.

71. Steinberg, B.E., Goldenberg, N.M., and Lee, W.L. (2012). Do viral infections mimic bacterial sepsis? The role of microvascular permeability: A review of mechanisms and methods. Antiviral Res. *93*, 2–15.

72. Siddall, E., Khatri, M., and Radhakrishnan, J. (2017). Capillary leak syndrome: etiologies, pathophysiology, and management. Kidney Int. *92*, 37–46.

73. Watterson, D., Modhiran, N., Muller, D.A., Stacey, K.J., and Young, P.R. (2018). Plugging the Leak in Dengue Shock. In Dengue and Zika: Control and Antiviral Treatment Strategies (Singapore: Springer), pp. 89–106.

74. Puerta-Guardo, H. (2022). Editorial: From Pathogenic Infections to Inflammation and Disease - the Tumultuous Road of the 'Cytokine Storm.' Front. Cell. Infect. Microbiol. *11*, 1–6.

75. Halstead, S.B. (1979). In Vivo Enhancement of Dengue Virus Infection in Rhesus Monkeys by Passively Transferred Antibody. J. Infect. Dis. *140*, 527–533.

76. Balsitis, S.J., Williams, K.L., Lachica, R., Flores, D., Kyle, J.L., Mehlhop, E., Johnson, S., Diamond, M.S., Beatty, P.R., and Harris, E. (2010). Lethal Antibody Enhancement of Dengue Disease in Mice Is Prevented by Fc Modification. PLoS Pathog. *6*, e1000790.

77. Kliks, S.C., Brandt, W.E., Wahl, L., Nisalak, A., and Burke, D.S. (1989). Antibody-Dependent Enhancement of Dengue Virus Growth in Human Monocytes as a Risk Factor for Dengue Hemorrhagic Fever. Am. J. Trop. Med. Hyg. *40*, 444–451.

78. Zellweger, R.M., Prestwood, T.R., and Shresta, S. (2010). Enhanced Infection of Liver Sinusoidal Endothelial Cells in a Mouse Model of Antibody-Induced Severe Dengue Disease. Cell Host Microbe *7*, 128–139.

79. Katzelnick, L.C., Gresh, L., Halloran, M.E., Mercado, J.C., Kuan, G., Gordon, A., Balmaseda, A., and Harris, E. (2017). Antibody-dependent enhancement of severe dengue disease in humans. Science *358*, 929–932.

80. Katzelnick, L.C., Narvaez, C., Arguello, S., Lopez Mercado, B., Collado, D., Ampie, O., Elizondo, D., Miranda, T., Bustos Carillo, F., Mercado, J.C., *et al.* (2020). Zika virus infection enhances

future risk of severe dengue disease. Science *369*, 1123–1128.

81. Waggoner, J.J., Katzelnick, L.C., Burger-Calderon, R., Gallini, J., Moore, R.H., Kuan, G., Balmaseda, A., Pinsky, B.A., and Harris, E. (2020). Antibody-Dependent Enhancement of Severe Disease Is Mediated by Serum Viral Load in Pediatric Dengue Virus Infections. J. Infect. Dis. *221*, 1846–1854.

82. Chen, H.R., Chuang, Y.C., Lin, Y.S., Liu, H.S., Liu, C.C., Perng, G.C., and Yeh, T.M. (2016). Dengue Virus Non-structural Protein 1 Induces Vascular Leakage through Macrophage Migration Inhibitory Factor and Autophagy. PLoS Negl. Trop. Dis. *10*, e0004828.

83. Reitsma, S., Slaaf, D.W., Vink, H., Van Zandvoort, M.A.M.J., and Oude Egbrink, M.G.A. (2007). The endothelial glycocalyx: Composition, functions, and visualization. Pflugers Arch. Eur. J. Physiol. *454*, 345–359.

84. Dejana, E. (2004). Endothelial cell-cell junctions: Happy together. Nat. Rev. Mol. Cell Biol. *5*, 261–270.

85. Bazzoni, G., and Dejana, E. (2004). Endothelial Cell-to-Cell Junctions: Molecular Organization and Role in Vascular Homeostasis. Physiol. Rev. *84*, 869–901.

86. Cerutti, C., and Ridley, A.J. (2017). Endothelial cell-cell adhesion and signaling. Exp. Cell Res. *358*, 31–38.

87. Otani, T., and Furuse, M. (2020). Tight Junction Structure and Function Revisited. Trends Cell Biol. *30*, 805–817.

88. Steed, E., Balda, M.S., and Matter, K. (2010). Dynamics and functions of tight junctions. Trends Cell Biol. *20*, 142–149.

89. Weinbaum, S., Tarbell, J.M., and Damiano, E.R. (2007). The Structure and Function of the Endothelial Glycocalyx Layer. Annu. Rev. Biomed. Eng. *9*, 121–167.

90. Pomin, V.H., and Mulloy, B. (2018). Glycosaminoglycans and proteoglycans. Pharmaceuticals *11*, 1–9.

91. Lin, C.-Y., Kolliopoulos, C., Huang, C.-H., Tenhunen, J., Heldin, C.-H., Chen, Y.-H., and Heldin, P. (2019). High levels of serum hyaluronan is an early predictor of dengue warning signs and perturbs vascular integrity. EBioMedicine *48*, 425–441.

92. Tang, T.H.-C., Alonso, S., Ng, L.F.-P., Thein, T.-L., Pang, V.J.-X., Leo, Y.-S., Lye, D.C.-B., and Yeo, T.-W. (2017). Increased Serum Hyaluronic Acid and Heparan Sulfate in Dengue Fever: Association with Plasma Leakage and Disease Severity. Sci. Rep. *7*, 46191.

93. Honsawek, S., Kongtawelert, P., Pothacharoen, P., Khongphatthanayothin, A., Chongsrisawat, V., and Poovorawan, Y. (2007). Increased levels of serum hyaluronan in patients with dengue infection. J. Infect. *54*, 225–229.

94. Suwarto, S., Sasmono, R.T., Sinto, R., Ibrahim, E., and Suryamin, M. (2017). Association of endothelial glycocalyx and tight and adherens junctions with severity of plasma leakage in dengue infection. J. Infect. Dis. *215*, 992–999.

95. Buijsers, B., Garishah, F.M., Riswari, S.F., van Ast, R.M., Pramudo, S.G., Tunjungputri, R.N., Overheul, G.J., van Rij, R.P., van der Ven, A., Alisjahbana, B., *et al.* (2021). Increased Plasma Heparanase Activity and Endothelial Glycocalyx Degradation in Dengue Patients Is Associated With Plasma Leakage. Front. Immunol. *12*, 1–12.

96. Espinosa, D.A., Beatty, P.R., Puerta-Guardo, H., Islam, M.N., Belisle, J.T., Perera, R., and Harris, E. (2019). Increased serum sialic acid is associated with morbidity and mortality in a murine

model of dengue disease. J. Gen. Virol. *100*, 1515–1522.

97. Paranavitane, S.A., Gomes, L., Kamaladasa, A., Adikari, T.N., Wickramasinghe, N., Jeewandara, C., Shyamali, N.L.A., Ogg, G.S., and Malavige, G.N. (2014). Dengue NS1 antigen as a marker of severe clinical disease. BMC Infect. Dis. *14*, 570.

98. Libraty, D.H., Young, P.R., Pickering, D., Endy, T.P., Kalayanarooj, S., Green, S., Vaughn, D.W., Nisalak, A., Ennis, F.A., and Rothman, A.L. (2002). High Circulating Levels of the Dengue Virus Non-structural Protein NS1 Early in Dengue Illness Correlate with the Development of Dengue Hemorrhagic Fever. J. Infect. Dis. *186*, 1165–1168.

99. Muller, D.A., Depelsenaire, A.C.I., and Young, P.R. (2017). Clinical and Laboratory Diagnosis of Dengue Virus Infection. J. Infect. Dis. *215*, S89–S95.

100. Young, P.R., Hilditch, P.A., Bletchly, C., and Halloran, W. (2000). An Antigen Capture Enzyme-Linked Immunosorbent Assay Reveals High Levels of the Dengue Virus Protein NS1 in the Sera of Infected Patients. J. Clin. Microbiol. *38*, 1053–1057.

101. Flamand, M., Megret, F., Mathieu, M., Lepault, J., Rey, F.A., and Deubel, V. (1999). Dengue Virus Type 1 Non-structural Glycoprotein NS1 Is Secreted from Mammalian Cells as a Soluble Hexamer in a Glycosylation-Dependent Fashion. J. Virol. *73*, 6104–6110.

102. Edeling, M.A., Diamond, M.S., and Fremont, D.H. (2014). Structural basis of Flavivirus NS1 assembly and antibody recognition. Proc. Natl. Acad. Sci. *111*, 4285–4290.

103. Akey, D.L., Brown, W.C., Jose, J., Kuhn, R.J., and Smith, J.L. (2015). Structure-guided insights on the role of NS1 in flavivirus infection. BioEssays *37*, 489–494.

104. Scaturro, P., Cortese, M., Chatel-Chaix, L., Fischl, W., and Bartenschlager, R. (2015). Dengue Virus Non-structural Protein 1 Modulates Infectious Particle Production via Interaction with the Structural Proteins. PLoS Pathog. *11*, e1005277.

105. Płaszczyca, A., Scaturro, P., Neufeldt, C.J., Cortese, M., Cerikan, B., Ferla, S., Brancale, A., Pichlmair, A., and Bartenschlager, R. (2019). A novel interaction between dengue virus non-structural protein 1 and the NS4A-2K-4B precursor is required for viral RNA replication but not for formation of the membranous replication organelle. PLoS Pathog. *15*, e1007736.

106. Hackett, B.A., and Cherry, S. (2018). Flavivirus internalization is regulated by a size-dependent endocytic pathway. Proc. Natl. Acad. Sci. *115*, 4246–4251.

107. Gutsche, I., Coulibaly, F., Voss, J.E., Salmon, J., D'Alayer, J., Ermonval, M., Larquet, E., Charneau, P., Krey, T., Mégret, F., *et al.* (2011). Secreted dengue virus non-structural protein NS1 is an atypical barrel-shaped high-density lipoprotein. Proc. Natl. Acad. Sci. *108*, 8003–8008.

108. Muller, D.A., and Young, P.R. (2013). The flavivirus NS1 protein: Molecular and structural biology, immunology, role inpathogenesis and application asadiagnostic biomarker. Antiviral Res. *98*, 192–208.

109. Winkler, G., Maxwell, S., Ruemmler, C., and Stollar, V. (1989). Newly synthesized dengue-2 virus non-structural protein NS1 is a soluble protein but becomes partially hydrophobic and membrane-associated after dimerization. Virology *171*, 302–305.

110. Benfrid, S., Park, K., Dellarole, M., Voss, J.E., Tamietti, C., Pehau-Arnaudet, G., Raynal, B., Brûlé, S., England, P., Zhang, X., *et al.* (2022). Dengue virus NS1 protein conveys pro-inflammatory signals by docking onto high-density lipoproteins. EMBO Rep., 1–14.

111. Tamura, T., Torii, S., Kajiwara, K., Anzai, I., Fujioka, Y., Noda, K., Taguwa, S., Morioka, Y., Suzuki, R., Fauzyah, Y., *et al.* (2022). Secretory glycoprotein NS1 plays a crucial role in the particle formation of flaviviruses. PLoS Pathog. *18*, e1010593.

112. Avirutnan, P., Fuchs, A., Hauhart, R.E., Somnuke, P., Youn, S., Diamond, M.S., and Atkinson, J.P. (2010). Antagonism of the complement component C4 by flavivirus non-structural protein NS1. J. Exp. Med. *207*, 793–806.

113. Chung, K.M., Liszewski, M.K., Nybakken, G., Davis, A.E., Townsend, R.R., Fremont, D.H., Atkinson, J.P., and Diamond, M.S. (2006). West Nile virus non-structural protein NS1 inhibits complement activation by binding the regulatory protein factor H. Proc. Natl. Acad. Sci. *103*, 19111–19116.

114. Pan, P., Li, G., Shen, M., Yu, Z., Ge, W., Lao, Z., Fan, Y., Chen, K., Ding, Z., Wang, W., *et al.* (2021). DENV NS1 and MMP-9 cooperate to induce vascular leakage by altering endothelial cell adhesion and tight junction. PLoS Pathog. *17*, 1–30.

115. Chen, H.R., Chao, C.H., Liu, C.C., Ho, T.S., Tsai, H.P., Perng, G.C., Lin, Y.S., Wang, J.R., and Yeh, T.M. (2018). Macrophage migration inhibitory factor is critical for dengue NS1-induced endothelial glycocalyx degradation and hyperpermeability. PLoS Pathog. *14*, e1007033.

116. Barbachano-Guerrero, A., Endy, T.P., and King, C.A. (2020). Dengue virus non-structural protein 1 activates the p38 MAPK pathway to decrease barrier integrity in primary human endothelial cells. J. Gen. Virol. *101*, 484–496.

117. Modhiran, N., Watterson, D., Blumenthal, A., Baxter, A.G., Young, P.R., and Stacey, K.J. (2017). Dengue virus NS1 protein activates immune cells via TLR4 but not TLR2 or TLR6. Immunol. Cell Biol. *95*, 491–495.

118. Chen, J., Ng, M.M.-L., and Chu, J.J.H. (2015). Activation of TLR2 and TLR6 by Dengue NS1 Protein and Its Implications in the Immunopathogenesis of Dengue Virus Infection. PLoS Pathog. *11*, e1005053.

119. Silva, T., Gomes, L., Jeewandara, C., Ogg, G.S., and Malavige, G.N. (2022). Dengue NS1 induces phospholipase A2 enzyme activity, prostaglandins, and inflammatory cytokines in monocytes. Antiviral Res. *202*, 105312.

120. Sung, P.-S., Huang, T.-F., and Hsieh, S.-L. (2019). Extracellular vesicles from CLEC2-activated platelets enhance dengue virus-induced lethality via CLEC5A/TLR2. Nat. Commun. *10*, 2402.

121. Riswari, S.F., Tunjungputri, R.N., Kullaya, V., Garishah, F.M., Utari, G.S.R., Farhanah, N., Overheul, G.J., Alisjahbana, B., Gasem, M.H., Urbanus, R.T., *et al.* (2019). Desialylation of platelets induced by Von Willebrand Factor is a novel mechanism of platelet clearance in dengue. PLoS Pathog. *15*, e1007500.

122. Hottz, E.D., Medeiros-de-Moraes, I.M., Vieira-de-Abreu, A., de Assis, E.F., Vals-de-Souza, R., Castro-Faria-Neto, H.C., Weyrich, A.S., Zimmerman, G.A., Bozza, F.A., and Bozza, P.T. (2014). Platelet Activation and Apoptosis Modulate Monocyte Inflammatory Responses in Dengue. J. Immunol. *193*, 1864–1872.

123. Chuang, Y.-C., Lin, J., Lin, Y.-S., Wang, S., and Yeh, T.-M. (2016). Dengue Virus Non-structural Protein 1–Induced Antibodies Cross-React with Human Plasminogen and Enhance Its Activation. J. Immunol. *196*, 1218–1226.

124. Liu, I.J., Chiu, C.Y., Chen, Y.C., and Wu, H.C. (2011). Molecular mimicry of human endothelial cell antigen by autoantibodies to non-structural protein 1 of dengue virus. J. Biol. Chem. *286*, 9726–9736.

125. Lai, Y.C., Chuang, Y.C., Liu, C.C., Ho, T.S., Lin, Y.S., Anderson, R., and Yeh, T.M. (2017). Antibodies Against Modified NS1 Wing Domain Peptide Protect Against Dengue Virus Infection. Sci. Rep. *7*, 69–75.

126. Coelho, D.R., Carneiro, P.H., Mendes-Monteiro, L., Conde, J.N., Andrade, I., Cao, T., Allonso, D., White-Dibiasio, M., Kuhn, R.J., and Mohana-Borges, R. (2021). ApoA1 Neutralizes Proinflammatory Effects of Dengue Virus NS1 Protein and Modulates Viral Immune Evasion. J. Virol. *95*, e01974-20.

127. Säemann, M.D., Poglitsch, M., Kopecky, C., Haidinger, M., Hörl, W.H., and Weichhart, T. (2010). The versatility of HDL: a crucial anti-inflammatory regulator. Eur. J. Clin. Invest. *40*, 1131–1143.

128. Birner-Gruenberger, R., Schittmayer, M., Holzer, M., and Marsche, G. (2014). Understanding high-density lipoprotein function in disease: Recent advances in proteomics unravel the complexity of its composition and biology. Prog. Lipid Res. *56*, 36–46.

129. Alcalá, A.C., Maravillas, J.L., Meza, D., Ramirez, O.T., Ludert, J.E., and Palomares, L.A. (2022). Dengue Virus NS1 Uses Scavenger Receptor B1 as a Cell Receptor in Cultured Cells. J. Virol. *96*, e01664-21.

130. Song, H., Qi, J., Haywood, J., Shi, Y., and Gao, G.F. (2016). Zika virus NS1 structure reveals diversity of electrostatic surfaces among flaviviruses. Nat. Struct. Mol. Biol. *23*, 456–458.

131. Xu, X., Song, H., Qi, J., Liu, Y., Wang, H., Su, C., Shi, Y., and Gao, G.F. (2016). Contribution of intertwined loop to membrane association revealed by Zika virus full-length NS1 structure. EMBO J. *35*, 2170–2178.

132. Liu, Y., Liu, J., Du, S., Shan, C., Nie, K., Zhang, R., Li, X.F., Zhang, R., Wang, T., Qin, C.F., *et al.* (2017). Evolutionary enhancement of Zika virus infectivity in Aedes aegypti mosquitoes. Nature *545*, 482–486.

133. Liu, J., Liu, Y., Nie, K., Du, S., Qiu, J., Pang, X., Wang, P., and Cheng, G. (2016). Flavivirus NS1 protein in infected host sera enhances viral acquisition by mosquitoes. Nat. Microbiol. *1*, 1–11.

134. Chung, K.M., and Diamond, M.S. (2008). Defining the levels of secreted non-structural protein NS1 after West Nile virus infection in cell culture and mice. J. Med. Virol. *80*, 547–556.

135. Jurado, K.A., Simoni, M.K., Tang, Z., Uraki, R., Hwang, J., Householder, S., Wu, M., Lindenbach, B.D., Abrahams, V.M., Guller, S., *et al.* (2016). Zika virus productively infects primary human placenta-specific macrophages. JCI Insight *1*, e88461.

136. Li, Y., Shi, S., Xia, F., Shan, C., Ha, Y., Zou, J., Adam, A., Zhang, M., Wang, T., Liu, H., *et al.* (2021). Zika virus induces neuronal and vascular degeneration in developing mouse retina. Acta Neuropathol. Commun. *9*, 97.

137. Bhardwaj, U., and Singh, S.K. (2021). Zika Virus NS1 Suppresses VE-Cadherin and Claudin-5 via hsa-miR-101-3p in Human Brain Microvascular Endothelial Cells. Mol. Neurobiol. *58*, 6290–6303.

138. Furnon, W., Fender, P., Confort, M., Desloire, S., Nangola, S., Kitidee, K., Leroux, C., Ratinier, M., Arnaud, F., Lecollinet, S., *et al.* (2019). Remodeling of the Actin Network Associated with the Non-Structural Protein 1 (NS1) of West Nile Virus and Formation of NS1-Containing Tunneling Nanotubes. Viruses *11*, 901.

139. Wessel, A.W., Dowd, K.A., Biering, S.B., Zhang, P., Edeling, M.A., Nelson, C.A., Funk, K.E., DeMaso, C.R., Klein, R.S., Smith, J.L., *et al.* (2021). Levels of Circulating NS1 Impact West Nile Virus Spread to the Brain. J. Virol. *95*, e00844-21.

140. Puerta-Guardo, H., Glasner, D.R., Espinosa, D.A., Biering, S.B., Patana, M., Ratnasiri, K., Wang, C., Beatty, P.R., and Harris, E. (2019). Flavivirus NS1 Triggers Tissue-Specific Vascular Endothelial Dysfunction Reflecting Disease Tropism. Cell Rep. *26*, 1598-1613.e8.

141. de Almeida, R.R., Paim, B., de Oliveira, S.A., Souza, A.S., Gomes, A.C.P., Escuissato, D.L., Zanetti, G., and Marchiori, E. (2017). Dengue Hemorrhagic Fever: A State-of-the-Art Review Focused in Pulmonary Involvement. Lung *195*, 389–395.

142. Wang, C., Puerta-Guardo, H., Biering, S.B., Glasner, D.R., Tran, E.B., Patana, M., Gomberg, T.A., Malvar, C., Lo, N.T.N., Espinosa, D.A., *et al.* (2019). Endocytosis of flavivirus NS1 is required for NS1-mediated endothelial hyperpermeability and is abolished by a single N-glycosylation site mutation. PLoS Pathog. *15*, e1007938.

143. Biering, S.B., Akey, D.L., Wong, M.P., Brown, W.C., Lo, N.T.N., Puerta-Guardo, H., Tramontini Gomes de Sousa, F., Wang, C., Konwerski, J.R., Espinosa, D.A., *et al.* (2021). Structural basis for antibody inhibition of flavivirus NS1–triggered endothelial dysfunction. Science *371*, 194–200.

144. Avirutnan, P., Zhang, L., Punyadee, N., Manuyakorn, A., Puttikhunt, C., Kasinrerk, W., Malasit, P., Atkinson, J.P., and Diamond, M.S. (2007). Secreted NS1 of dengue virus attaches to the surface of cells via interactions with heparan sulfate and chondroitin sulfate E. PLoS Pathog. *3*, 1798–1812.

145. Kim, S.Y., Koetzner, C.A., Payne, A.F., Nierode, G.J., Yu, Y., Wang, R., Barr, E., Dordick, J.S., Kramer, L.D., Zhang, F., *et al.* (2019). Glycosaminoglycan Compositional Analysis of Relevant Tissues in Zika Virus Pathogenesis and in Vitro Evaluation of Heparin as an Antiviral against Zika Virus Infection. Biochemistry *58*, 1155–1166.

146. Domínguez-Alemán, C.A., Sánchez-Vargas, L.A., Hernández-Flores, K.G., Torres-Zugaide, A.I., Reyes-Sandoval, A., Cedillo-Barrón, L., Remes-Ruiz, R., and Vivanco-Cid, H. (2021). Dengue Virus Induces the Expression and Release of Endocan from Endothelial Cells by an NS1–TLR4-Dependent Mechanism. Microorganisms *9*, 1305.

147. Carpio, K.L., and Barrett, A.D.T. (2021). Flavivirus ns1 and its potential in vaccine development. Vaccines *9*, 1–21.

148. Akey, D.L., Brown, W.C., Dutta, S., Konwerski, J., Jose, J., Jurkiw, T.J., DelProposto, J., Ogata, C.M., Skiniotis, G., Kuhn, R.J., *et al.* (2014). Flavivirus NS1 Structures Reveal Surfaces for Associations with Membranes and the Immune System. Science *343*, 881–885.

149. Brown, W.C., Akey, D.L., Konwerski, J.R., Tarrasch, J.T., Skiniotis, G., Kuhn, R.J., and Smith, J.L. (2016). Extended surface for membrane association in Zika virus NS1 structure. Nat. Struct. Mol. Biol. *23*, 865–867.

150. Somnuke, P., Hauhart, R.E., Atkinson, J.P., Diamond, M.S., and Avirutnan, P. (2011). N-linked glycosylation of dengue virus NS1 protein modulates secretion, cell-surface expression, hexamer stability, and interactions with human complement. Virology *413*, 253–264.

151. Shu, B., Ooi, J.S.G., Tan, A.W.K., Ng, T., Dejnirattisai, W., Mongkolsapaya, J., Fibriansah, G., Shi, J., Kostyuchenko, V.A., Screaton, G., *et al.* (2022). CryoEM structures of the multimeric secreted NS1 , a major factor for dengue hemorrhagic fever. bioRxiv, 1–36. doi:https://doi.org/10.1101/2022.04.04.487075

152. Liang, B., Chew, A., Ngoh, A.Q., Phoo, W.W., Chan, K.W.K., Lim, S.S., Jie, M., Weng, M.J.G., Watanabe, S., Choy, M.M., *et al.* (2022). Secreted dengue virus NS1 is predominantly dimeric and in complex with high-density lipoprotein Affiliations : bioRxiv, 1–14. doi:https://doi.org/10.1101/2022.04.06.487425

153. Hertz, T., Beatty, P.R., MacMillen, Z., Killingbeck, S.S., Wang, C., and Harris, E. (2017). Antibody Epitopes Identified in Critical Regions of Dengue Virus Non-structural 1 Protein in Mouse Vaccination and Natural Human Infections. J. Immunol. *198*, 4025–4035.

154. Modhiran, N., Song, H., Liu, L., Bletchly, C., Brillault, L., Amarilla, A.A., Xu, X., Qi, J., Chai, Y.,

Cheung, S.T.M., *et al.* (2021). A broadly protective antibody that targets the flavivirus NS1 protein. Science *371*, 190–194.

155. Kraivong, R., Traewachiwiphak, S., Nilchan, N., Tangthawornchaikul, N., Pornmun, N., Poraha, R., Sriruksa, K., Limpitikul, W., Avirutnan, P., Malasit, P., *et al.* (2022). Cross-reactive antibodies targeting surface-exposed non-structural protein 1 (NS1) of dengue virus-infected cells recognize epitopes on the spaghetti loop of the β-ladder domain. PLoS One *17*, e0266136.

156. FDA (2020). Dengvaxia. Available at: https://www.fda.gov/vaccines-blood-biologics/dengvaxia.

157. Zimmerman, M.G., Quicke, K.M., O'Neal, J.T., Arora, N., Machiah, D., Priyamvada, L., Kauffman, R.C., Register, E., Adekunle, O., Swieboda, D., *et al.* (2018). Cross-Reactive Dengue Virus Antibodies Augment Zika Virus Infection of Human Placental Macrophages. Cell Host Microbe *24*, 731-742.e6.

158. Espinosa, D.A., Beatty, P.R., Reiner, G.L., Sivick, K.E., Hix Glickman, L., Dubensky, T.W., and Harris, E. (2019). Cyclic Dinucleotide–Adjuvanted Dengue Virus Non-structural Protein 1 Induces Protective Antibody and T Cell Responses. J. Immunol. *202*, 1153–1162.

159. Lee, P.X., Ting, D.H.R., Boey, C.P.H., Tan, E.T.X., Chia, J.Z.H., Idris, F., Oo, Y., Ong, L.C., Chua, Y.L., Hapuarachchi, C., *et al.* (2020). Relative contribution of non-structural protein 1 in dengue pathogenesis. J. Exp. Med. *217*, e20191548.

160. Lin, C.-F., Lei, H.-Y., Shiau, A.-L., Liu, H.-S., Yeh, T.-M., Chen, S.-H., Liu, C.-C., Chiu, S.-C., and Lin, Y.-S. (2002). Endothelial Cell Apoptosis Induced by Antibodies Against Dengue Virus Non-structural Protein 1 Via Production of Nitric Oxide. J. Immunol. *169*, 657–664.

161. Lin, C.F., Lei, H.Y., Shiau, A.L., Liu, C.C., Liu, H.S., Yeh, T.M., Chen, S.H., and Lin, Y.S. (2003). Antibodies from dengue patient sera cross-react with endothelial cells and induce damage. J. Med. Virol. *69*, 82–90.

162. Lin, C.-F., Lei, H.-Y., Shiau, A.-L., Liu, H.-S., Yeh, T.-M., Chen, S.-H., Liu, C.-C., Chiu, S.-C., and Lin, Y.-S. (2014). Endothelial Cell Apoptosis Induced by Antibodies Against Dengue Virus Non-structural Protein 1 Via Production of Nitric Oxide. J. Immunol. *169*, 657–664.

163. Lin, Y.S., Yeh, T.M., Lin, C.F., Wan, S.W., Chuang, Y.C., Hsu, T.K., Liu, H.S., Liu, C.C., Anderson, R., and Lei, H.Y. (2011). Molecular mimicry between virus and host and its implications for dengue disease pathogenesis. Exp. Biol. Med. *236*, 515–523.

164. Chen, H.R., Lai, Y.C., and Yeh, T.M. (2018). Dengue virus non-structural protein 1: A pathogenic factor, therapeutic target, and vaccine candidate. J. Biomed. Sci. *25*, 1–11.

165. Wang, W.-H., Urbina, A.N., Lin, C.-Y., Yang, Z.-S., Assavalapsakul, W., Thitithanyanont, A., Lu, P.-L., Chen, Y.-H., and Wang, S.-F. (2021). Targets and strategies for vaccine development against dengue viruses. Biomed. Pharmacother. *144*, 112304.

166. Sharma, M., Glasner, D.R., Watkins, H., Puerta-Guardo, H., Kassa, Y., Egan, M.A., Dean, H., and Harris, E. (2020). Magnitude and Functionality of the NS1-Specific Antibody Response Elicited by a Live-Attenuated Tetravalent Dengue Vaccine Candidate. J. Infect. Dis. *221*, 867–877.

167. Rivera, L., Biswal, S., Sáez-Llorens, X., Reynales, H., López-Medina, E., Borja-Tabora, C., Bravo, L., Sirivichayakul, C., Kosalaraksa, P., Martinez Vargas, L., *et al.* (2021). Three-year Efficacy and Safety of Takeda's Dengue Vaccine Candidate (TAK-003). Clin. Infect. Dis.

168. López-Medina, E., Biswal, S., Saez-Llorens, X., Borja-Tabora, C., Bravo, L., Sirivichayakul, C., Vargas, L.M., Alera, M.T., Velásquez, H., Reynales, H., *et al.* (2022). Efficacy of a Dengue Vaccine Candidate (TAK-003) in Healthy Children and Adolescents 2 Years after Vaccination. J. Infect. Dis. *225*, 1521–1532.

169. Wan, S.-W., Chen, P.-W., Chen, C.-Y., Lai, Y.-C., Chu, Y.-T., Hung, C.-Y., Lee, H., Wu, H.F., Chuang, Y.-C., Lin, J., *et al.* (2017). Therapeutic Effects of Monoclonal Antibody against Dengue Virus NS1 in a STAT1 Knockout Mouse Model of Dengue Infection. J. Immunol. *199*, 2834–2844.

170. Krishna, V.D., Rangappa, M., and Satchidanandam, V. (2009). Virus-Specific Cytolytic Antibodies to Non-structural Protein 1 of Japanese Encephalitis Virus Effect Reduction of Virus Output from Infected Cells. J. Virol. *83*, 4766–4777.

171. Tien, S.-M., Chang, P.-C., Lai, Y.-C., Chuang, Y.-C., Tseng, C.-K., Kao, Y.-S., Huang, H.-J., Hsiao, Y.-P., Liu, Y.-L., Lin, H.-H., *et al.* (2022). Therapeutic efficacy of humanized monoclonal antibodies targeting dengue virus non-structural protein 1 in the mouse model. PLoS Pathog. *18*, e1010469.

172. Chang, J., Schul, W., Butters, T.D., Yip, A., Liu, B., Goh, A., Lakshminarayana, S.B., Alonzi, D., Reinkensmeier, G., Pan, X., *et al.* (2011). Combination of α-glucosidase inhibitor and ribavirin for the treatment of dengue virus infection in vitro and in vivo. Antiviral Res. *89*, 26–34.

173. Qu, X., Pan, X., Weidner, J., Yu, W., Alonzi, D., Xu, X., Butters, T., Block, T., Guo, J.T., and Chang, J. (2011). Inhibitors of endoplasmic reticulum α-glucosidases potently suppress hepatitis C virus virion assembly and release. Antimicrob. Agents Chemother. *55*, 1036–1044.

174. Wu, S.-F., Lee, C.-J., Liao, C.-L., Dwek, R.A., Zitzmann, N., and Lin, Y.-L. (2002). Antiviral Effects of an Iminosugar Derivative on Flavivirus Infections. J. Virol. *76*, 3596–3604.

175. Block, T.M., and Jordan, R. (2001). Iminosugars as possible broad spectrum anti hepatitis virus agents: The glucovirs and alkovirs. Antivir. Chem. Chemother. *12*, 317–325.

176. Perry, S.T., Buck, M.D., Plummer, E.M., Penmasta, R.A., Batra, H., Stavale, E.J., Warfield, K.L., Dwek, R.A., Butters, T.D., Alonzi, D.S., *et al.* (2013). An iminosugar with potent inhibition of dengue virus infection in vivo. Antiviral Res. *98*, 35–43.

177. Plummer, E., Buck, M.D., Sanchez, M., Greenbaum, J.A., Turner, J., Grewal, R., Klose, B., Sampath, A., Warfield, K.L., Peters, B., *et al.* (2015). Dengue Virus Evolution under a Host-Targeted Antiviral. J. Virol. *89*, 5592–5601.

178. Warfield, K.L., Plummer, E.M., Sayce, A.C., Alonzi, D.S., Tang, W., Tyrrell, B.E., Hill, M.L., Caputo, A.T., Killingbeck, S.S., Beatty, P.R., *et al.* (2016). Inhibition of endoplasmic reticulum glucosidases is required for in vitro and in vivo dengue antiviral activity by the iminosugar UV-4. Antiviral Res. *129*, 93–98.

179. Franco, E.J., Warfield, K.L., and Brown, A.N. (2022). UV-4B potently inhibits replication of multiple SARS-CoV-2 strains in clinically relevant human cell lines. Front. Biosci. *27*, 1.

180. National Library of Medicine (USA) (2020). Safety and Pharmacokinetics of UV-4B Solution Administered Orally as Multiple Ascending Doses to Healthy Subjects. Clin. Identifier NCT02696291.

Chapter 2

Molecular Determinants of Tissue Specificity of Flavivirus Non-structural Protein 1 Interaction with Endothelial Cells

This chapter was submitted as:

Lo, N.T.N. (羅子甯), Roodsari, S.Z., Tin, N.L., Wong, M.P., Biering, S.B., and Harris, E. (2022). Molecular Determinants of Tissue Specificity of Flavivirus Non-structural Protein 1 Interaction with Endothelial Cells. *J. Virol*. doi**:** https://doi.org/10.1101/2022.04.28.489972

Abstract

Members of the mosquito-borne flavivirus genus such as dengue (DENV), West Nile (WNV), and Zika (ZIKV) viruses cause distinct diseases and affect different tissues. We previously found that the secreted flaviviral non-structural protein 1 (NS1) interacts with endothelial cells and disrupts endothelial barrier function in a tissue-specific manner consistent with the disease tropism of the respective viruses. However, the underlying molecular mechanism of this tissue-specific NS1-endothelial cell interaction is not well understood. To elucidate the distinct role(s) that the wing and β-ladder domains of NS1 play in NS1 interactions with endothelial cells, we constructed flavivirus NS1 chimeras that exchanged the wing and β-ladder domains in a pair-wise manner between DENV, WNV, and ZIKV NS1. We found that both the NS1 wing and β-ladder domains conferred NS1 tissue-specific endothelial dysfunction, with the wing conferring cell binding and the β-ladder involved in inducing endothelial hyperpermeability as measured by trans-endothelial electrical resistance assay. To narrow down the amino acids dictating cell binding specificity, we utilized the DENV-WNV NS1 chimera and identified residues 91 to 93 (GDI) of DENV NS1 as a molecular motif determining binding specificity. Further, using an *in vivo* mouse model of localized leak, we found that the GDI motif of the wing domain was essential for triggering DENV NS1-induced vascular leak in mouse dermis. Taken together, we identify molecular determinants of flavivirus NS1 that confer NS1 binding and vascular leak and highlight the importance of the NS1 wing domain for flavivirus pathogenesis.

Importance

Flavivirus non-structural protein 1 (NS1) is secreted into the bloodstream from infected cells during a viral infection. Dengue virus NS1 contributes to severe dengue pathology such as endothelial dysfunction and vascular leak independently of the virus. We have shown that multiple flavivirus NS1 proteins result in endothelial dysfunction in a tissue-specific manner consistent with their respective viral tropism. Here, we aimed to identify the molecular determinants that make some, but not other, flavivirus NS1 proteins bind to select endothelial cells in vitro and cause vascular leak in a mouse model. We identified the wing domain of NS1 as a primary determinant conferring differential endothelial dysfunction and vascular leak and narrowed the contributing amino acid residues to a three-residue motif within the wing domain. The insights from this study pave the way for future studies on the effects of flavivirus NS1 on viral dissemination and pathogenesis and offer potential new avenues for antiviral therapies.

Introduction

Dengue virus (DENV) is a mosquito-borne positive-stranded RNA virus of the *Flavivirus* genus, consisting of four serotypes (DENV1-4). DENV causes ~100 million symptomatic infections per year globally, ranging from classic dengue fever to the more severe dengue haemorrhagic fever and dengue shock syndrome [1–3]. The severe forms of dengue are characterized by clinical presentation of vascular leak as a result of endothelial dysfunction [4]. Traditionally, endothelial dysfunction has been attributed to a hyperactivated immune response as a result of uncontrolled viral infection and immune cell activation [5,6]. Recently, we and others have demonstrated that the secreted non-structural protein 1 (NS1) directly contributes to endothelial dysfunction and vascular leak through interactions with endothelial and immune cells that result in the breakdown of endothelial barriers such as the endothelial glycocalyx and intercellular junctions [7–14]. In addition to DENV, West Nile (WNV) and Zika (ZIKV) viruses are also members of the *Flavivirus* genus that cause human diseases of public health significance. Like DENV NS1, the NS1 proteins of WNV and ZIKV have also been shown to modulate endothelial barriers. WNV NS1 also has been shown to contribute to WNV infection in the brain [15], while ZIKV NS1 has been shown to modulate the barrier integrity of placental explants [11] as well as the testis, contributing to ZIKV infection of Sertoli cells [10,16].

NS1 is a ~55-kDa glycoprotein that is highly conserved across the flaviviruses [17]. It dimerizes in the endoplasmic reticulum and is found as a component of the viral replication complex. The dimers can also trimerize to form hexamers that are secreted by DENV-infected cells into the bloodstream as a soluble lipoprotein containing lipid cargo [18–20]. In severe dengue patients, the levels of detectable NS1 in the blood are generally reported as 1-10 μg/mL [21,22]. Secreted NS1 has been shown to associate with components of the innate immune system such as toll-like receptors [13,23] and complement proteins [24–26], as well as components of the blood-clotting cascade such as platelets [27–29], which results in both host immune evasion and modulation of barrier integrity of endothelial cells. Separately, NS1 can also directly disrupt endothelial cell barrier integrity by promoting the degradation of endothelial glycocalyx components that line the surface of endothelial cells [7,8,30,31] and disrupting junctional proteins that mediate cell-cell interactions [9,32,33]. In mouse models, NS1 vaccination has been shown to be protective against lethal DENV challenge. Conversely, addition of NS1 to sub-lethal DENV infection was shown to exacerbate pathology resulting in a lethal infection, suggesting the potential of NS1 as a vaccine component and therapeutic target [7].

NS1 proteins from multiple flaviviruses have been shown to interact with endothelial cells of distinct tissue origin in a manner consistent with the tropism of their respective flaviviruses [34]. For example, DENV NS1 interacts with multiple cell lines including human pulmonary microvascular endothelial cells (HPMEC), which correlates with the systemic nature of DENV infection that can be observed in the lungs. In contrast, WNV NS1 interacts well with brain endothelial cells but minimally with HPMEC, as WNV causes neurological pathologies, such as meningitis and encephalitis, but not pulmonary pathology. Similarly, ZIKV NS1 interacts well with both brain and umbilical vein endothelial cells but minimally with HPMEC, as ZIKV causes neurological and congenital but not pulmonary pathologies. However, how these tissue-specific NS1 interactions are modulated remains unclear.

Flavivirus NS1 contains three domains that are highly conserved: the β-roll (residues 1–29), wing (residues 30–180), and β-ladder (residues 181–352) [35]. The NS1 wing domain contains many hydrophobic residues that are predicted to interact with the cell's plasma membrane and lipid cargo in its hexameric form [36,37]. Interestingly, these surface-exposed residues are

conserved among DENV serotypes but divergent across the *Flavivirus* genus (e.g., between DENV and WNV), suggesting their possible roles in mediating NS1 tissue-specific interactions. Additionally, prior studies have suggested that the three domains of NS1 may have distinct functions. DENV NS1 wing domain has been shown to be immunodominant in both humans and mice [7,38,39], where conserved, hydrophobic residues in the flexible loop (residues 108–129) within the wing domain (Trp-115, Trp-118, Gly-119) have been identified to partially contribute to DENV NS1 binding to HPMEC [36,40]. In contrast, select residues in the β-ladder domain (such as residues N207, A303, E326, and D327) have been implicated as important for NS1-induced endothelial hyperpermeability, while being dispensable for binding endothelial cells [32,40]. While these data offer clues about NS1 molecular determinants of tissue-specific interactions with endothelial cells, a systematic investigation of these different domains in distinct flavivirus NS1 proteins has not been undertaken.

In this study, we provide new insights on the tissue-specific interactions between flavivirus NS1 and endothelial cells using NS1 chimeras that exchange the wing and β-ladder domains of DENV, WNV, and ZIKV in a pair-wise manner with one another. We found that both the wing and β-ladder domains confer tissue-specific barrier dysfunction, with the wing influencing initial attachment to endothelial cells and the β-ladder involved in inducing endothelial hyperpermeability *in vitro*. We further identified a variable 3-amino acid (aa) motif in the wing domain as a molecular determinant for tissue specificity. Finally, we identify the wing domain and the 3-aa motif as a driver of DENV-triggered vascular leak *in vivo*. Taken together, our results provide insights into the tissue-specific interactions of flavivirus NS1.

Results

The wing domain of flavivirus NS1 confers tissue-specific binding to endothelial cells

In previous work, we showed that DENV NS1 binds to human lung endothelial cells (HPMEC) at higher levels than WNV and ZIKV NS1 [34], correlating with the capacity of DENV NS1 but not WNV or ZIKV NS1 to cause endothelial hyperpermeability of HPMEC and pleural effusion in humans. Similarly, DENV and ZIKV NS1 exhibited higher binding than WNV NS1 to human umbilical vein microvascular endothelial cells (HUVEC) and caused endothelial hyperpermeability of HUVEC [34]. To uncover the molecular determinants of flavivirus NS1 that dictate this tissue-specific endothelial cell tropism, we generated chimeric NS1 proteins that exchanged either the wing or the β-ladder domains between DENV and WNV NS1 (Fig. 1A). We cloned and expressed the C-terminally His-tagged NS1 proteins in HEK-293 cells, which were successfully secreted, and then purified NS1 oligomers using cobalt affinity chromatography (Fig. 2). Chimeric proteins are annotated by their 3 domains from the respective flavivirus NS1 proteins in sequence "β-roll–wing–β-ladder" (e.g., D-D-W designating DENV β-roll – DENV wing – WNV β-ladder). We treated HPMEC with either wild-type (WT) or DENV-WNV chimeric NS1 proteins and measured the levels of NS1 binding to HPMEC using an immunofluorescence microscopy assay (IFA). We found that the chimeric NS1 constructs containing DENV NS1 wing domain (D-**D**-W and W-**D**-W) bound to HPMEC at comparable levels to WT DENV NS1, whereas the constructs containing WNV NS1 wing (W-**W**-D and D-**W**-D) exhibited significantly lower binding than WT DENV NS1, but at comparable levels to WT WNV NS1 (Fig. 1B and C). A similar pattern was observed when we treated HUVEC with the same DENV-WNV chimeric NS1 proteins, where constructs containing the DENV NS1 wing domain drove binding to HUVEC at comparable levels as WT DENV NS1 (Fig. 1D and E).

To investigate whether the wing domain of other flaviviruses conferred NS1 binding to endothelial cells, we constructed similar chimeric NS1 proteins that exchanged the wing and β-ladder domains between WNV and ZIKV NS1 and DENV and ZIKV NS1, respectively (Fig. 3A and D). We treated HUVEC with WNV-ZIKV chimeric NS1 and found that constructs containing the ZIKV NS1 wing domain (Z-**Z**-W and W-**Z**-W) bound to HUVEC at comparable levels to WT ZIKV NS1, whereas the constructs containing the WNV NS1 wing (W-**W**-Z and Z-**W**-Z) bound to HUVEC at lower levels, consistent with WT WNV NS1 (Fig. 3B and C). We subsequently treated HPMEC with DENV-ZIKV chimeric NS1 and found that while constructs with ZIKV NS1 wing (Z-**Z**-D and D-**Z**-D) exhibited significantly diminished binding to HPMEC, the constructs with DENV NS1 wing (D-**D**-Z and Z-**D**-Z) did not gain binding to HPMEC comparably to WT DENV NS1 (Fig. 3E and F), possibly due to differential effects of interdomain interactions between flaviviruses. Overall, these results indicate that the tissue-specific patterns of flavivirus NS1 binding to endothelial cells are driven by the wing domain of NS1.

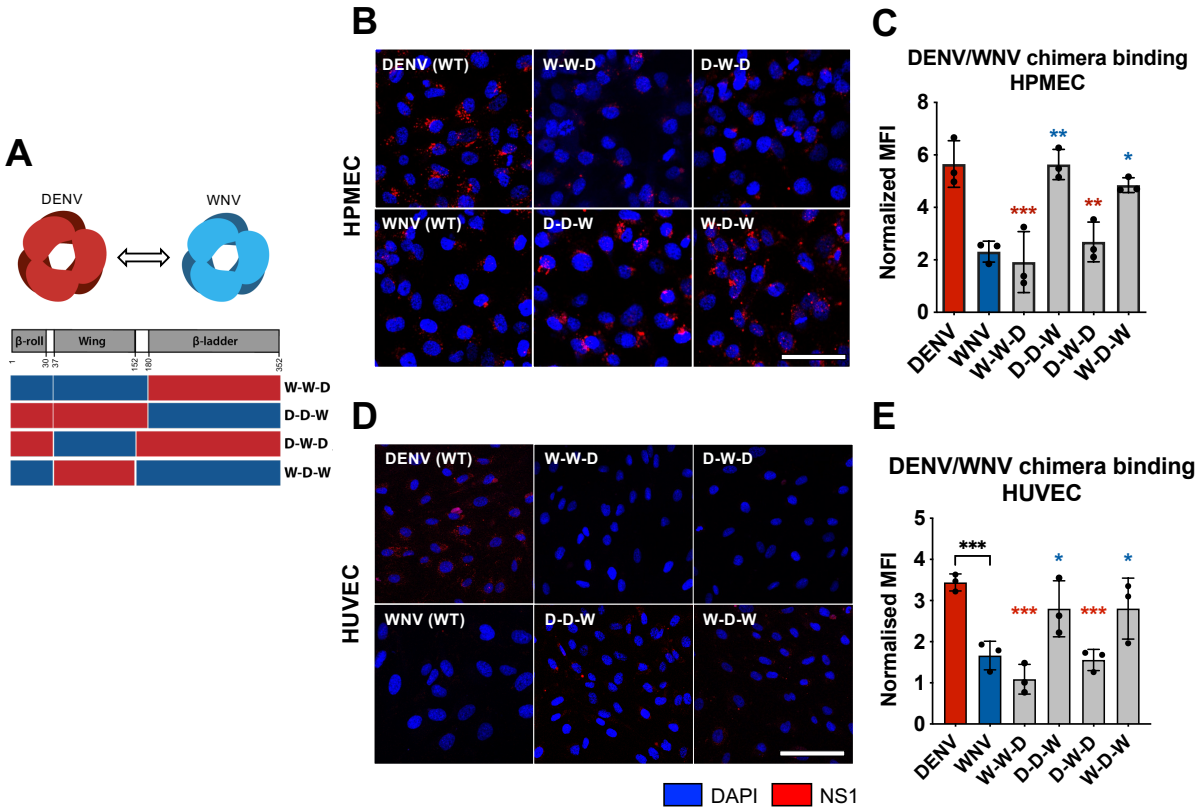

Figure 1. The wing domain of DENV NS1 confers tissue-specific binding to endothelial cells.
(A) Schematic representation of chimeric NS1 proteins that exchange wing or β-ladder domains between DENV and WNV NS1. Red box represents DENV NS1, and blue box represents WNV NS1. **(B)** Recombinant WT or chimeric NS1 (10 µg/mL) was added to HPMEC and incubated at 37ºC for 1 hour. NS1 binding was assessed by immunofluorescence microscopy, and representative images from three experiments are shown. **(C)** Quantification of (B), normalized to untreated controls. **(D)** NS1 binding as in (B), but on HUVEC. **(E)** Quantification of (D), normalized to untreated controls. MFI, mean fluorescence intensity. Images represent 3 independent experiments. Scale bars, 100µm. Data plotted as mean ± standard deviation (SD). *p<0.05, **p<0.01, ***p<0.005, ****p<0.001 by one-way ANOVA with multiple comparisons. Star colors indicate the respective control to which each construct was compared.

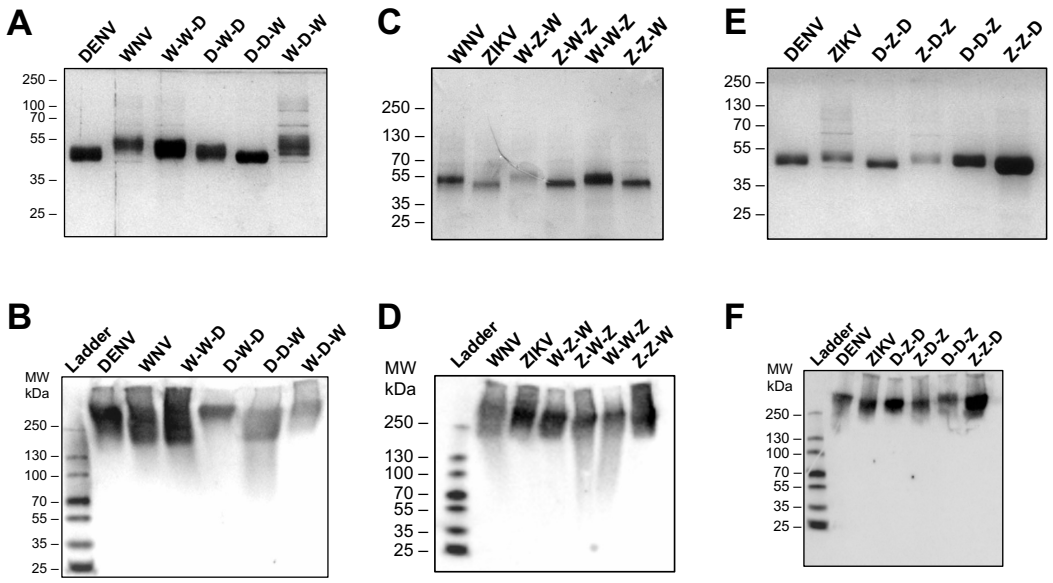

Figure 2. Production and quality control of flavivirus NS1 chimeric constructs.
Proteins were evaluated by silver stain following SDS-PAGE (A, C, E) and native PAGE (B, D, F). 2 µg of each NS1 construct was used. For native gels, proteins were detected using anti-His mAb. **(A)** Silver stain of DENV-WNV NS1 chimeras. **(B)** Native PAGE of DENV-WNV NS1 chimeras. **(C)** Silver stain of WNV-ZIKV NS1 chimeras. **(D)** Native PAGE of WNV-ZIKV NS1 chimeras. **(E)** Silver stain of DENV-ZIKV NS1 chimeras. **(F)** Native PAGE of DENV-ZIKV NS1 chimeras.

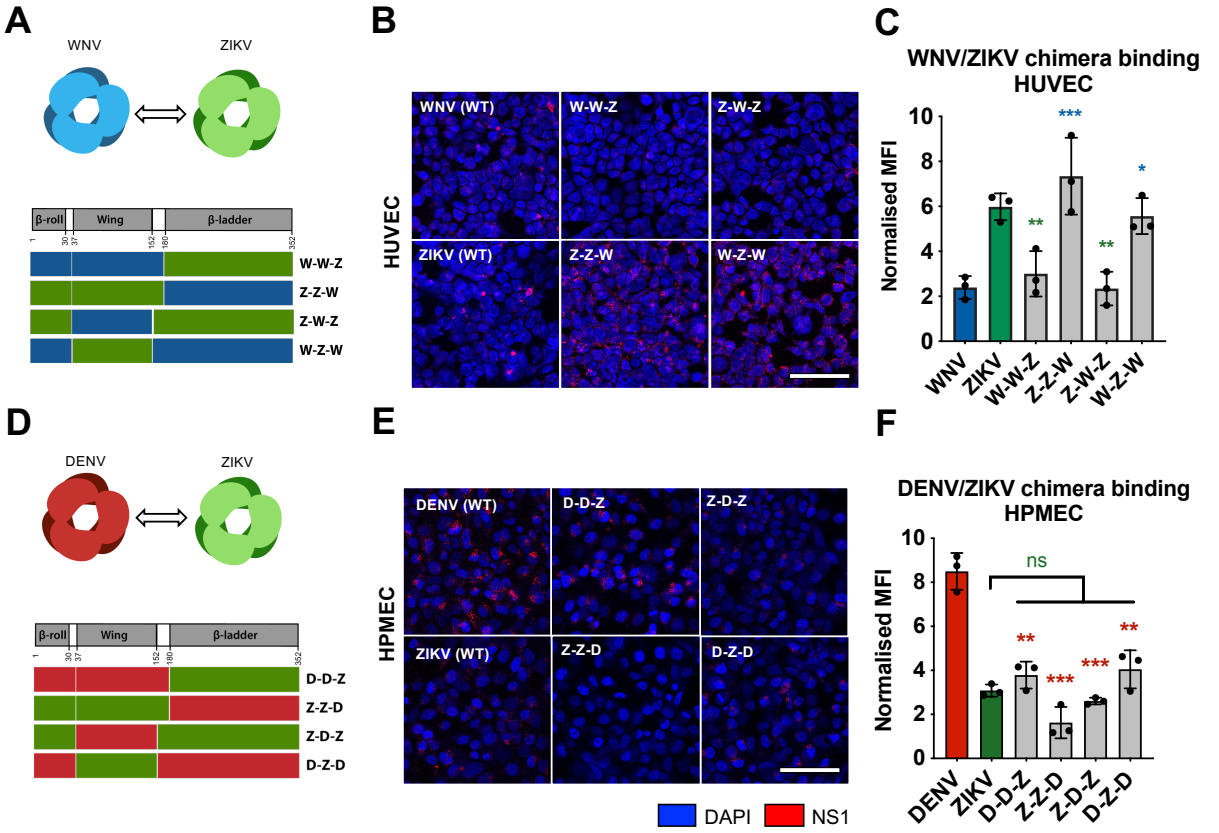

Figure 3. The wing domain of flavivirus NS1 confers tissue-specific binding to endothelial cells. **(A, D)** Schematic representation of chimeric NS1 proteins produced with WNV and ZIKV NS1 (A) or DENV and ZIKV NS1 (D). Red box represents DENV NS1, blue box represents WNV NS1, and green box represents ZIKV NS1. **(B)** Recombinant WT or WNV-ZIKV chimeric NS1 (10 µg/mL) was added to HUVEC and incubated at 37ºC for 1 hour. NS1 binding was assessed by immunofluorescence microscopy, and representative images from three experiments are shown. **(C)** Quantification of (B), normalized to untreated controls. **(E)** NS1 binding as in (B), but with DENV-ZIKV chimeric NS1 to HPMEC. **(F)** Quantification of (E), normalized to untreated controls. MFI, mean fluorescence intensity. Images represent 3 independent experiments. Scale bars, 100 µm. Data plotted as mean ± SD. *p<0.05, **p<0.01, ***p<0.005, ****p<0.001 by one-way ANOVA with multiple comparisons. Star colors indicate the respective control to which each construct was compared.

The wing and β-ladder domains of flavivirus NS1 proteins are necessary for inducing endothelial hyperpermeability

Following binding to endothelial cells, DENV NS1 is taken up by cells via clathrin-mediated endocytosis, trafficks to endosomes, and activates enzymes that degrade the endothelial glycocalyx and disrupt intercellular junctional complexes [8,11,14,30,32]. This results in disruption of endothelial barrier integrity, making endothelial cells hyperpermeable to solutes and fluids. We have previously shown that DENV NS1 can cause endothelial barrier dysfunction by inducing endothelial hyperpermeability independently of the virus [7,8,30]. Given this finding, we next explored whether the NS1 wing domain that conferred DENV NS1 binding to HPMEC was also responsible for causing HPMEC hyperpermeability. To investigate how different flavivirus NS1 domains influence the capacity of NS1 to trigger endothelial hyperpermeability, we utilized the DENV-WNV NS1 chimeras in a trans-endothelial electrical resistance (TEER) assay. We treated HPMEC seeded in the apical chamber of a Transwell with either WT or chimeric NS1 (2.5 μg/ml) and measured the TEER values between the apical and the basolateral chambers of the Transwell (Fig. 4A and B). Consistent with previous observations [34], WT DENV NS1 resulted in significantly greater TEER reduction of HPMEC than WNV NS1, indicating greater endothelial barrier hyperpermeability. Interestingly, the constructs containing either the DENV wing or β-ladder domain (D-**D**-W, W-**D**-W, W-W-**D**, D-W-**D**) were unable to cause TEER reduction to the same extent as WT DENV NS1, indicating that while the wing domain confers cell binding, both the DENV wing and the DENV β-ladder domains are required for NS1 to trigger endothelial hyperpermeability of HPMEC.

Since we have previously observed that NS1 triggers endothelial hyperpermeability in a dose-dependent manner [8,9], we tested whether our chimeric NS1 proteins would trigger endothelial hyperpermeability when cells were treated with a higher concentration. We repeated the TEER experiments using 5 and 10 μg/mL of our NS1 proteins (Fig. 4C to F), and observed that at both concentrations, the constructs containing the DENV NS1 β-ladder (W-W-**D** and D-W-**D**) caused a decrease in TEER on HPMEC comparably to WT DENV NS1, whereas the constructs containing the WNV β-ladder domain (D-D-**W** and W-D-**W**) did not cause endothelial hyperpermeability, similar to WT WNV NS1. This implicates a role for the DENV β-ladder in inducing endothelial hyperpermeability as measured by TEER, consistent with our previous findings [32,40].

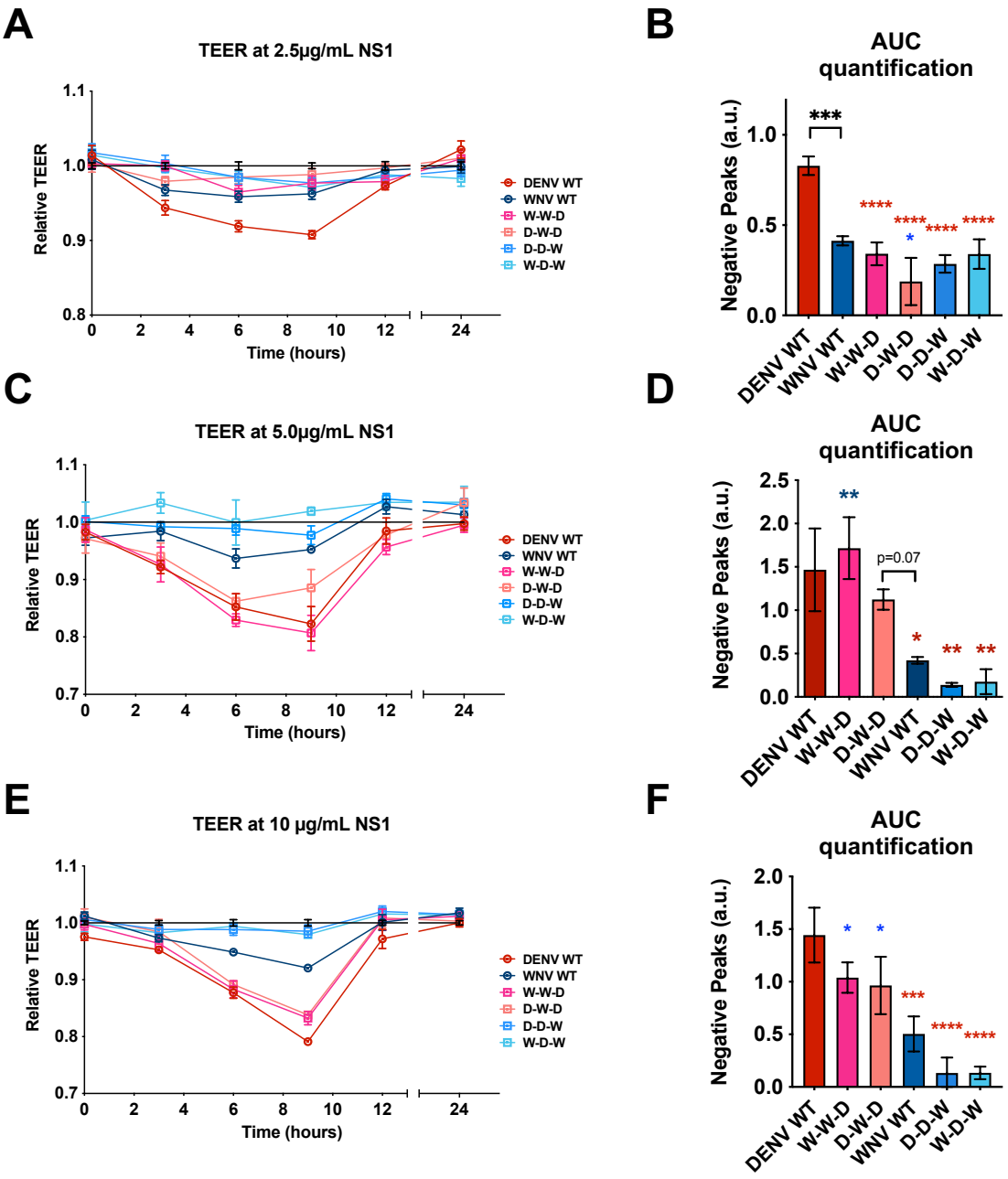

Figure 4. The wing and β-ladder domains of flavivirus NS1 are necessary for inducing endothelial cell hyperpermeability.

(A) HPMEC monolayer was seeded in the apical chambers of 24-well Transwell inserts and treated with either WT or chimeric NS1 proteins at 2.5 µg/mL. The trans-endothelial electrical resistance (TEER) between the apical and basolateral chamber were measured over time and normalized to the untreated controls at each respective timepoint. **(B)** Quantification of the area between the curve and Y=1.0 in (A) ("area under curve"), correlating to a decrease in electrical resistance and an increase in permeability. **(C, E)** Endothelial hyperpermeability (TEER) assay as in (A), but with the indicated NS1 protein at (C) 5 and (E) 10 µg/mL, respectively. **(D, F)** Area of the curve of (C) and (E), respectively. AUC, area under the curve. a.u., arbitrary units. Data represent at least n=3 biological replicates, plotted as mean ± standard error of the mean (SEM). *p<0.05, **p<0.01, ***p<0.005, ****p<0.001 by one-way ANOVA with multiple comparisons. Star colors indicate the respective control to which each construct was compared.

A 3-amino acid motif in the wing domain of DENV NS1 confers endothelial cell binding specificity between DENV and WNV NS1

While NS1 is highly conserved across the *Flavivirus* genus [41], regions of variability can be found within the wing domain, specifically between amino acid (aa) residues 90 and 120 (Fig. 5A). We have previously identified the same stretch of residues within the NS1 wing domain to be immunodominant, eliciting robust antibody responses in DENV2-infected mice and natural human infections [38]. Multiple structural studies have reported a flexible loop structure located near residues 90-120 that is thought to be critical for endothelial cell binding, given its exposure on the surface of dimeric NS1 and its predicted proximity to cell membranes [36,42]. This suggests a functional importance that could explain the tissue-specificity of flavivirus NS1. As such, we hypothesized that amino acids within residues 90 to 120 of the wing domain confer tissue-specific endothelial binding.

To test this hypothesis, we aligned the DENV and WNV NS1 sequences to identify differentially conserved residues that were predicted to be surface-exposed, reasoning that these divergent residues may dictate tissue specificity of NS1 [36,42]. We identified five sites of 3-4aa between residues 90 and 120 that contained divergent residues across flaviviruses, but were conserved within each flavivirus (Fig. 5A). To test the involvement of these residues in the differential DENV-WNV NS1 cell binding phenotype, we generated 5 pairs of site-specific mutants that exchanged these motifs between DENV and WNV NS1 (Figs. 5 and 6). We then treated HPMEC with either WT NS1 or site-specific NS1 mutants and measured the levels of NS1 binding to HPMEC by IFA (Fig. 5B). Interestingly, we found that while 4 pairs retained the binding pattern of their parental NS1 protein, one pair exhibited the opposite pattern. WNV NS1 containing DENV2 residues 91-93 (WNV-GDI) gained the capacity to bind to HPMEC at comparable levels to WT DENV NS1, whereas the DENV NS1 containing residues 91-93 from WNV NS1 (DENV-EKQ) had reduced capacity to bind to HPMEC, exhibiting levels similar to WT WNV NS1 (Fig. 5B and C). These results suggest that residues 91-93 of DENV NS1 form a motif that contributes to the DENV-WNV tissue-specific endothelial cell binding pattern we observe.

To determine if residues 91-93 conferring NS1 cell binding specificity between DENV-WNV also dictate the capacity of DENV-WNV NS1 to trigger endothelial hyperpermeability, we conducted a TEER assay on HPMEC with NS1 mutants swapped at residues 91-93 and 101-103 for comparison (Fig. 5D). Similar to our observations above, at low NS1 levels (2.5 μg/mL), only WT DENV NS1 was able to induce endothelial hyperpermeability, in contrast to WT WNV and mutants from the DENV-WNV 91-93 and 101-103 swaps that did not noticeably alter permeability, suggesting that while the residues in the wing domain are important for inducing endothelial hyperpermeability, they alone are not sufficient.

We next repeated the TEER experiments at 5 μg/mL to confirm if the wing deficiency phenotype of DENV NS1 could be overcome by utilization of a higher dose of NS1 (Fig. 5E). WT DENV NS1 and NS1 constructs containing WNV motifs of either residues 91-93 and 101-103 (both containing DENV β-ladder) were able to trigger endothelial hyperpermeability, whereas WT WNV NS1 caused less TEER decrease, and WNV NS1 constructs containing DENV NS1 motifs of both residues 91-93 and 101-103 (both containing WNV β-ladder) remained unable to cause TEER decrease. Together, these results are consistent with the previous TEER data involving NS1 domain chimeras (Fig. 4), where at the higher NS1 concentrations of 5 and 10 μg/mL, only the constructs containing DENV β-ladder triggered endothelial hyperpermeability. Using a published

DENV2 NS1 structure at 2.89Å resolution [40], we highlight the location and orientation of the GDI motif (Fig. 5F and G), indicating its predicted interaction with the plasma membrane.

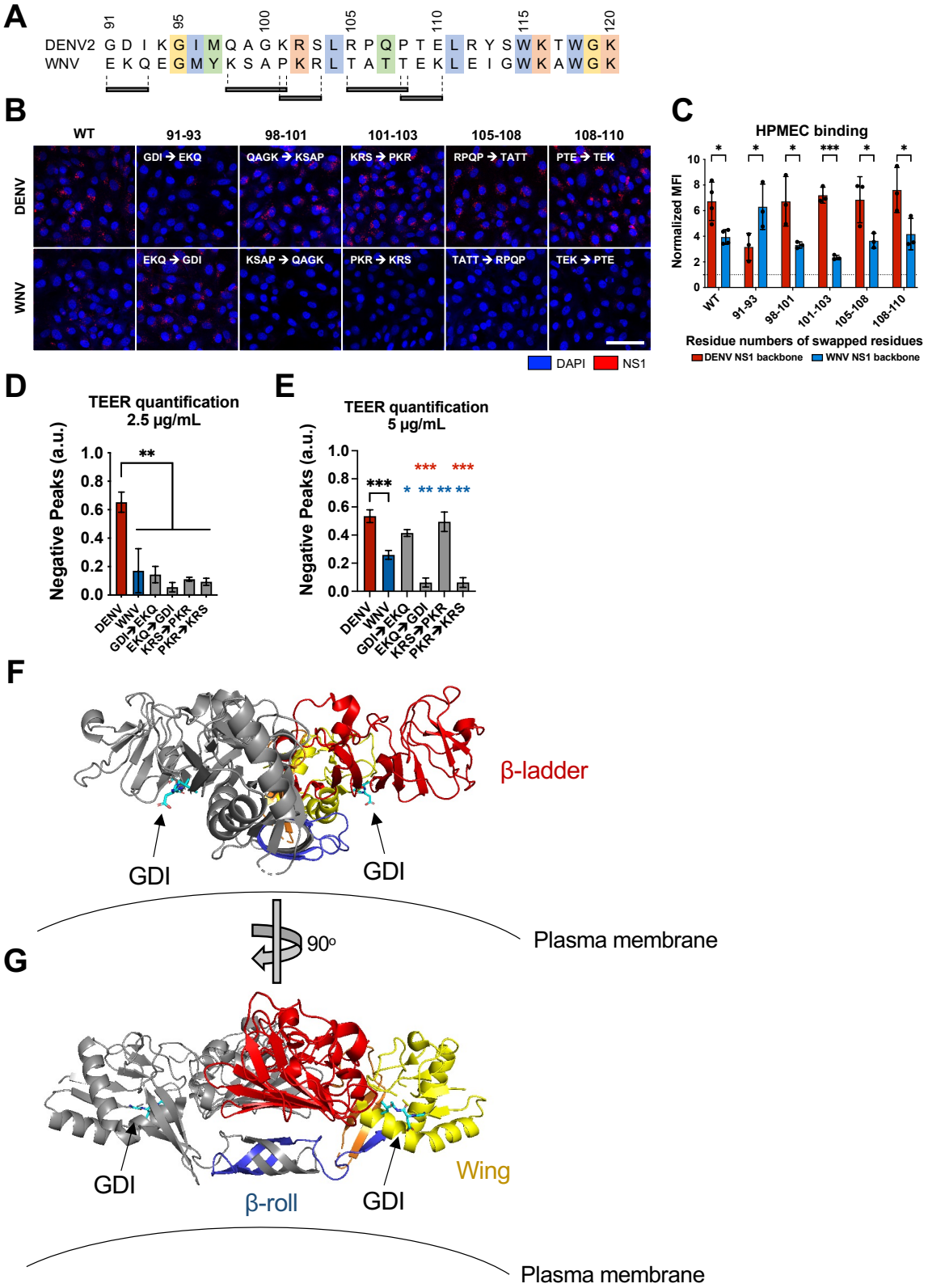
A
DENV2 G D I K G I M Q A G K R S L R P Q P T E L R Y S W K T W G K
WNV E K Q E G M Y K S A P K R L T A T T E K L E I G W K A W G K
B
WT
91-93
98-101
101-103
105-108
108-110
DENV
WNV
GDI → EKQ
QAGK → KSAP
KRS → PKR
RPQP → TATT
PTE → TEK
EKQ → GDI
KSAP → QAGK
PKR → KRS
TATT → RPQP
TEK → PTE
DAPI
NS1
C
HPMEC binding
Normalized MFI
Residue numbers of swapped residues
DENV NS1 backbone
WNV NS1 backbone
D
TEER quantification
2.5 μg/mL
Negative Peaks (a.u.)
E
TEER quantification
5 μg/mL
Negative Peaks (a.u.)
F
β-ladder
GDI
GDI
Plasma membrane
G
90°
GDI
β-roll
GDI
Wing
Plasma membrane

Figure 5. Residues 91-93 of DENV NS1 drive DENV NS1-endothelial cell interactions.
(A) Sequence alignment of DENV and WNV NS1 from amino acid residue 91 to 120, with black bars indicating the 3-4 residue motifs swapped in the site-directed mutants between DENV and WNV NS1. Colors of the residues indicate their similarities based on biochemical properties. **(B)** NS1 binding assay where 10μg/mL of WT or mutant NS1 as indicated were added to HPMEC and imaged using immunofluorescence microscopy. **(C)** Quantification of (B). **(D)** HPMEC monolayer was seeded in the apical chamber of a Transwell and treated with either WT or site-directed mutant NS1 proteins at 2.5μg/mL. Trans-endothelial electrical resistance (TEER) was measured over time, normalized to the untreated controls of respective timepoints. Area-under-the-curve (AUC) quantification of TEER curves is shown. **(E)** Same as (D) but treating with NS1 proteins at 5.0 μg/mL. AUC quantification of TEER curves is shown. **(F, G)** Dimeric DENV2 NS1 structure at 2.89Å (PDB 7K93 [40]) was annotated to denote the location of the 91-93 GDI motif within the wing domain in spatial and structural reference to the rest of NS1. One monomer is coloured grey while the other monomer is coloured as follows: blue for β-roll, yellow for wing, red for β-ladder, and orange for inter-domain connecting regions. Arrows point towards GDI motif on both monomers, coloured in cyan. Plasma membrane is shown to indicate the position in which NS1 is proposed to interact. (F) and (G) are rotated 90º along the Y-axis from each other. All data are from at least 3 biological replicates, plotted as mean ± SEM. *p<0.05, **p<0.01, ***p<0.005, ****p<0.001 by one-way ANOVA with multiple comparisons. a.u., arbitrary units. Star colors indicate the respective control to which each construct has been compared.

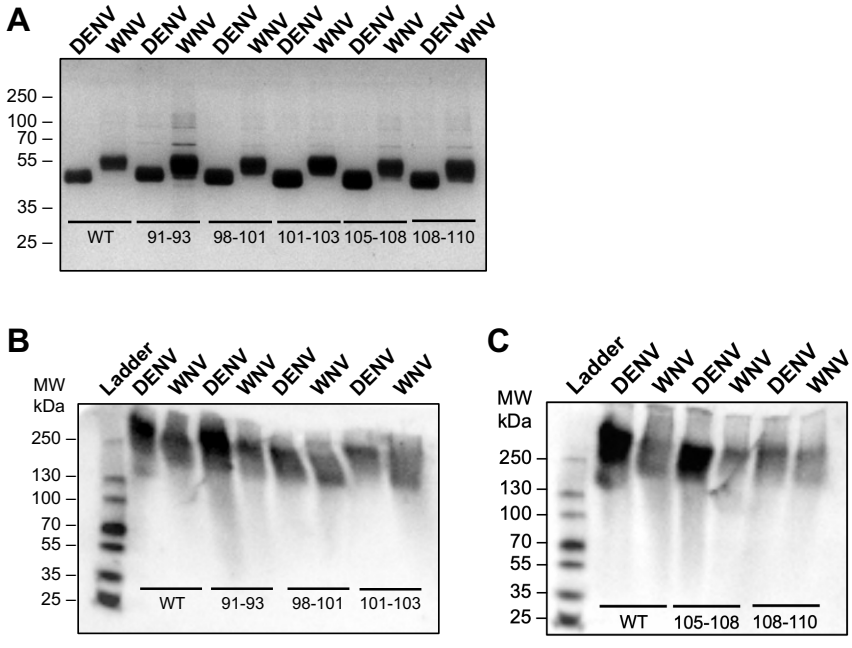

Figure 6. Production and quality control of flavivirus NS1 site-directed mutants.
Proteins were evaluated by silver stain following SDS-PAGE gel (A) and native PAGE (B, C). 2 μg of each NS1 construct was used. For native gels, proteins were detected using anti-His mAb. Top row labels indicate the flavivirus NS1 backbone. Numbering under bands refer to the residues that were swapped between DENV and WNV NS1. **(A)** Silver stain of site-directed NS1 mutants between DENV and WNV NS1. **(B, C)** Native PAGE of site-directed NS1 mutants between DENV and WNV NS1, divided into two gels each with respective WT DENV and WNV NS1 controls. WT, wild-type.

The wing domain of DENV NS1 confers NS1-induced vascular leak *in vivo*

To explore whether the tissue-specific NS1-endothelial cell interactions we observed *in vitro* could be recapitulated *in vivo*, we next asked which NS1 domains were required for tissue-specific vascular leak *in vivo*. We used a mouse model of localized dermal leak, in which we have previously shown that DENV NS1 causes significantly higher leak than WNV NS1 [30]. We shaved the hair from the back (dorsal side) of wild-type C57BL/6 mice and administered injections intradermally (ID): PBS as baseline vehicle control, WT parental NS1, and DENV-WNV NS1 chimeras. Immediately following ID injections, we retro-orbitally administered dextran conjugated to Alexa-680. Two hours post-NS1 treatment, we excised the dorsal dermis and used a fluorescent scanner to measure the extent of vascular leak as indicated by dextran-associated fluorescence, since dextran is a small molecule that can extravasate into tissues (Fig. 7A and B).

Using this model, we found that the NS1 chimeras containing DENV wing domain (D-**D**-W and W-**D**-W) caused comparable levels of leak as WT DENV NS1, which is significantly higher leak than the leak caused by WT WNV NS1 (Fig. 7C). Conversely, the NS1 chimeras containing WNV wing domain – and DENV β-ladder (W-**W**-D and D-**W**-D) – caused leak comparable to WT WNV NS1, and significantly less than WT DENV NS1. It should be noted that while WT WNV NS1 caused visible vascular leak, the leak was not statistically significant when compared to PBS. These data suggest that the DENV NS1 wing is driving NS1-induced vascular leak in the dorsal dermis of mice *in vivo*.

Since we identified residues 91-93 of DENV as a determinant of wing-mediated endothelial hyperpermeability *in vitro*, we asked whether this motif was also a determinant for wing-mediated dermal leak *in vivo*. Using the same dermal leak model as above, we intradermally injected PBS, WT parental NS1 proteins, and DENV NS1 with WNV NS1 residues 91-93 and *vice versa*, followed by retro-orbital administration of Dextran-A680 (Fig. 7D). We found that WNV NS1 with DENV residues 91-93 gained the ability to trigger vascular leak at comparable levels as WT DENV NS1, while DENV NS1 with WNV residues 91-93 caused significantly less leak, comparable to WT WNV NS1 (Fig. 7E). Taken together, these results suggest that the DENV NS1 wing domain, along with residues 91-93 (GDI), are required to trigger localized vascular leak in this *in vivo* model.

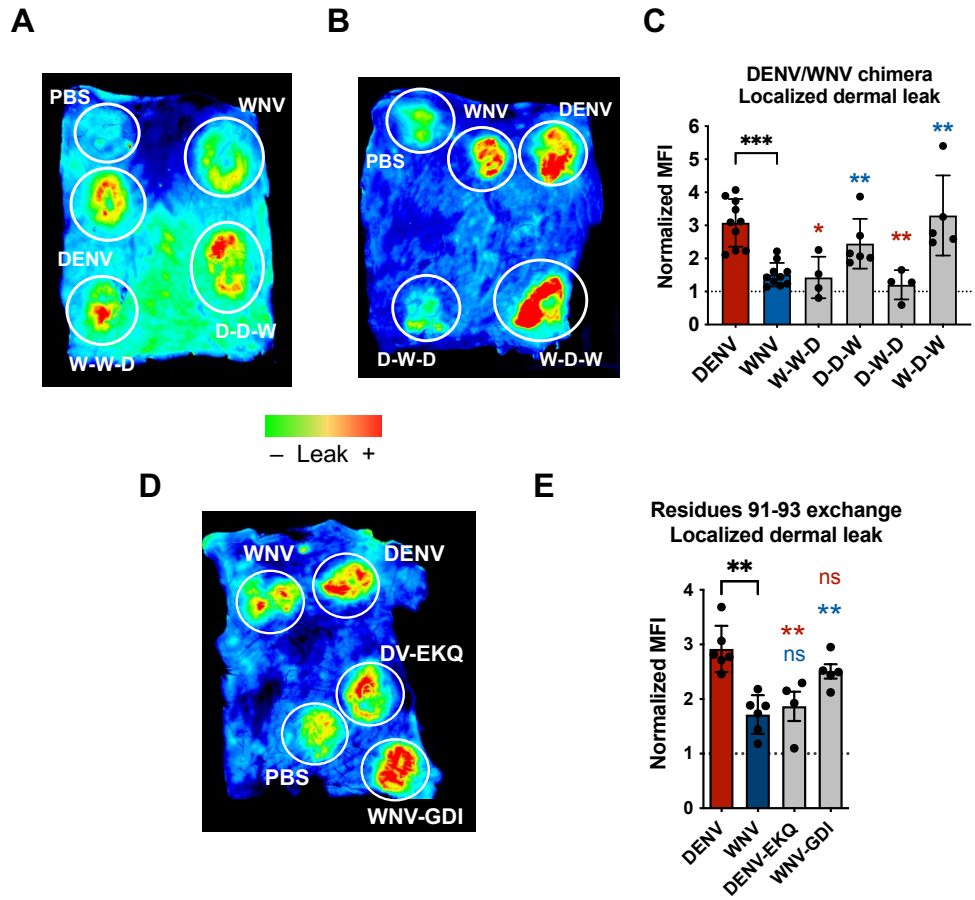

Figure 7. The wing domain of DENV NS1 and residues 91 to 93 within the wing domain confer NS1-induced localized vascular leak *in vivo*.

(A, B) Wild-type C57BL/6J mice were shaved by removing hair from their backs 3 days before the experiment. On the day of experiment, PBS, WT and chimeric NS1 proteins (15 µg) were administered intradermally into discrete spots on the shaved dorsal dermis. Immediately following NS1 injections, 25 µg of Dextran conjugated to Alexa Fluor 680 was administered retro-orbitally. Two hours post-injection, the dermis of each mouse was collected and visualized using a fluorescent scanner. Representative images of the dorsal dermis from 4 to 6 mice are shown. Chimeric proteins were analyzed in different mice with each mouse containing both positive and negative controls (WT DENV and WNV NS1, respectively). **(C)** Mean fluorescent intensity (MFI) quantification of (A) and (B), normalized to PBS injection. **(D)** Same as (A) and (B), but using site-directed NS1 mutants that exchanged residues 91 to 93 between DENV and WNV NS1. Representative image of the dorsal dermis from 4 mice backs are shown. **(E)** MFI quantification of (D), normalized to PBS injection. Data plotted as mean ± SEM. *p<0.05, **p<0.01, ***p<0.005, ****p<0.001 by unpaired Mann-Whitney U test. Star colours indicate the respective control to which each construct was compared.

Discussion

In this study, we determined that both the wing and β-ladder domains of flavivirus NS1 proteins drive differential interactions with human endothelial cells, with the wing influencing binding to endothelial cells and the β-ladder involved in inducing endothelial hyperpermeability *in vitro*. We further identified residues 91 to 93 (GDI) within the flexible loop of the DENV NS1 wing domain as a critical molecular determinant for tissue-specific NS1-endothelial cell binding. Finally, we showed that the wing domain, along with the GDI motif, also dictate the capacity of NS1 to trigger vascular leak *in vivo*. Our finding that the NS1 wing domain contributes to endothelial binding and hyperpermeability is consistent with our previous observations [40] and with studies reporting that in DENV NS1-vaccinated mice, anti-wing antibodies were highly protective against lethal DENV infection [39]. While in its cell-bound dimeric form, residues within the 90 to 120 region of the wing domain are expected to interact with the plasma membrane [35–37,42], which our findings support. In addition, the hydrophobic residues in the DENV NS1 wing domain have also been implicated to be involved in membrane remodeling [43].

It could be expected that flavivirus NS1 contains both conserved core residues mediating interactions with endothelial cells, as well as divergent residues that confer tissue-specificity. In agreement with this hypothesis, previous work from our group uncovered NS1 residues involved in endothelial cell binding that are conserved across the *Flavivirus* genus (W115-W118-G119); these residues are located in the flexible loop within the wing domain [40]. In that study, we mutated the W-W-G residues to alanines; the DENV NS1-WWG mutant bound to HPMEC at lower levels than WT DENV NS1 and had reduced capacity to cause endothelial hyperpermeability in HPMEC. This finding suggests that the highly conserved WWG residues may mediate a baseline level of NS1-endothelial cell binding across all flavivirus NS1 proteins, while the tissue-specificity is likely mediated by non-conserved molecular determinants. The conserved WWG residues contrast with the DENV-GDI motif we identified in the present study, which is highly variable among flaviviruses.

One interesting observation in our data was how the DENV-WNV NS1 chimeras that bound weakly at 2.5 μg/mL to HPMEC (W-**W**-**D** and D-**W**-**D**, containing WNV NS1 wing domain and DENV NS1 β-ladder), at much lower levels than WT DENV NS1, could induce HPMEC hyperpermeability at comparable levels to WT DENV NS1 at the higher NS1 concentrations of 5 and 10 μg/mL (Fig. 4). We observed the same trend again when we tested the capacity of the site-directed mutants to cause endothelial hyperpermeability, where at higher concentrations, the DENV-EKQ mutant NS1 bound at a low level to HPMEC while remaining able to cause HPMEC hyperpermeability, whereas WNV-GDI NS1 bound HPMEC but could not cause HPMEC hyperpermeability. This implicates the β-ladder in conferring endothelial cell hyperpermeability, and is consistent with prior studies that identified residues in the β-ladder as important for endothelial hyperpermeability at a step following endothelial cell binding. A glutamine point mutant of the glycosylated residue N207 [32] and targeted mutations at residues T301, A303, E326, D327 [40], which are in the β-ladder domain, were able to bind to HPMEC but were deficient in causing hyperpermeability. While the present study tested the relative contributions of the wing and β-ladder domains to binding and hyperpermeability, the contribution of the β-roll domain cannot be ruled out.

It is important to note that while WT WNV NS1 bound to HPMEC less efficiently than DENV NS1, it did bind at detectable levels, although this level of binding was not sufficient to trigger endothelial hyperpermeability (Fig. 4) (14). In the TEER model used to measure endothelial hyperpermeability *in vitro*, cells are treated with NS1 and left undisturbed over time under static

conditions, in contrast to DENV infection *in vivo*, where NS1 travels through the bloodstream with constant blood flow. As a result, when the DENV-WNV NS1 chimeras (containing WNV wing but DENV β-ladder) that bound poorly to HPMEC were left undisturbed on HPMEC in TEER assays, we hypothesize that their low-level binding was then sufficient to induce hyperpermeability, which was driven by the DENV β-ladder domain. In the *in vivo* environment, we observed that the vascular leak phenotype was conferred by the wing domain, which is consistent with the observation of wing-driven endothelial binding *in vitro*. This suggests that in the fluid condition of the *in vivo* environment, it is critical for NS1 to have strong interactions with host factors on the cell surface such that NS1 binding, which is mediated by the wing domain, can occur despite blood flow.

Further, the complexity of the *in vivo* condition likely accounts for the discrepancy we observe between the *in vitro* endothelial permeability system and the *in vivo* murine dermal leak model, where constructs containing DENV wing and WNV β-ladder could cause vascular leak *in vivo* despite not causing endothelial hyperpermeability *in vitro*. The *in vitro* TEER assay contains only endothelial cells, whereas in the *in vivo* mouse model, other non-endothelial intrinsic factors may be at play, which could be mediated by the wing domain of NS1. In addition, the kinetics differed in our *in vivo* model of localized leak versus *in vitro* TEER assay. Finally, the NS1 proteins might have different effects on the dermal cells in the *in vivo* system as compared to pulmonary cells in the *in vitro* system. Future studies are needed to fully characterize the relative contribution of non-endothelial factors to NS1-mediated vascular leak.

A critical question to address next is the mechanism by which the residues 91-93 of the wing domain mediate tissue-specific endothelial cell binding. We propose two models to explain the manner in which residues 91 to 93 may mediate tissue-specific interactions. One possibility is that the motif directly interacts with specific host factors on the surface of endothelial cells such as glycans or proteins. In particular, the carboxylate side chain of D92 points directly towards the cell surface; it may interact with host factors, distinct from the WWG motif, which may facilitate association with the plasma membrane (Fig. 5F, G). A second possibility is that the aa 91-93 motif modulates the flexibility of the flexible loop containing the WWG motif [40], which is ultimately the site predicted to interact with endothelial cells.

On the other side of NS1 tissue-specific interactions lies the host endothelial cell. The endothelial cell surface is made up of the endothelial glycocalyx, which is a network of luminal membrane-bound glycoproteins and proteoglycans with both short, branched carbohydrates and long, unbranched glycosaminoglycan side-chains [44,45]. Glycocalyx components include sialic acid, heparan sulfate, chondroitin sulfate, and hyaluronan [44]. The composition and ratio of the components that make up the glycocalyx can vary significantly depending on the tissue of origin of endothelial cells, which in turn can result in differential binding of viral proteins to distinct tissues. As such, different residues in both the aa 91-93 motif and the broader wing domain may influence the interactions with specific types of glycans on different endothelial cells.

Our study begins to uncover the molecular determinants for flavivirus NS1 binding and tissue tropism. We establish the flavivirus NS1 wing domain to be important for binding endothelial cells and causing vascular leak, and in the case of DENV NS1, identify residues 91 to 93 within the wing domain as key determinants driving such interactions. This new molecular insight into what determines flavivirus NS1 tissue specificity is crucial for understanding pan-flaviviral pathogenesis and offers new approaches for antiviral therapies.

TABLE 1 Primers used for mutagenesis in this study.

Construct	NS1 Backbone	Mutation / Insertion	Primer Direction	Sequence
-	Plasmid pMAB	-	Forward	CTCTAGACCGGTACGCGTGCCGCCACC
-	Plasmid pMAB	-	Reverse	GGATCCCTGCAGCTCGAGTCAGTGATGGTGATGGTGATG
W-W-D	WNV	DENV β-ladder	Forward	AACACAACTGAATGCGACTCAAAACTCATGTCAGCG
	WNV	DENV β-ladder	Reverse	TGACATGAGTTTTGAGTCGCATTCAGTTGTGTTGC
D-D-W	DENV	WNV β-ladder	Forward	AGGATGTATTCTGCGACTCGAAGATCATTGG
	DENV	WNV β-ladder	Reverse	AATGATCTTCGAGTCGCAGAATACATCCTG
D-W-D	DENV	DENV β-roll + WNV wing	Reverse	TAGGCCTTGTGGCGTTTCTGGTTGGAAC
	DENV	DENV β-roll + WNV wing	Forward	AAGTTCCAACCAGAAACGCCACAAGG
	DENV	WNV wing + DENV β-ladder	Reverse	AACTTCCAACGAATTCCAAGCGCG
	DENV	WNV wing + DENV β-ladder	Forward	ATCGCGCTTGGAATTCGTTGGAAGTTG
W-D-W	WNV	WNV β-roll + DENV wing	Reverse	GTTTTGAAGGGGATTCAGGGTAATACTTGTAC
	WNV	WNV β-roll + DENV wing	Forward	GTACAAGTATTACCCTGAATCCCCTTCAAAAC
	WNV	DENV wing + WNV β-ladder	Reverse	TCCACTTCTAAGCTATTCCAAGCTC
	WNV	DENV wing + WNV β-ladder	Forward	TAGAGCTTGGAATAGCTTAGAAGTGG
W-Z-W	WNV	WNV β-roll + ZIKV wing	Reverse	TCTACGGGGGGATTCAGGGTAATAC
	WNV	WNV β-roll + ZIKV wing	Forward	TATTACCCTGAATCCCCCCGTAGATTGG
	WNV	ZIKV wing + WNV β-ladder	Reverse	TCCACTTCTAAGCTGTTCCATGCTCTATG
	WNV	ZIKV wing + WNV β-ladder	Forward	ATAGAGCATGGAACAGCTTAGAAGTGGAGG
Z-W-Z	ZIKV	ZIKV β-roll + WNV wing	Reverse	TAGGCCTTGTGGCGTGTCAGGATGGTAC
	ZIKV	ZIKV β-roll + WNV wing	Forward	TACCATCCTGACACGCCACAAGG
	ZIKV	WNV wing + ZIKV β-ladder	Reverse	ACAAGAAAGCTATTCCAAGC
	ZIKV	WNV wing + ZIKV β-ladder	Forward	TTGGAATAGCTTTCTTGTGG

W-W-Z	WNV	ZIKV β-ladder	Reverse	AATAACGGCTGGGTCGCATTCAGTTG
	WNV	ZIKV β-ladder	Forward	AACTGAATGCGACCCAGCCGTTATTGG
Z-Z-W	ZIKV	WNV β-ladder	Reverse	TGATCTTCGAATCACACTC
	ZIKV	WNV β-ladder	Forward	AGAGTGTGATTCGAAGATCATTGG
D-Z-D	DENV	DENV β-roll + ZIKV wing	Reverse	ATCTACGGGGGGATTCTGGTTGGAAC
	DENV	DENV β-roll + ZIKV wing	Forward	AGTTCCAACCAGAATCCCCCCGTAGATTGG
	DENV	ZIKV wing + DENV β-ladder	Reverse	TCAACTTCCAACGAGTTCCATGCTCTATG
	DENV	ZIKV wing + DENV β-ladder	Forward	TAGAGCATGGAACTCGTTGGAAGTTG
Z-D-Z	ZIKV	ZIKV β-roll + DENV wing	Reverse	AGTTTTGAAGGGGAGTCAGGATGGTAC
	ZIKV	ZIKV β-roll + DENV wing	Forward	TACCATCCTGACTCCCCTTCAAAAC
	ZIKV	DENV wing + ZIKV β-ladder	Reverse	ACAAGAAAGCTATTCCAAGCTCT
	ZIKV	DENV wing + ZIKV β-ladder	Forward	TAGAGCTTGGAATAGCTTTCTTGTGG
D-D-Z	DENV	ZIKV β-ladder	Reverse	ATAACGGCTGGGTCGCAGAATAC
	DENV	ZIKV β-ladder	Forward	TATTCTGCGACCCAGCCGTTATTG
Z-Z-D	ZIKV	DENV β-ladder	Reverse	ACATGAGTTTTGAATCACACTCTAATGA
	ZIKV	DENV β-ladder	Forward	AGAGTGTGATTCAAAACTCATG
Site-directed mutants	DENV	91-93 EKQ (WNV sequence)	Forward	AACTATTATGACAGAGAAACAGAAAGGAATCATGCAGG
	DENV	91-93 EKQ (WNV sequence)	Reverse	TGCATGATTCCTTTCTGTTTCTCTGTCATAATAGTTAAC
	WNV	91-93 GDI (DENV sequence)	Forward	TAGTGTCGTGGTTGGAGACATCGAGGGAATGTACAAG
	WNV	91-93 GDI (DENV sequence)	Reverse	TTGTACATTCCCTCGATGTCTCCAACCACGACACTAAGG
	DENV	98-101 KSAP (WNV sequence)	Forward	ACATCAAAGGAATCATGAAGTCAGCACCTCGATCTCTGCGGCCTCAGC
	DENV	98-101 KSAP (WNV sequence)	Reverse	TGAGGCCGCAGAGATCGAGGTGCTGACTTCATGATTCCTTTGATGTC
	WNV	98-101 QAGK (DENV sequence)	Forward	AACAGGAGGGAATGTACCAGGCAGGAAAAAAACGCCTCACCGCC
	WNV	98-101 QAGK (DENV sequence)	Reverse	TGGCGGTGAGGCGTTTTTTTCCTGCCTGGTACATTCCCTCCTGTTTC
	DENV	101-103 PKR (WNV)	Forward	TGCAGGCAGGACCTAAACGCCTGCGGCCTCAGC

	DENV	101-103 PKR (WNV)	Reverse	TGAGGCCGCAGGCGTTTAGGTCCTGCCTGCATG
	WNV	101-103 KRS (DV)	Forward	TACAAGTCAGCAAAACGATCTCTCACCGCCACC
	WNV	101-103 KRS (DV)	Reverse	TGGCGGTGAGAGATCGTTTTGCTGACTTGTAC
	DENV	105-108 TATT (WNV)	Forward	AAAACGATCTCTGACCGCCACCACGACTGAGCTGAAG
	DENV	105-108 TATT (WNV)	Reverse	TTCAGCTCAGTCGTGGTGGCGGTCAGAGATCGTTTTCC
	WNV	105-108 RPQP (DV)	Forward	ACCTAAACGCCTCCGGCCTCAGCCCGAAAAATTGGAA
	WNV	105-108 RPQP (DV)	Reverse	TTCCAATTTTTCGGGCTGAGGCCGGAGGCGTTTAGGTG
	DENV	108-110 TEK (WNV)	Forward	TCTGCGGCCTCAGACGGAAAAACTGAAGTATTCATG
	DENV	108-110 TEK (WNV)	Reverse	ATGAATACTTCAGTTTTTCCGTCTGAGGCCGCAG
	WNV	108-110 PTE (DV)	Forward	TCACCGCCACCCCCACTGAGTTGGAAATTGGC
	WNV	108-110 PTE (DV)	Reverse	AGCCAATTTCCAACTCAGTGGGGGTGGCGGTGAG

Materials and Methods

Cell lines

FreeStyle 293F suspension cells (Thermo Fisher Scientific) were used for production of recombinant NS1 proteins. 293F cells were cultured in FreeStyle 293 Expression medium (Thermo Fisher Scientific) containing 1% penicillin/streptomycin (P/S) and grown in a CO_2 incubator at 37°C with 8% CO_2 and maintained on a cell shaker at ~130 rpm. HPMEC (HPMEC-ST1.6r) were kindly donated by Dr. J.C. Kirkpatrick at Johannes Gutenberg University, Germany, and were used for NS1 cell binding and TEER assays. HUVEC were kindly gifted from Dr. Melissa Lodoen at the University of California, Irvine. HUVEC are primary endothelial cells obtained from a single female donor (Lonza). Both HPMEC and HUVEC cell lines were propagated (passages 5–10) and maintained in endothelial growth medium 2 (EGM-2) using the EGM-2 bullet kit from Lonza following the manufacturer's specifications and grown in a CO_2 incubator at 37ºC with 5% CO_2.

NS1 mutagenesis and cloning chimeric NS1 proteins

Chimeric NS1 proteins were produced by amplifying fragments of β-roll, wing, and β-ladder domains from the WT DENV2 NS1 (Thailand/16681), WNV NS1 (NY99), or ZIKV NS1 (Uganda MR766), using primers listed in Table 1. The N-terminus of β-roll and C-terminus of β-ladder primer sequences were flanked with nucleotide bases complementary to the protein expression vector plasmid "pMAB". The pMAB vector encodes a N-terminal CD33 signal sequence and C-terminal 6xHis tag, a kind gift from Dr. Michael Diamond, Washington University at St. Louis. The domain fragments and pMAB vector were fused together using overlap extension PCR. Site-directed NS1 mutants were produced using a site-directed mutagenesis kit (QuikChange XL Site-Directed Mutagenesis Kit, Agilent) following the manufacturer's instructions, with primers listed in Table 1. All mutant NS1 constructs were sequence-verified with 5' and 3' primers that recognize the pMAB vector beyond the mutagenesis insertion region.

NS1 protein production and purification

Plasmids containing WT or mutant NS1 sequence were transfected into FreeStyle 293F cells using polyethylenimine (PEI) (40K) (Sigma) according to the manufacturer's instructions. 48 to 72 hours post-transfection, NS1-containing supernatants were collected, filtered through a 0.45 μm cellulose acetate membrane to remove cell debris, and stored at -80º prior to protein purification. The NS1-containing supernatants were thawed, mixed 1:1 with binding buffer (20 mM sodium phosphate, 500 mM sodium chloride, 20 mM imidazole, pH 7.4), and bound to HisPur cobalt resin (Thermo Fisher Scientific) with shaking for 2 hours at room temperature. The NS1-resin mixture then transferred to a column and washed 5 times in wash buffer (20 mM sodium phosphate, 500 mM sodium chloride, 25 mM imidazole, pH 7.4). NS1 was then eluted from the HisPur cobalt resin with elution buffer (20 mM sodium phosphate, 500 mM sodium chloride, 200 mM imidazole, pH 7.4) over 5 fractions. The purified NS1 stocks were then subjected to dialysis against 1X PBS for 48 hours at 4ºC and concentrated using Amicon filters with 10,000 molecular weight cut-off (Millipore). The Pierce BCA protein quantitation kit (Thermo Fisher Scientific) was used to quantify the purified recombinant proteins according to manufacturer's instructions. These proteins were used for all experiments within this study.

SDS-PAGE and western blot

Recombinant proteins were collected in protein sample buffer (0.1 M Tris pH 6.8, 4% SDS, 4 mM EDTA, 286 mM 2-mercaptoethanol, 3.2 M glycerol, 0.05% bromophenol blue) and then resolved by SDS-PAGE. For native gels, the same protocol was followed except that the sample buffer contained no SDS and 2-mercaptoethanol. Proteins were then transferred onto nitrocellulose membranes and probed with primary antibodies diluted in Tris-buffered saline with 0.1% Tween20 (TBST) containing 5% nonfat dry milk. Membranes and antibodies were incubated overnight rocking at 4°C. The next day, membranes were washed three times with TBST before being probed with anti-mouse HRP secondary antibodies diluted in 5% milk in TBST at a dilution of 1:5,000 at room temperature for 1 hour. Afterwards, membranes were washed with TBST three more times before being developed with ECL reagents and imaged on a ChemiDoc system with Image Lab software (Bio-Rad). The following antibodies were used: mouse anti-His (MA1-21315, Thermo Scientific), goat anti-mouse HRP (405306, Biolegend).

NS1 cell binding assays

To measure binding of WT and mutant NS1 proteins to HPMEC and HUVEC, $1x10^5$ cells were seeded on glass coverslips in 24-well plates. Cells were allowed to form a fully confluent monolayer for 3 days, with medium change every other day. On the day of experiment, 10 µg/mL (3 µg in 300 µL) of NS1 proteins were prepared in 10 µL medium, then added to the cells. Untreated wells were used as negative controls. NS1 and cells were incubated for 1 hour at 37ºC. Mouse anti-6xHis antibody conjugated to Alexa Fluor 647 (Novus Biologicals) was then added at a dilution of 1:200, together with Hoechst 33342 (Immunochemistry) at a 1:2000 dilution for staining of nuclei, for 30 minutes at 37ºC. Cells were then washed twice in 1X PBS followed by fixation in 4% formaldehyde diluted in 1X PBS (Thermo Fisher Scientific). Coverslips were mounted onto microscope slides on a drop of ProLong Gold (Thermo Fisher Scientific) and imaged using a Zeiss LSM 710 inverted confocal microscope (CRL Molecular Imaging Center, UC Berkeley). Images were processed using ImageJ software.

Trans-endothelial electrical resistance (TEER)

The trans-endothelial electrical resistance assay was used to measure the functional effect of NS1 on endothelial barrier function in HPMEC as previously described [34]. Briefly, $1x10^5$ cells (HPMEC) were seeded in 300 µL of medium on the polycarbonate membrane insert of a trans-well (Transwell permeable support, 0.4 µm, 6.5 mm insert; Corning Inc.). The trans-well is placed in a well on a 24-well plate, becoming the apical (upper) chamber. 1.5 mL of media is added to the basolateral (lower) chamber. Cells were allowed to form a monolayer for 3 days with media changes in both apical and basolateral chambers every day, until the inter-chamber electrical resistance reaches about 60Ω difference between trans-wells seeded with (~150Ω) and without cells (~90Ω). On the day of experiment, 2.5, 5, or 10 µg/mL of indicated NS1 proteins (0.75 or 1.5 µg proteins, respectively) were mixed with media up to 10µL, and added to the apical chambers of the trans-wells. Electrical resistance between the apical and basolateral chambers is measured in ohms using an Epithelial Volt Ohm Meter (EVOM) with an electrode pair (World Precision Instruments), at the times indicated in the figures. Trans-wells containing no cells and untreated trans-wells containing only cells were used as negative controls to calculate the baseline electrical resistance at each timepoint. Relative TEER is calculated as a ratio of resistance values $((\Omega_{experimental} - \Omega_{media\ only}) / (\Omega_{untreated\ cells} - \Omega_{media\ only}))$. Area under the curve (AUC) analyses were calculated using the area between TEER curves and Y=1.

Mouse model of localized vascular leak

Five- to eight-week-old WT C57BL/6 male mice were purchased from the Jackson Laboratory (Bar Harbor, ME) and maintained under specific pathogen-free conditions at the University of California, Berkeley, Animal Facility. Mice were housed in a controlled temperature environment on a 12-hour light/dark cycle, with food and water provided *ad libitum*. All experimental procedures involving animals were pre-approved by the Animal Care and Use Committee (ACUC) of the University of California, Berkeley. Three to four days prior to experiment, the dorsal dermises of 6- to 10-week-old WT C57BL/6 female mice (Jackson Laboratory) were shaved using hair clippers, and residual hair removed using Nair (Church & Dwight). On the day of experiment, 15 µg of WT or mutant NS1 was mixed with PBS in a total volume 50 µL each. NS1 mixtures and PBS were then injected intradermally (ID) into discrete spots in the shaved mouse dermis. Immediately following ID injections, 25 µg of 10-kDa dextran conjugated to Alexa Fluor 680 (1 mg/mL; Sigma) was delivered intravenously (IV) through the retro-orbital route. Two hours post-injection, mice were euthanized, and the dorsal dermis was removed and placed in Petri dishes. The dermis was then placed on a fluorescent scanner (LI-COR Odyssey CLx Imaging System) to visualize the fluorescence signal accumulation at a wavelength of 700 nm. Vascular leak at the ID injection sites was quantified using Image Studio software (LI-COR Biosciences) as described previously [30,32].

Statistics

All quantitative analyses were conducted, and all data were plotted, using GraphPad Prism 9 software. Experiments were repeated at least 3 times, to ensure reproducibility. All experiments were designed and performed with both positive and negative controls (indicated in the figures), which were used for inclusion/exclusion determination. For immunofluorescence microscopy experiments, images of random fields were captured. For all experiments with quantitative analysis, data are displayed as mean ± standard error of the mean (SEM). All cell binding and TEER quantitative data were analyzed using a One-way ANOVA analysis with Tukey's multiple comparisons test. For the localized dermal leak experiments, a non-parametric, unpaired Mann-Whitney U test was used to determine statistical significance between groups. The resulting p-values from the above statistical tests were displayed as n.s., not significant; $p > 0.05$; *$p < 0.05$; **$p < 0.01$; ***$p < 0.001$; ****$p < 0.0001$.

References
Chapter 2

1. Bhatt, S., Gething, P.W., Brady, O.J., Messina, J.P., Farlow, A.W., Moyes, C.L., Drake, J.M., Brownstein, J.S., Hoen, A.G., Sankoh, O., *et al.* (2013). The global distribution and burden of dengue. Nature *496*, 504–507.

2. Stanaway, J.D., Shepard, D.S., Undurraga, E.A., Halasa, Y.A., Coffeng, L.E., Brady, O.J., Hay, S.I., Bedi, N., Bensenor, I.M., Castañeda-Orjuela, C.A., *et al.* (2016). The global burden of dengue: an analysis from the Global Burden of Disease Study 2013. Lancet Infect. Dis. *16*, 712–723.

3. Pierson, T.C., and Diamond, M.S. (2020). The continued threat of emerging flaviviruses. Nat. Microbiol. *5*, 796–812.

4. Glasner, D.R., Puerta-Guardo, H., Beatty, P.R., and Harris, E. (2018). The Good, the Bad, and the Shocking: The Multiple Roles of Dengue Virus Non-structural Protein 1 in Protection and Pathogenesis. Annu. Rev. Virol. *5*, 227–253.

5. Srikiatkhachorn, A., Mathew, A., and Rothman, A.L. (2017). Immune-mediated cytokine storm and its role in severe dengue. Semin. Immunopathol. *39*, 563–574.

6. Malavige, G.N., Jeewandara, C., and Ogg, G.S. (2020). Dysfunctional Innate Immune Responses and Severe Dengue. Front. Cell. Infect. Microbiol. *10:590004*.

7. Beatty, P.R., Puerta-Guardo, H., Killingbeck, S.S., Glasner, D.R., Hopkins, K., and Harris, E. (2015). Dengue virus NS1 triggers endothelial permeability and vascular leak that is prevented by NS1 vaccination. Sci. Transl. Med. *7*, 304ra141.

8. Puerta-Guardo, H., Glasner, D.R., and Harris, E. (2016). Dengue Virus NS1 Disrupts the Endothelial Glycocalyx, Leading to Hyperpermeability. PLoS Pathog. *12*, e1005738.

9. Rastogi, M., and Singh, S.K. (2020). Zika virus NS1 affects the junctional integrity of human brain microvascular endothelial cells. Biochimie *176*, 52–61.

10. Hui, L., Nie, Y., Li, S., Guo, M., Yang, W., Huang, R., Chen, J., Liu, Y., Lu, X., Chen, Z., *et al.* (2020). Matrix metalloproteinase 9 facilitates Zika virus invasion of the testis by modulating the integrity of the blood-testis barrier. PLoS Pathog. *16*, e1008509.

11. Puerta-Guardo, H., Tabata, T., Petitt, M., Dimitrova, M., Glasner, D.R., Pereira, L., and Harris, E. (2020). Zika Virus Non-structural Protein 1 Disrupts Glycosaminoglycans and Causes Permeability in Developing Human Placentas. J. Infect. Dis. *221*, 313–324.

12. Singh, S., Anupriya, M.G., Modak, A., and Sreekumar, E. (2018). Dengue virus or NS1 protein induces trans-endothelial cell permeability associated with VE-Cadherin and RhoA phosphorylation in HMEC-1 cells preventable by Angiopoietin-1. J. Gen. Virol. *99*, 1658–70.

13. Modhiran, N., Watterson, D., Muller, D.A., Panetta, A.K., Sester, D.P., Liu, L., Hume, D.A., Stacey, K.J., and Young, P.R. (2015). Dengue virus NS1 protein activates cells via Toll-like receptor 4 and disrupts endothelial cell monolayer integrity. Sci. Transl. Med. *7*, 304ra142.

14. Puerta-Guardo, H., Biering, S.B., de Sousa, F.T.G., Shu, J., Glasner, D.R., Li, J., Blanc, S.F., Beatty, P.R., and Harris, E. (2022). Flavivirus NS1 Triggers Tissue-Specific Disassembly of Intercellular Junctions Leading to Barrier Dysfunction and Vascular Leak in a GSK-3β-Dependent Manner. Pathogens *11*, 615.

15. Wessel, A.W., Dowd, K.A., Biering, S.B., Zhang, P., Edeling, M.A., Nelson, C.A., Funk, K.E., DeMaso, C.R., Klein, R.S., Smith, J.L., *et al.* (2021). Levels of Circulating NS1 Impact West Nile

Virus Spread to the Brain. J. Virol. *95*, e00844-21.

16. Siemann, D., Strange, D., Maharaj, P., Shi, P.Y., and Verma, S. (2017). Zika Virus Infects Human Sertoli Cells. J. Virol. *91*, e00623-17.

17. Flamand, M., Megret, F., Mathieu, M., Lepault, J., Rey, F.A., and Deubel, V. (1999). Dengue Virus Type 1 Non-structural Glycoprotein NS1 Is Secreted from Mammalian Cells as a Soluble Hexamer in a Glycosylation-Dependent Fashion. J. Virol. *73*, 6104–6110.

18. Gutsche, I., Coulibaly, F., Voss, J.E., Salmon, J., D'Alayer, J., Ermonval, M., Larquet, E., Charneau, P., Krey, T., Mégret, F., *et al.* (2011). Secreted dengue virus non-structural protein NS1 is an atypical barrel-shaped high-density lipoprotein. Proc. Natl. Acad. Sci. *108*, 8003–8008.

19. Muller, D.A., and Young, P.R. (2013). The flavivirus NS1 protein: Molecular and structural biology, immunology, role inpathogenesis and application asadiagnostic biomarker. Antiviral Res. *98*, 192–208.

20. Edeling, M.A., Diamond, M.S., and Fremont, D.H. (2014). Structural basis of Flavivirus NS1 assembly and antibody recognition. Proc. Natl. Acad. Sci. *111*, 4285–4290.

21. Young, P.R., Hilditch, P.A., Bletchly, C., and Halloran, W. (2000). An Antigen Capture Enzyme-Linked Immunosorbent Assay Reveals High Levels of the Dengue Virus Protein NS1 in the Sera of Infected Patients. J. Clin. Microbiol. *38*, 1053–1057.

22. Libraty, D.H., Young, P.R., Pickering, D., Endy, T.P., Kalayanarooj, S., Green, S., Vaughn, D.W., Nisalak, A., Ennis, F.A., and Rothman, A.L. (2002). High Circulating Levels of the Dengue Virus Non-structural Protein NS1 Early in Dengue Illness Correlate with the Development of Dengue Hemorrhagic Fever. J. Infect. Dis. *186*, 1165–1168.

23. Modhiran, N., Watterson, D., Blumenthal, A., Baxter, A.G., Young, P.R., and Stacey, K.J. (2017). Dengue virus NS1 protein activates immune cells via TLR4 but not TLR2 or TLR6. Immunol. Cell Biol. *95*, 491–495.

24. Avirutnan, P., Fuchs, A., Hauhart, R.E., Somnuke, P., Youn, S., Diamond, M.S., and Atkinson, J.P. (2010). Antagonism of the complement component C4 by flavivirus non-structural protein NS1. J. Exp. Med. *207*, 793–806.

25. Avirutnan, P., Hauhart, R.E., Somnuke, P., Blom, A.M., Diamond, M.S., and Atkinson, J.P. (2011). Binding of Flavivirus Non-structural Protein NS1 to C4b Binding Protein Modulates Complement Activation. J. Immunol. *187*, 424–433.

26. Chung, K.M., Liszewski, M.K., Nybakken, G., Davis, A.E., Townsend, R.R., Fremont, D.H., Atkinson, J.P., and Diamond, M.S. (2006). West Nile virus non-structural protein NS1 inhibits complement activation by binding the regulatory protein factor H. Proc. Natl. Acad. Sci. *103*, 19111–19116.

27. Malavige, G.N., and Ogg, G.S. (2017). Pathogenesis of vascular leak in dengue virus infection. Immunology *151*, 261–269.

28. Riswari, S.F., Tunjungputri, R.N., Kullaya, V., Garishah, F.M., Utari, G.S.R., Farhanah, N., Overheul, G.J., Alisjahbana, B., Gasem, M.H., Urbanus, R.T., *et al.* (2019). Desialylation of platelets induced by Von Willebrand Factor is a novel mechanism of platelet clearance in dengue. PLoS Pathog. *15*, e1007500.

29. Chao, C.-H., Wu, W.-C., Lai, Y.-C., Tsai, P.-J., Perng, G.-C., Lin, Y.-S., and Yeh, T.-M. (2019). Dengue virus non-structural protein 1 activates platelets via Toll-like receptor 4, leading to thrombocytopenia and hemorrhage. PLoS Pathog. *15*, e1007625.

30. Glasner, D.R., Ratnasiri, K., Puerta-Guardo, H., Espinosa, D.A., Beatty, P.R., and Harris, E.

(2017). Dengue virus NS1 cytokine-independent vascular leak is dependent on endothelial glycocalyx components. PLoS Pathog. *13*, e1006673.

31. Avirutnan, P., Zhang, L., Punyadee, N., Manuyakorn, A., Puttikhunt, C., Kasinrerk, W., Malasit, P., Atkinson, J.P., and Diamond, M.S. (2007). Secreted NS1 of dengue virus attaches to the surface of cells via interactions with heparan sulfate and chondroitin sulfate E. PLoS Pathog. *3*, 1798–1812.

32. Wang, C., Puerta-Guardo, H., Biering, S.B., Glasner, D.R., Tran, E.B., Patana, M., Gomberg, T.A., Malvar, C., Lo, N.T.N., Espinosa, D.A., *et al.* (2019). Endocytosis of flavivirus NS1 is required for NS1-mediated endothelial hyperpermeability and is abolished by a single N-glycosylation site mutation. PLoS Pathog. *15*, e1007938.

33. Barbachano-Guerrero, A., Endy, T.P., and King, C.A. (2020). Dengue virus non-structural protein 1 activates the p38 MAPK pathway to decrease barrier integrity in primary human endothelial cells. J. Gen. Virol. *101*, 484–496.

34. Puerta-Guardo, H., Glasner, D.R., Espinosa, D.A., Biering, S.B., Patana, M., Ratnasiri, K., Wang, C., Beatty, P.R., and Harris, E. (2019). Flavivirus NS1 Triggers Tissue-Specific Vascular Endothelial Dysfunction Reflecting Disease Tropism. Cell Rep. *26*, 1598-1613.e8.

35. Akey, D.L., Brown, W.C., Dutta, S., Konwerski, J., Jose, J., Jurkiw, T.J., DelProposto, J., Ogata, C.M., Skiniotis, G., Kuhn, R.J., *et al.* (2014). Flavivirus NS1 Structures Reveal Surfaces for Associations with Membranes and the Immune System. Science *343*, 881–885.

36. Brown, W.C., Akey, D.L., Konwerski, J.R., Tarrasch, J.T., Skiniotis, G., Kuhn, R.J., and Smith, J.L. (2016). Extended surface for membrane association in Zika virus NS1 structure. Nat. Struct. Mol. Biol. *23*, 865–867.

37. Xu, X., Song, H., Qi, J., Liu, Y., Wang, H., Su, C., Shi, Y., and Gao, G.F. (2016). Contribution of intertwined loop to membrane association revealed by Zika virus full-length NS1 structure. EMBO J. *35*, 2170–2178.

38. Hertz, T., Beatty, P.R., MacMillen, Z., Killingbeck, S.S., Wang, C., and Harris, E. (2017). Antibody Epitopes Identified in Critical Regions of Dengue Virus Non-structural 1 Protein in Mouse Vaccination and Natural Human Infections. J. Immunol. *198*, 4025–4035.

39. Lai, Y.C., Chuang, Y.C., Liu, C.C., Ho, T.S., Lin, Y.S., Anderson, R., and Yeh, T.M. (2017). Antibodies Against Modified NS1 Wing Domain Peptide Protect Against Dengue Virus Infection. Sci. Rep. *7*, 69–75.

40. Biering, S.B., Akey, D.L., Wong, M.P., Brown, W.C., Lo, N.T.N., Puerta-Guardo, H., Tramontini Gomes de Sousa, F., Wang, C., Konwerski, J.R., Espinosa, D.A., *et al.* (2021). Structural basis for antibody inhibition of flavivirus NS1–triggered endothelial dysfunction. Science *371*, 194–200.

41. Rastogi, M., Sharma, N., and Singh, S.K. (2016). Flavivirus NS1: a multifaceted enigmatic viral protein. Virol. J. *13*, 131.

42. Akey, D.L., Brown, W.C., Jose, J., Kuhn, R.J., and Smith, J.L. (2015). Structure-guided insights on the role of NS1 in flavivirus infection. BioEssays *37*, 489–494.

43. Ci, Y., Liu, Z.Y., Zhang, N.N., Niu, Y., Yang, Y., Xu, C., Yang, W., Qin, C.F., and Shi, L. (2020). Zika NS1-induced ER remodeling is essential for viral replication. J. Cell Biol. *219*, e201903062.

44. Weinbaum, S., Tarbell, J.M., and Damiano, E.R. (2007). The Structure and Function of the Endothelial Glycocalyx Layer. Annu. Rev. Biomed. Eng. *9*, 121–167.

45. Srikiatkhachorn, A., and Kelley, J.F. (2014). Endothelial cells in dengue hemorrhagic fever. Antiviral Res. *109*, 160–170.

Chapter 3

Structure-function studies of dengue virus non-structural protein 1

Abstract

The mosquito-borne, positive-sense RNA dengue virus (DENV) causes up to 400 million infections globally each year and continues to cause substantial dengue cases in tropical and sub-tropical regions. While most symptomatic cases present as the milder dengue fever, some can develop severe dengue, which is characterized by vascular leak. DENV non-structural protein 1 (NS1) is a secreted glycoprotein with 3 domains: the β-roll, wing, and β-ladder. We previously found that NS1 can directly induce endothelial cell (EC) barrier dysfunction, leading to EC hyperpermeability *in vitro* and vascular leak *in vivo* independently of the virus. We further discovered that different flavivirus NS1 proteins bind to human EC and induce vascular leak in a tissue-specific manner, consistent with the virus's respective disease tropism. For example, NS1 from systemic DENV affects EC from all tissues including the lungs, while NS1 from neurotropic West Nile (WNV) only affects brain EC. In the preceding chapter, I established that the NS1 wing domain confers flavivirus NS1-EC binding and drives DENV NS1-induced vascular leak, as well as identified residues 91-93 as the molecular determinants of binding and vascular leak. In this chapter, I include all the data that contributed to the publication of the previous chapter, as well as extended NS1 structure-function data that I accumulated during my studies. I show that the β-ladder N207Q mutant of DENV NS1 that abrogates NS1-induced EC dysfunction could cause localized vascular leak in our dorsal dermal mouse model comparable to wild-type NS1; that the highly conserved W-W-G motif in the NS1 wing domain mediates binding to pulmonary EC; that NS1 wing domain confers binding to EC surface glycans; and that the 2B7 mouse mAb that protects against lethal DENV challenge binds unequivocally to the β-ladder of DENVNS1 blockade and binding. Taken together, results in this chapter will help guide future flavivirus NS1, host factors, and therapeutic studies.

Introduction

The four dengue virus serotypes (DENV1-4) are mosquito-borne positive-stranded RNA viruses of the *Flavivirus* genus which cause up to 400 million annual infections worldwide, of which up to 100 million result in symptomatic infections [1]. These can be categorized into mostly classic dengue fever (DF) or less commonly, severe dengue, which includes dengue haemorrhagic fever (DHF) and dengue shock syndrome (DSS). Severe dengue is characterized by increased vascular leak, where fluids accumulate in tissues after extravasating form the vasculature; the sudden and rapid loss of fluids can lead to shock, which can be fatal [2]. In dengue, one of the most common clinical presentations of vascular leak is pleural effusion resulting in respiratory distress.

DENV, along with other flaviviruses such as Zika (ZIKV) and West Nile (WNV) viruses, contains a 10.7 kb genome that encodes three structural and seven non-structural proteins, including non-structural protein 1 (NS1). NS1 is produced by DENV-infected cells and exists as membrane-bound dimers intracellularly [3]. While intracellular NS1 plays a role in membrane remodeling and viral replication [4–6], NS1 can also be secreted as an oligomeric lipoprotein [7]. The specific oligomeric states of secreted NS1 as well as the roles its lipid cargo plays have recently become points of active discussion in the field where open questions remain [8–10]. Nonetheless, secreted NS1 is multifaceted and involved in pathogenesis [11,12], viral dissemination [13,14], and immune evasion [15,16].

While vascular leak in severe dengue has traditionally been attributed to aberrant immune responses to the virus, we and other groups have shown that NS1 can directly cause vascular dysfunction that results in leak, independently of the virus. NS1-induced vascular leak can occur by promoting the degradation of endothelial glycocalyx components that line the surface of endothelial cells to compromise the endothelial barrier [11,17–19], as well as by disrupting interjunctional proteins that mediate the physical cell-cell interactions [20–22].

NS1 is highly conserved across flaviviruses. We have shown that, intriguingly, NS1 proteins from multiple flaviviruses interact with endothelial cells of distinct tissue origins in a manner consistent with the tropism of its 'parental' flavivirus [23]. For example, DENV NS1 interacts with multiple cell lines including human pulmonary microvascular endothelial cells (HPMEC), which correlates with the systemic nature of DENV infection that can be observed in the lungs. In contrast, WNV NS1 interacts well with human brain microvascular endothelial cells (HBMEC) but minimally with HPMEC, as WNV causes neurological pathologies, such as meningitis and encephalitis, but not pulmonary pathology. However, how these tissue-specific NS1 interactions are modulated has remained unclear and is the central research question of the preceding chapter.

Flavivirus NS1 contains three domains that are highly conserved: the β-roll (residues 1–29), wing (residues 30–180), and β-ladder (residues 181–352) [24]. The NS1 β-roll and wing domains contain many hydrophobic residues that are predicted to interact with the cell's plasma membrane and the lipid cargo within the secreted oligomeric NS1 lipoprotein [25,26]. Interestingly, these surface-exposed residues are conserved among DENV serotypes but divergent across the flavivirus genus (e.g., between DENV and WNV), suggesting their possible roles in mediating NS1 tissue-specific interactions. Additionally, prior studies have suggested that the three domains of NS1 may have distinct functions. DENV NS1 wing domain has been shown to be immunodominant [11,27,28]; conserved, hydrophobic residues in the flexible loop (residues 108–129) within the wing domain (Trp-115, Trp-118, Gly-119) have been identified to partially contribute to DENV NS1 binding to HPMEC [25,29]. In contrast, select residues in the β-ladder domain (such as residues N207, A303, E326, and E327) have been implicated as important for NS1-induced

endothelial hyperpermeability, while being dispensable for binding to endothelial cells [20,29]. One notable residue in the β-ladder domain is the Asn-207 glycosylation site, as we have shown that the N207Q mutant in DENV NS1 binds to endothelial cells comparably to wild-type (WT) DENV NS1 but abrogates NS1's capacity to internalize into cells and cause endothelial dysfunction [20]. These data offer clues about NS1 molecular determinants of tissue-specific interactions with endothelial cells, and a systematic investigation of the different domains has been described in Chapter 2.

Some of the open questions in the flavivirus NS1 field are the identity and roles that the cognate receptor, as well as various glycan association factors, play in mediating NS1-induced pathogenesis. The surface of endothelial cells is decorated with the glycocalyx , which is a complex network of membrane-bound glycoproteins and proteoglycans that contribute to the endothelial barrier integrity. The glycocalyx is a dense, kelp forest-like matrix that protects the underlying endothelial cells from shear force generated by blood flow [30]. Major components of the glycocalyx include sialic acid (Sia) and glycosaminoglycans (GAGs) such as heparan sulfate, chondroitin sulfate, and hyaluronic acid. While this dissertation focuses on the NS1 molecular determinants of tissue specificity, the flip side of this tropism are the host determinants, one of which is believed to be the differential GAG composition across endothelial cells of distinct tissue origins. Part of this chapter begins to address this question by using short protein-bound glycans that have different lengths and sulfation levels to evaluate their relative binding capacity with various DENV/WNV NS1 chimeras.

As mentioned in the introduction, NS1 is a promising therapeutic target candidate to treat dengue, as no specific therapeutics are currently available. As severe dengue is significantly associated with NS1, targeting NS1 with an anti-NS1 monoclonal antibody (mAb) could potentially protect against severe dengue. This chapter covers my involvement in the project characterizing 2B7, a mouse anti-NS1 mAb that is protective in a DENV lethal challenge model in mice, and blocks NS1-induced endothelial hyperpermeability *in vitro* [29]. We showed that 2B7 binds to the β-ladder domain of NS1 and blocks the wing domain-driven interactions with endothelial cells through steric hindrance, demonstrating a proof-of-concept for anti-NS1 mAb therapeutics [29].

Overall, this chapter highlights additional structure-function studies of DENV NS1 that I performed. This includes negative data, data that were included as part of bigger studies, as well as several pilot experiments that will form parts of more complete stories in the future.

Results

Residues 101-135 of DENV NS1 are necessary but not sufficient for NS1 binding to endothelial cells

In work leading up to this dissertation project, we had identified amino acid (aa) residues 101 to 135 of the DENV NS1 wing domain to be immunodominant [27]. Following up on this observation, we made chimeric NS1 proteins that exchanged residues 101-135 between DENV and WNV NS1. Additionally, we made chimeric NS1 that swapped a smaller region of residues 110-122 from WNV into DENV NS1; the smaller region contained highly conserved Trp and Gly residues (W115, W118, G119) and Lys residues (K116 and K120) (Fig. 1A). We cloned and expressed the C-terminally His-tagged NS1 proteins in HEK-293 cells, which were successfully secreted, and then purified NS1 oligomers using cobalt ion affinity chromatography. We treated human pulmonary endothelial cells (HPMEC) with either wild-type (WT) NS1 or DENV/WNV chimeric NS1 proteins and measured the levels of NS1 binding to HPMEC using an immunofluorescence microscopy assay (IFA) (Fig. 1B, C). We found that the DENV NS1 mutants containing WNV NS1 residues 101 to 135 ($DENV^{WNV101-135}$) showed lower levels of binding to HPMEC compared to WT DENV NS1, at a level comparable to WT WNV NS1, suggesting that the stretch of residues contain the molecular determinants for specificity or that the chimeric protein was not folded correctly.

Interestingly, the reciprocal chimera with WNV NS1 containing residues 101-135 of DENV NS1 ($WNV^{DENV101-135}$) did not bind HPMEC differently from WT WNV NS1, suggesting that this stretch of residues alone was not sufficient for HPMEC binding. However, the DENV NS1 mutant containing the smaller region of WNV NS1 ($DENV^{WNV110-122}$) bound HPMEC at comparable levels to WT DENV, suggesting the possibility for residues within the smaller region to be mediating conserved, pan-flavivirus baseline binding, while the residues responsible conferring tissue specificity are outside the smaller region.

To further investigate this inconsistency, we subjected the $DENV^{WNV101-135}$ NS1 mutant to size-exclusion chromatography (SEC) on a fast protein liquid chromatography (FPLC) system (Fig. 1D). We found that the $DENV^{WNV101-135}$ mutant exhibited different elution profiles compared to both WT DENV NS1 made in the laboratory and WT DENV NS1 acquired from a commercial source. Its elution profile suggested that the protein was likely aggregated as a result of disruption of secondary protein structures during the chimerization process. This was supported by native PAGE gel that showed a smearing band for $DENV^{WNV101-135}$ construct compared to distinct bands of WT DENV NS1 (data not shown). Residues 101-135 were not resolved in any of the DENV NS1 structures solved via X-ray crystallography due to the flexible nature of this region [24]. This region was resolved only for ZIKV NS1, which had overall structural difference compared to DENV NS1 [25,26]; in ZIKV NS1, contiguous secondary β-sheets span through residues 101-135, which could explain the protein aggregation phenotype of construct $DENV^{WNV101-135}$. Nonetheless, since the swap of resides 110-122 (NS1 $DENV^{WNV110-122}$) did not affect the NS1 binding phenotype, this suggested that NS1 residues 110-120 are likely not driving NS1 tissue-specific interactions.
Current crystal structures of DENV NS1 have not been able to resolve residues 101-135. However, this region has been resolved for ZIKV NS1 and was revealed to contain a flexible loop that is thought to be disordered [25]. To investigate how residues 101-135 could be presented on DENV NS1, we used AlphaFold to predict the DENV2 NS1 crystal structure in its dimeric form (Fig. 1E) [31]. The predicted structure revealed an alpha helix within residues 101-135 (in green) of the wing domain (in yellow). While this predicted structure is similar to the crystallized ZIKV NS1 structure, ZIKV NS1 does not contain secondary structures within the flexible loop [25].

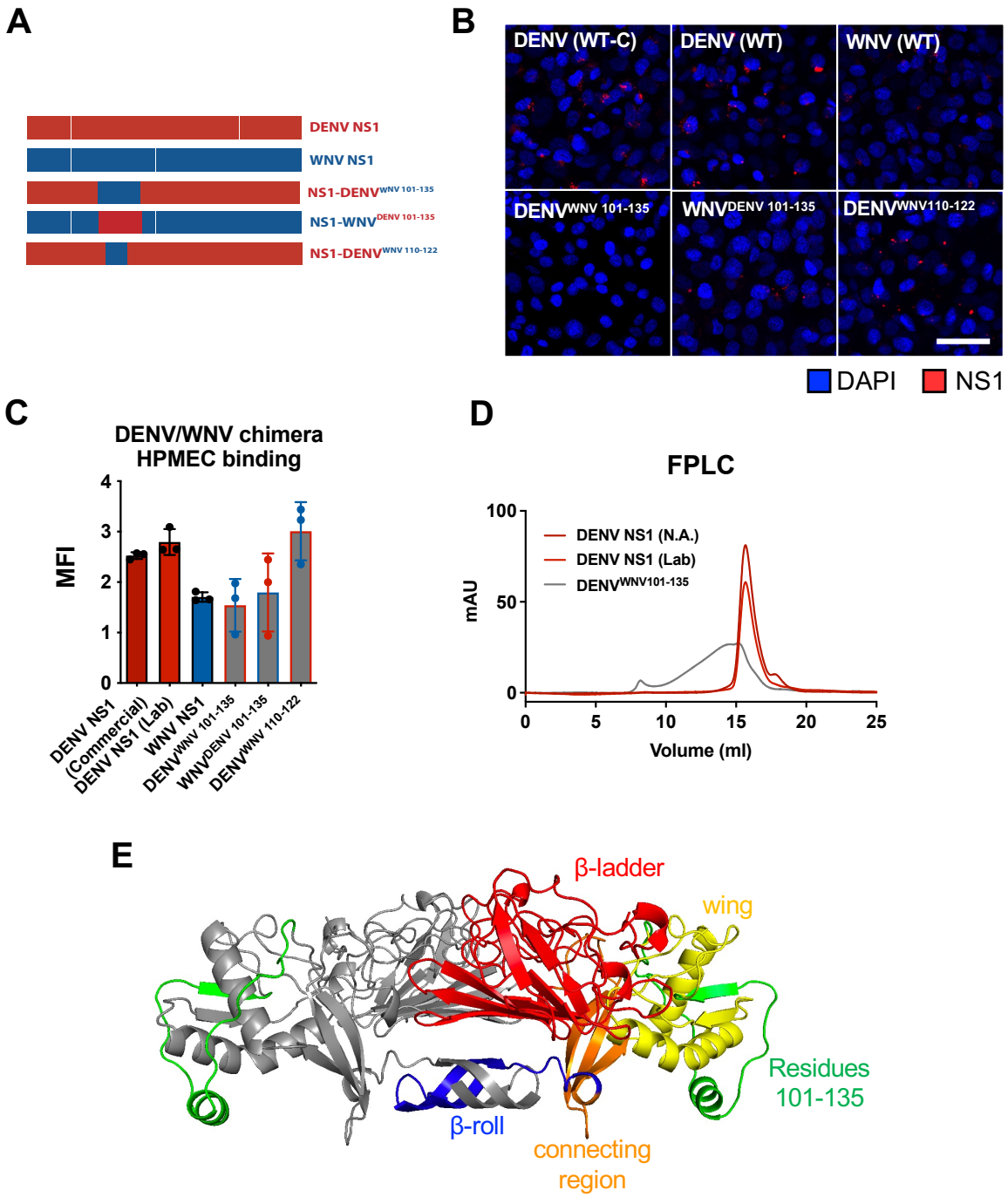

Figure 1. Residues 101-135 of DENV NS1 are necessary for NS1 binding to cells but not sufficient. **(A)** Schematic of chimeric NS1 proteins used in this figure. **(B)** WT or chimeric NS1 proteins were added to human pulmonary endothelial cells (HPMEC); cell binding was assessed by detection of conjugated anti-His antibody using immunofluorescence microscopy, quantified in **(C)**. **(D)** Size-exclusion chromatography plot of WT and chimeric NS1 proteins. **(E)** Dimeric DENV2 NS1 structure was predicted using AlphaFold. One monomer is coloured grey while the other monomer is coloured as follows: blue for β-roll, yellow for wing, red for β-ladder, and orange for inter-domain connecting regions. Residues 101-135 are highlighted in green. Data are representative of N=3 biological replicates, plotted as mean ± SEM. Scale bar, 50 μm.

Tissue-specific NS1-endothelial cell binding cannot be measured by flow cytometry

Concurrently, we were interested in establishing an alternate assay to measure NS1-endothelial cell binding. We explored flow cytometry, as it allows for high-throughput analysis with the ability to incorporate multiple NS1 concentrations in a given experiment. Following several studies that measured NS1 binding to glycosaminoglycans (GAGs) on the endothelial cell surface [17], we detached HPMEC from the cell culture flask before proceeding with the NS1 binding experiment, and then measured NS1 binding by flow cytometry using anti-His antibody conjugated to Alexa Fluor 647 (Fig. 2A, B). We found that all flavivirus NS1 proteins tested (DENV, WNV, ZIKV, and yellow fever virus [YFV]) bound to HPMEC, in contrast to previous data based on our standard IFA assay that had shown that DENV and YFV NS1 bound HPMEC at high levels whereas WNV and ZIKV NS1 exhibited only baseline binding to HPMEC [23]. We repeated the flow cytometry-based binding assay using human brain endothelial cells (HBMEC) (Fig. 2C, D), and found that all the flavivirus NS1 proteins tested (DENV, WNV, ZIKV) bound equally, consistent with the previous IFA data [23].

Overall, these data suggest that the tissue-specificity of NS1-endothelial cell binding cannot be captured by flow cytometry, possibly due to alteration of endothelial cell surface glycan components during the cell detachment process, which are known host factors to mediate tissue tropism of both virus and NS1. Notably, we also tried cell detachment after the NS1 cell binding step instead of before the binding step, which was also unsuccessful as the cell detachment step also removed the NS1 that was bound to the cells.

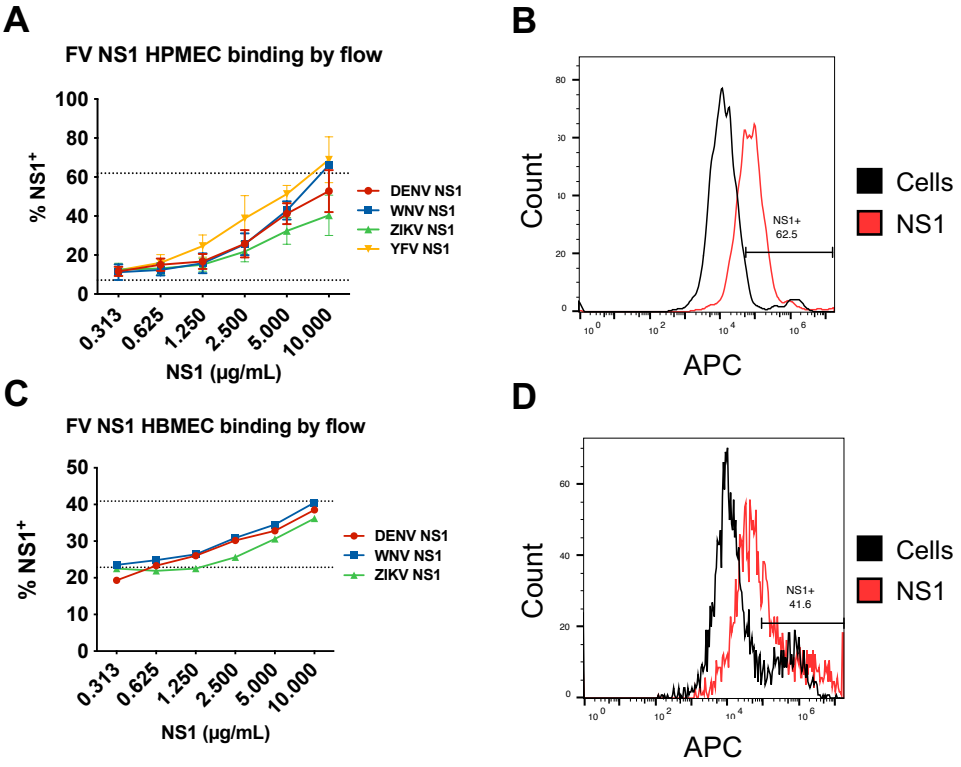

Figure 2. Tissue-specific NS1-endothelial cell binding cannot be measured by flow cytometry.
(A) HPMEC was suspended and treated with WT NS1 proteins from different flaviviruses (FV); NS1 binding was measured using flow cytometry. **(B)** Flow cytometry histogram of positive and negative controls of (A). **(C)** Same as (A), but with HBMEC. **(D)** Histogram of positive and negative controls of (C). APC, Allophycocyanin. Data are representative of n=3 biological replicates, plotted as mean ± SEM.

ZIKV NS1 causes partial endothelial hyperpermeability

As part of the manuscript revision process of the paper presented in Chapter 2, we included ZIKV NS1 in the TEER experiments. Here, the main point was that at higher NS1 concentrations, the endothelial cell hyperpermeability is driven by DENV NS1 β-ladder domain (W-W-D and D-W-D). Additionally, I found that like WNV NS1, ZIKV NS1 also induces partial endothelial hyperpermeability on HPMEC (Fig. 3).

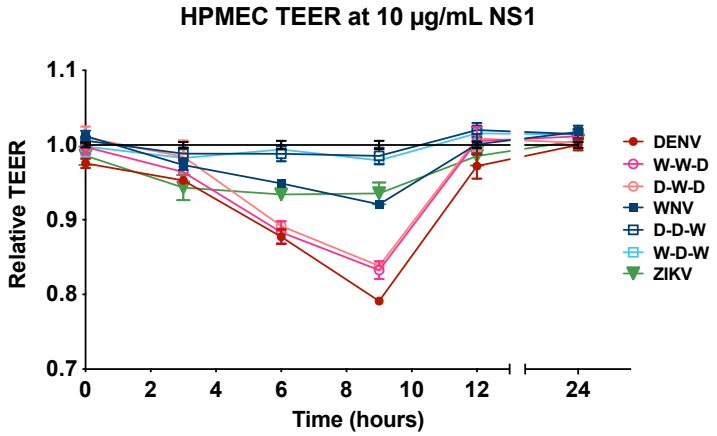

Figure 3. ZIKV NS1 causes partial endothelial hyperpermeability on HPMEC.
Extension of Figure 4 of Chapter 2. HPMEC seeded on Transwells were treated with WT or chimeric NS1 at 10 µg/mL. The trans-endothelial electrical resistance (TEER) between the apical and basolateral chamber was measured over time and normalized to the untreated controls at each timepoint. Data are representative of n=3 biological replicates, plotted as mean ± SEM.

Residues 123-130 do not affect NS1-endothelial cell binding

In the process of testing flow cytometry-based methods with HPMEC to measure cell binding, we also explored using suspension cells in flow cytometry, which would eliminate the need for cell detachment and would preserve the integrity of cell surface glycan attachment factors as well as NS1-cell binding. We tested NS1-cell binding on flow cytometry using HEK-293F cells that we use to produce NS1 proteins, and found that the NS1-HEK293F binding pattern by flow cytometry recapitulated the NS1-HPMEC binding data by IFA (Fig. 4A, B). WT DENV NS1 from both commercial and lab sources, as well as DENV$^{WNV110-122}$ NS1, bound HEK-293F at high levels, whereas WNV NS1, DENV$^{WNV101-135}$, and WNV$^{DENV101-135}$ NS1 exhibited low-level binding.

In addition to DENV$^{WNV110-122}$, we also divided the 101-135-residue portion into two additional parts – residues 101-109 and 123-135 (Fig. 4C) – and cloned and produced the proteins. We found that while construct DENV$^{WNV123-135}$ yielded comparable protein production as WT DENV NS1, construct DENV$^{WNV101-109}$ was poorly secreted (data not shown), suggesting that residues 101-109 harbour critical secondary structures that were disrupted in the chimeric protein. We tested NS1 binding to HEK293F using flow cytometry and found that construct DENV$^{WNV123-135}$ bound HEK293F at comparable levels to WT DENV NS1 (Fig. 4D, E), suggesting that these residues likely do not contain the molecular determinants for tissue-specific binding.

Using DENV2 NS1 structure previously predicted using AlphaFold (Fig. 1E), we show the locations of residues 101-109 (in pink) and 123-135 (in green) in the context of dimeric DENV NS1 (Fig. 4F, G). Residues 101-109 appear to be situated at a less surface-exposed location within the NS1 dimer than residues 123-135, which could be less amenable to chimerization and thus explain the poor secretion of the DENV$^{WNV101-109}$ chimera.

These data provided snippets of the bigger picture. Coupled with the structural integrity issues with several key NS1 chimeras, we decided to re-examine our approach and to re-start with chimeras that exchange the complete wing and β-ladder domains, which would minimize the risk of disrupting crucial secondary structures. These data and the story that developed were published and included in Chapter 2 of this dissertation.

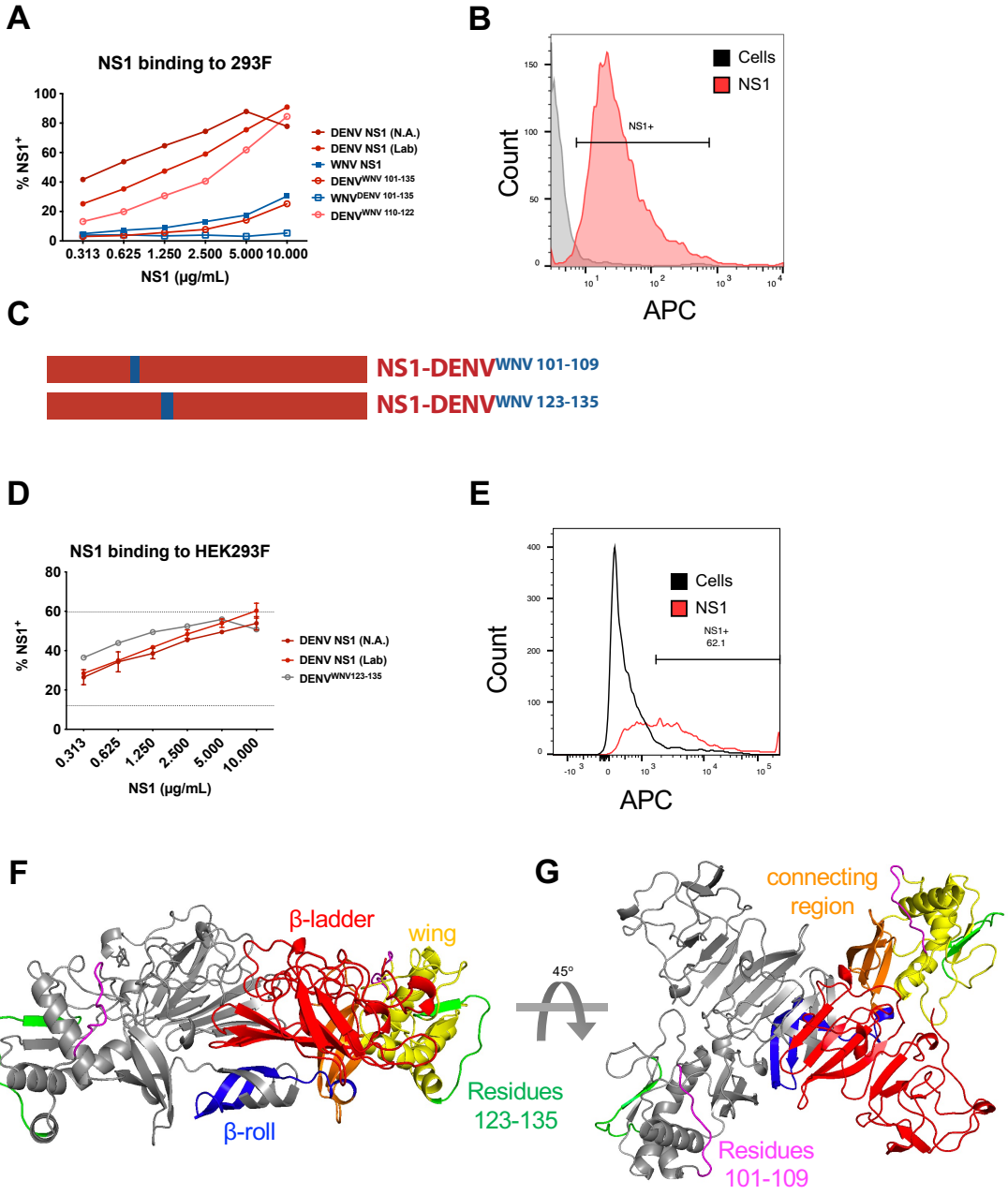

Figure 4. Residues 123-130 do not affect NS1-cell binding.
(A) HEK-293F cells were treated with WT or chimeric NS1 proteins that were previously measured by IFA on HPMEC. Binding was measured using flow cytometry. **(B)** Flow plot of positive and negative controls of (A). **(C)** Schematic of chimeric DENV NS1 proteins that exchanged specific wing domain residues with WNV NS1. **(D)** HEK-293F cells were treated with WT DENV NS1 from commercial or lab sources, or chimeric NS1 proteins and assessed for cell binding using flow cytometry. **(E)** Flow plot of positive and negative controls of (D). **(F, G)** Dimeric DENV2 NS1 structure was predicted using AlphaFold. One monomer is coloured grey while the other monomer is coloured as follows: blue for β-roll, yellow for wing, red for β-ladder, and orange for inter-domain connecting regions. Residues 101-109 are highlighted in pink, and residues 123-135 are highlighted in green. (F) and (G) are rotated 45º along the X-axis from each other. APC, Allophycocyanin.

WWG motif in the NS1 wing domain confers partial binding to HPMEC and HUVEC

While we were curious about the tissue-specific interactions of flavivirus NS1, we consistently observed a baseline level of NS1 binding to endothelial cells and wanted to determine the residues that might be mediating this conserved, baseline level of binding. Sequence alignment of NS1 proteins from multiple flaviviruses revealed that Trp-115, Trp-118, and Gly-119 residues within the wing domain are conserved across all flaviviruses, including tick-borne flaviviruses [32]. To determine whether the W115-W118-G119 motif mediated pan-flavivirus NS1 binding to endothelial cells, we mutated these residues to alanine ("DENV^{WWG}"), cloned and produced the proteins, and measured their capacity to bind HPMEC using IFA (Fig. 5A). We observed a partial binding reduction (Fig. 5B), suggesting a role for the WWG motif. To further examine whether the WWG motif also played a role in NS1-induced endothelial hyperpermeability, we treated HPMEC seeded on Transwells with either WT DENV or DENV^{WWG} NS1 and measured TEER as an inverse proxy for endothelial hyperpermeability (Fig. 5C). We found that DENV^{WWG} NS1 induced a lower TEER reduction (i.e., less hyperpermeability) than WT DENV NS1, suggesting that the WWG motif indeed also plays a role in endothelial hyperpermeability. This is consistent with our findings in Chapter 2 that identified the wing domain as playing a role in mediating NS1-induced TEER reduction.

Next, we explored whether the WWG motif also played a role in the binding of other flavivirus NS1 proteins to endothelial cells. We cloned and produced WWG mutants in WNV and ZIKV NS1 and treated HPMEC, HBMEC, and human umbilical vein endothelial cells (HUVEC) with these proteins to measure for cell binding using IFA (Fig. 5D–J). We normalized the mutant NS1 binding to that of WT NS1 binding, as each flavivirus NS1 bound each endothelial cell line at different levels. We found that the WWG mutant resulted in lower HPMEC binding compared to WT NS1 for all three flaviviruses tested, while having no effect on binding to HBMEC across all flavivirus NS1 proteins tested (Fig. 5K–M). Notably, WNV^{WWG} and ZIKV^{WWG} NS1 exhibited lower binding on HUVEC than their WT counterparts, suggesting a possible role for WWG for HUVEC binding as well (Fig. 5H, J).

Using DENV2 NS1 structure previously predicted using AlphaFold (Fig. 1E), we modeled the location of the WWG motif (in pink and labeled with black arrowheads) in the context of dimeric DENV NS1 (Fig. 5N, P). We found that the indole of Trp-115 and Trp-118 are predicted to protrude downwards on the exposed surface of NS1 dimer that is hypothesized to interact with the plasma membrane of cells – potentially explaining the roles of the WWG motif in endothelial binding and hyperpermeability.

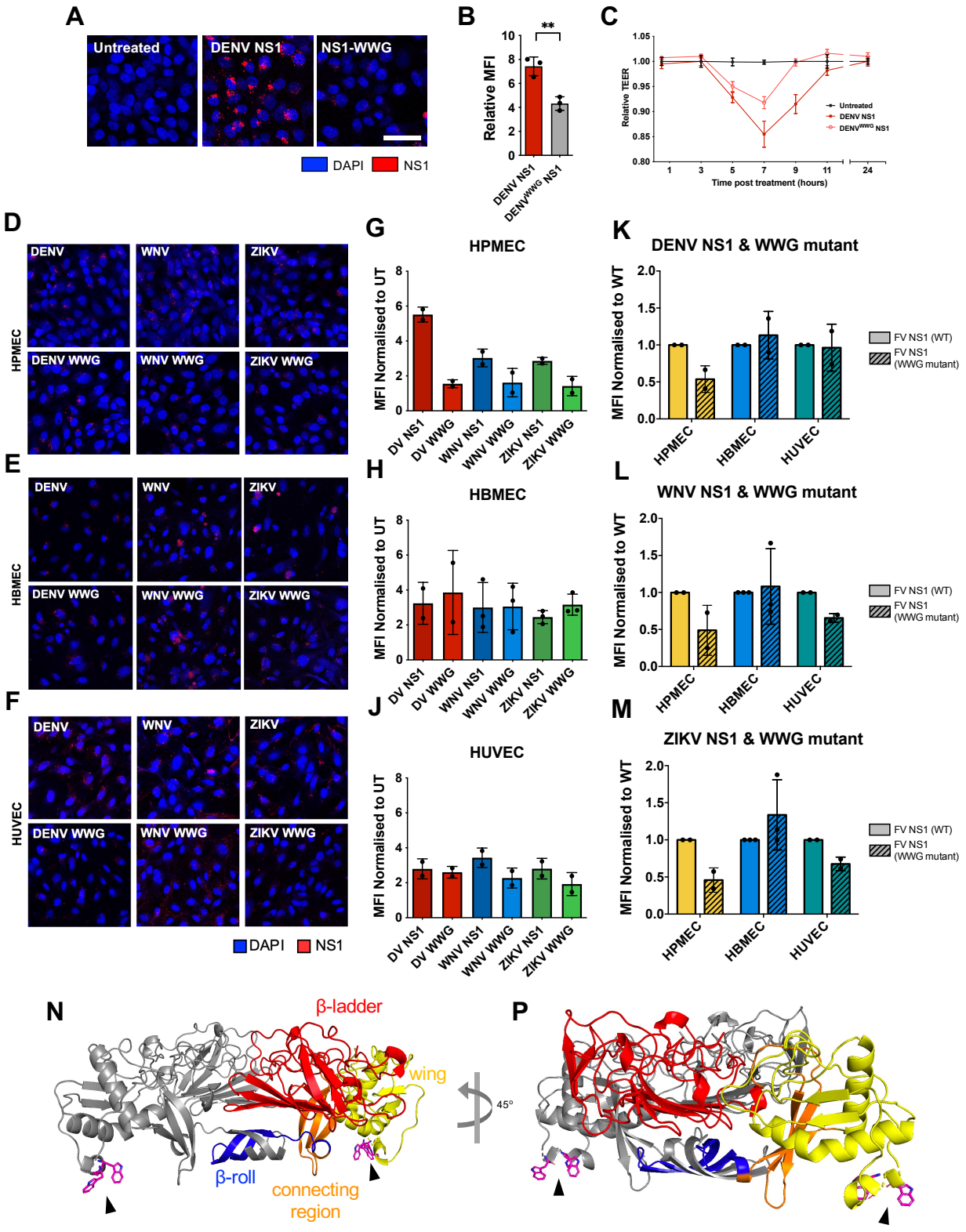

Figure 5. WWG motif in the NS1 wing domain confers partial binding to HPMEC.
(A) WT DENV or DENV W115A-W118A-G119A ("WWG") NS1 point mutant were treated on HPMEC and cell binding was assessed by immunofluorescence microscopy and quantified in **(B)**. (C) WT DENV or WWG NS1 mutant was treated on HPMEC seeded on trans-well. Endothelial hyperpermeability was

measured by TEER over time. **(D–F)** WT DENV, WNV, ZIKV NS1, and the respective WWG mutants were treated on (D) HPMEC, (E) HBMEC, and (F) HUVEC. Cell binding was measured by immunofluorescence microscopy and quantified based on either the cell types (**G–J)**, or the respective flavivirus NS1 or mutants in (**K**) DENV, (**L**) WNV, and (**M**) ZIKV. **(N, P)** Dimeric DENV2 NS1 structure was predicted using AlphaFold. WWG motif was denoted with its side chains in pink and indicated with black arrowheads. One monomer is coloured grey while the other monomer is coloured as follows: blue for β-roll, yellow for wing, red for β-ladder, and orange for inter-domain connecting regions. (N) and (P) are rotated 45º along the Y-axis from each other. Scale bar, 10μm. Data plotted representative of 3 biological replicates, as mean ± SEM. **$p<0.01$ by unpaired t-test.

Endocytosis-deficient DENV^{N207Q} NS1 mutant causes comparable leak as WT DENV NS1 in a mouse model of localized leak

Flavivirus NS1 contains two conserved N-linked glycans (N-glycans) at Asn-130 and Asn-207, with an additional site at Asn-175 for WNV, St. Louis encephalitis virus (SLEV), and Murray Valley encephalitis virus (MVEV) NS1 proteins. Previous studies from our laboratory demonstrated that Asn-207 glycosylation is particularly important for DENV NS1-mediated endothelial dysfunction [20]. The DENV^{N207Q} NS1 mutant was shown to exhibit comparable HPMEC binding to WT DENV NS1, while abrogating the capacity for both endocytosis and endothelial hyperpermeability as measured by TEER. As we discovered intriguingly in Chapter 2 that it was the wing, not β-ladder domain that appeared to drive vascular leak *in vivo* as measured by a mouse model of localized leak in the dorsal dermis, we explored whether Asn-207 glycosylation also affected vascular leak.

We administered PBS, WT NS1, or DENV^{N207Q} NS1 onto discrete spots of shaved dorsal dermis of mice, followed by intravascular injection of fluorophore-conjugated Dextran, and measured the relative fluorescence as a proxy for vascular leak (Fig. 6A, 6B). We found that while WT WNV NS1 caused lower levels of leak compared to WT DENV NS1 as expected, DENV^{N207Q} NS1 caused comparable levels of leak as WT DENV NS1. This suggests that while Asn-207 was critical for endocytosis and causing endothelial hyperpermeability *in vitro*, it does not play a role in vascular leak in the mouse dermis. Although unexpected, this result is supported by data from NS1 domain-exchanged chimeras in Chapter 2.

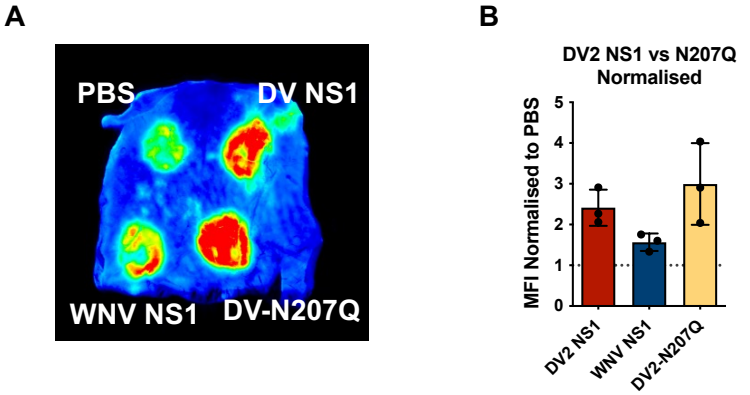

Figure 6. Endocytosis-deficient DENV N207Q NS1 mutant causes comparable leak as WT DENV NS1 in mouse model of localized leak.
The dorsal dermis of WT C57BL/6J mice were shaved 2 days prior to the experiment. PBS, WT, or mutant NS1 proteins were injected intradermally onto discrete spots in the shaved backs of mice, followed by intravascular injection of Alexa Fluor 648-conjugated Dextran. **(A)** The dorsal dermis was collected 2 hours post-treatment and measured for fluorescence indicating leak using fluorescent scanner, quantified in **(B).**

NS1 wing domain mediates binding to glycosaminoglycans on the endothelial cell surface

NS1 initiates its binding to endothelial cells via surface-bound GAGs. This is thought to be mediated by interactions between the positively charged residues on NS1 and the largely negatively charged GAGs on EC surfaces [17]. Endothelial cells have been shown to harbour distinct tissue-specific GAGs that contribute to NS1 tissue-specific binding to ECs [33].

Having shown that the DENV NS1 wing domain drives NS1-HPMEC binding, we wondered whether the presence of certain surface GAGs contributed to the higher binding levels of DENV NS1 compared to WNV NS1. We obtained HPMEC lines that had two genes individually knocked out (KO) by CRISPR-Cas9 technology for a different project in the laboratory [34]; the two genes, SLC35B2 and XYLT2, are involved in the heparan sulfate proteoglycan biosynthetic pathway. We confirmed by IFA that these KO HPMEC possessed less detectable heparan sulfate on the cell surface compared to control cells treated with non-targeting guide RNAs (Fig. 7A, B). We then treated non-targeted or XYLT2-KO HPMEC with the DENV/WNV NS1 proteins characterized in Chapter 2 – WT DENV, WNV, DENV/WNV chimera, and DENV/WNV NS1 that exchanged residues 91-93. We found that while all NS1 proteins showed reduced binding in XYLT2-KO HPMEC compared to the non-targeting control cells, the difference in binding levels between non-targeting and XYLT-KO cells were similar across NS1 proteins with both DENV and WNV backbones alike (Fig. 7C, D). This supports the overall hypothesis that EC surface-bound glycan components do play a significant role in overall NS1-EC binding, but the relative contribution of GAGs to NS1 tissue-specificity remains to be determined.

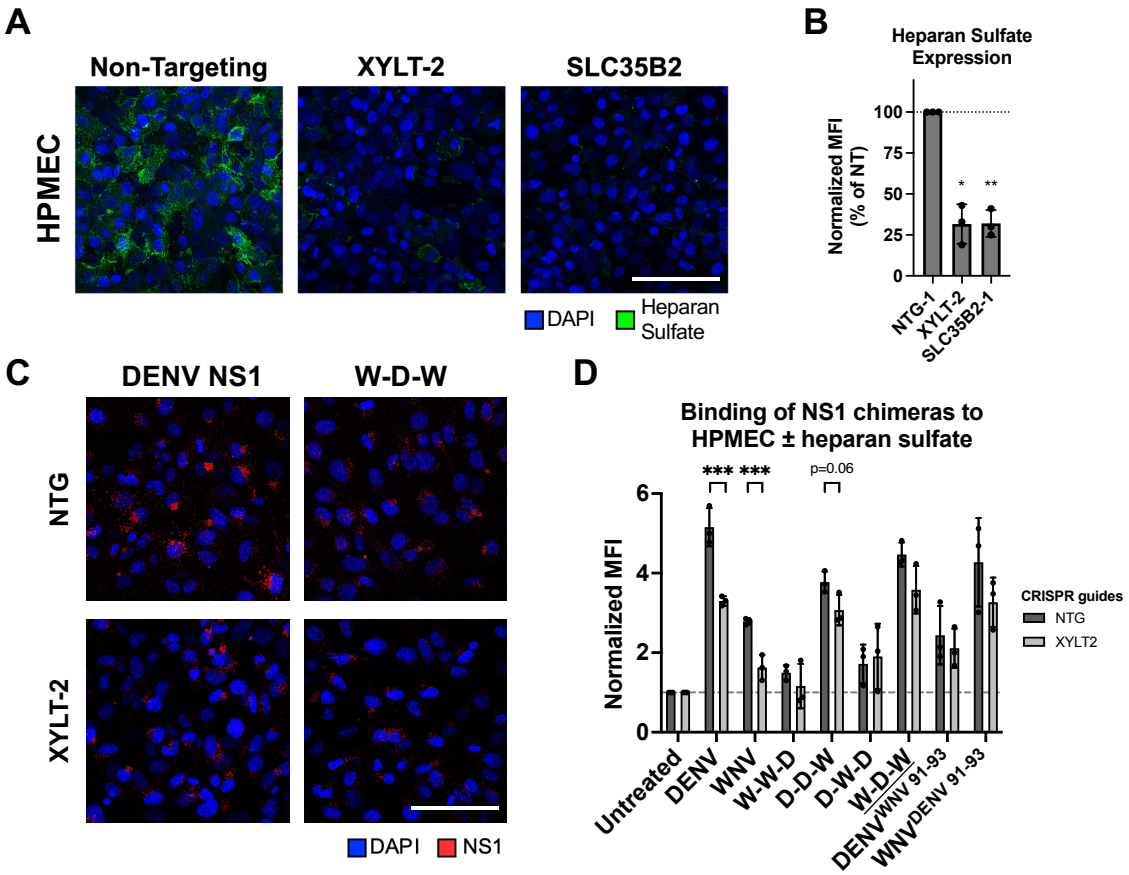

Figure 7. Depleting glycans on HPMEC surface reduces NS1 binding to HPMEC.
(A) Representative images of HPMEC transduced with lentivirus encoding the indicated guide RNAs for CRISPR knock-out cells, stained for heparan sulfate. **(B)** Quantification of (A), as a percentage of cells treated with the non-targeting guide (NTG). **(C)** 10µg/mL of WT or chimeric NS1 as indicated were added to HPMEC that had been transduced with lentivirus encoding the indicated guide RNAs, and cells were stained for NS1 on the cell surface. Images selected are representative of three independent experiments for two NS1 proteins that showed a significant difference between NTG and XYLT2. **(D)** Quantification of (C); constructs for images in (C) are underlined. Scale bars, 100µm; MFI, mean fluorescence intensity; NTG, non-targeting guide; XYLT2, xylosotransferase 2. Data plotted are 3 biological replicates, as mean ± SEM. *p<0.05, **p<0.01, ***p<0.005, ****p<0.001 by ANOVA with multiple comparisons (B) and Student's t-test (D), respectively.

Ongoing glycan-related projects in the Harris laboratory and with collaborators found that there are distinct heparan sulfate sulfation patterns across HPMEC, HBMEC, HUVEC, and dermal (HMEC) endothelial cells. To further explore whether levels of sulfation and what components of surface glycans are specifically mediating NS1 tissue-specificity from the host perspective, we obtained several bovine serum albumin (BSA)-conjugated glycans that were previously identified in a glycan array screen as part of an ongoing collaboration with Dr. Kamil Godula's laboratory at the University of California, San Diego. HS-1 is unsulfated, while HS-15, 16, 20, and 23 each contains varying levels and types of sulfation (Fig. 8A). We conducted an enzyme-linked immunosorbent assay (ELISA) that measured the binding levels of WT and chimeric DENV/WNV NS1 proteins added to plates coated with BSA-conjugated GAGs, including a BSA-heparin as

baseline control. We found that NS1 proteins bound all sulfated GAGs at higher levels than the non-sulfated HS-1 species, with little difference between each HS species. Unexpectedly, WNV NS1 bound all GAGs at higher levels than DENV NS1, and constructs W-**W**-D and D-**W**-D that contain the WNV NS1 wing domain bound higher than constructs D-**D**-W and W-**D**-W that contain the DENV NS1 wing domain (Fig. 8B). These data suggest that the NS1 wing domain drives NS1-GAG binding, which could partially contribute to the wing-driven NS1-endothelial cell binding. However, further studies are needed to solve the unexpectedly high levels of WNV NS1 wing-driven GAG binding versus DENV NS1 wing-driven EC binding.

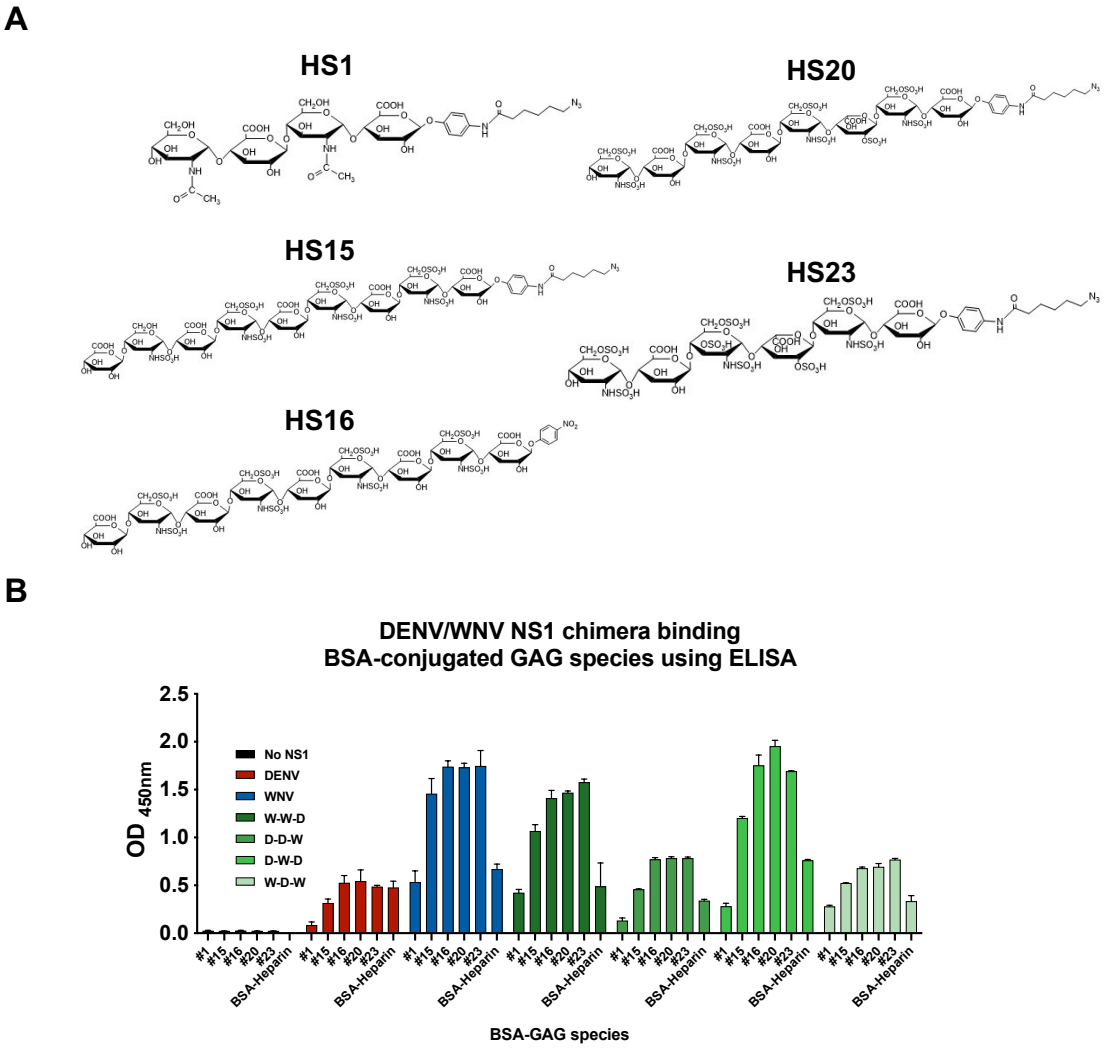

Figure 8. NS1 wing domain drives NS1 binding with select glycosaminoglycans.
(A) Structures of glycans identified in a previous glycan array screen; the glycans have varying disaccharide components and sulfation levels. **(B)** Glycans were coated on ELISA plates; WT or chimeric NS1 proteins were added and their binding capacity measured using ELISA. Data plotted are 3 biological replicates, as mean ± SEM**.**

Anti-DENV NS1 mouse monoclonal antibody 2B7 blocks NS1-endothelial cell binding and binds to the β-ladder domain of NS1

The Harris laboratory had previously shown that 2B7, an anti-DENV NS1 immunoglobulin G2b (IgG2b) monoclonal antibody (mAb), inhibits NS1-induced endothelial dysfunction *in vitro* [11]. As part of the follow-up study which resolved 2B7 crystal structure in complex with NS1 and characterized its effects *in vivo* and *in vitro* [29], we examined the *in vitro* mechanism of 2B7-NS1 blockade and binding.

We measured via IFA the levels of DENV NS1 binding to HPMEC that were treated with NS1 incubated with or without 2B7, 2B7 fragment antigen-binding (Fab) region, or an IgG control, and we found that both 2B7 and 2B7 Fab blocked NS1-HPMEC binding (Fig. 9A, 9B). This demonstrates that 2B7 potently blocks NS1-HPMEC binding in a manner independent of antibody Fc effector functions, which was repeated orthogonally in HEK-293F cells using flow cytometry (Fig. 9C).

The 2B7 structural study identified the NS1 epitopes to be in the β-ladder domain, specifically residues between residues 326 and 346. It was predicted that 2B7 binds to the β-ladder in a tilted orientation towards the NS1 hydrophobic surface in a manner that indirectly creates steric hindrance for the wing domain, blocking NS1-EC binding regardless of whether NS1 is in the dimeric or hexameric form [Ref 29, Fig. 4A, B]. As an additional confirmation that 2B7 blocks NS1 wing-driven endothelial cell binding by steric hindrance instead of direct inhibition, we conducted an ELISA with WT DENV NS1 and $DENV^{WWG}$ NS1 and found that 2B7 bound to both NS1 proteins equally, supporting the steric hindrance prediction (Fig. 9D).

At the beginning of the NS1-tissue specificity project before the co-crystal structure was solved, there were conflicting data as to where on NS1 2B7 bounds. As part of the 2B7 project, 2B7 binding profile to a number of different flavivirus NS1 proteins was assessed, and it was found to bind YFV NS1 at low levels compared to DENV NS1 [Ref 29, Fig. 3C]. Making use of this distinction, we constructed DENV/YFV NS1 chimera that exchanged YFV NS1 residues 101-135 and β-ladder separately into DENV NS1 (Fig. 9E). We conducted an ELISA with WT DENV, YFV, $DENV^{YFV101-135}$, and $DENV^{YFV\ \beta\text{-ladder}}$ NS1. We found that 2B7 bound WT DENV and $DENV^{YFV101-135}$ strongly, which contain the DENV NS1 β-ladder, whereas 2B7 bound WT YFV and $DENV^{YFV\ \beta\text{-ladder}}$ weakly, which contain YFV NS1 β-ladder (Fig. 9F). This suggests that the 2B7 binding pattern reflects the presence of the DENV NS1 β-ladder and supports the eventual identification of 2B7 epitopes on the β-ladder domain of NS1.

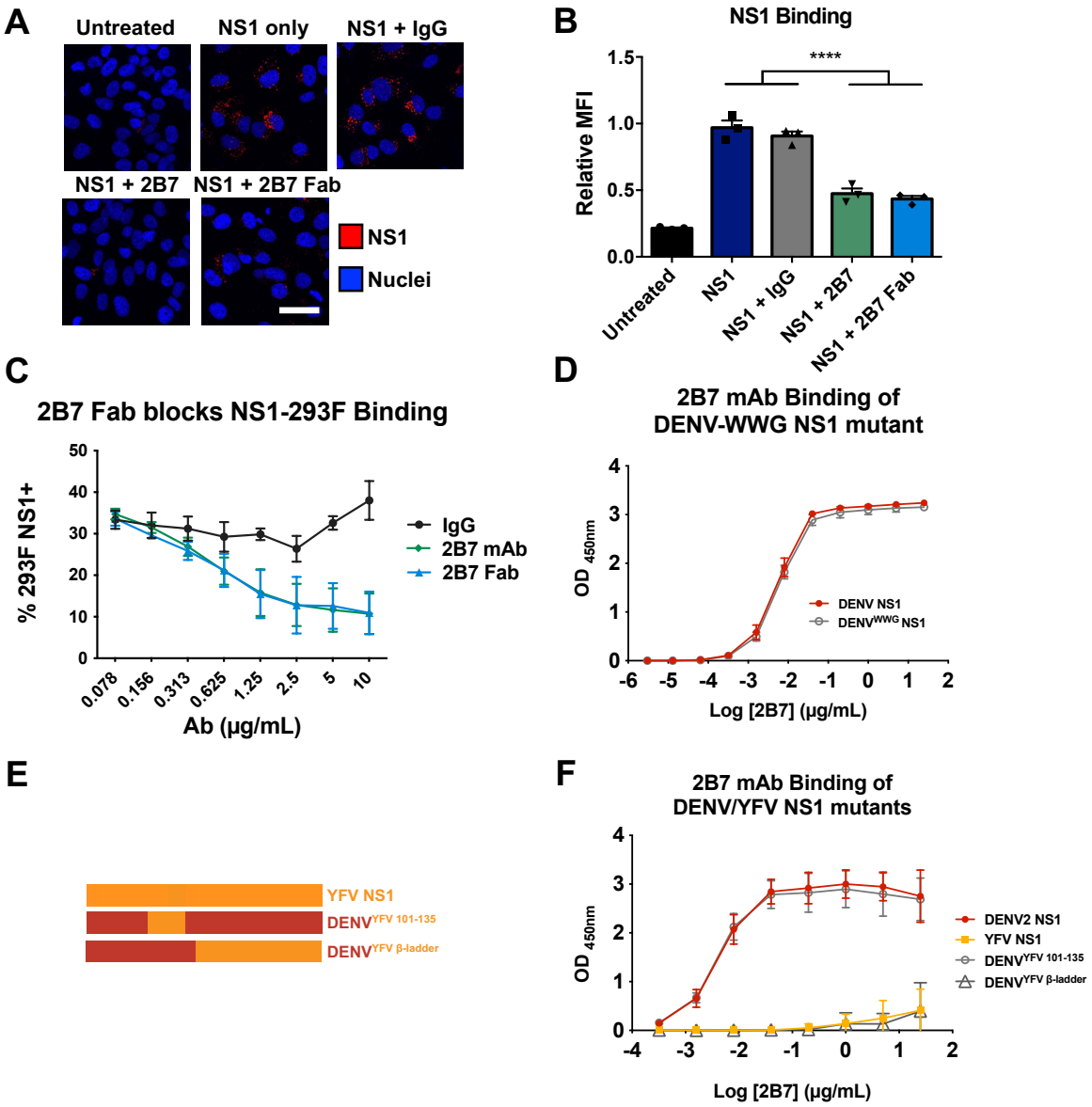

Figure 9. Anti-DENV NS1 mouse monoclonal antibody 2B7 blocks NS1-endothelial cell binding and binds to the β-ladder domain of NS1.

(A) DENV NS1-HPMEC binding in the presence or absence of full-length 2B7 mAb, the 2B7 Fab, or indicated controls, was measured by immunofluorescence assay (IFA) 90 minutes post-NS1 treatment and quantified in **(B). (C)** DENV NS1 cell binding assay using HEK-293F suspension cells. NS1 was incubated with indicated concentration of 2B7 mAb or 2B7 Fab and added to U-bottom 96-well plate containing 293F cells. NS1 binding to cells was assessed by flow cytometry. **(D)** Direct ELISA of WT DENV and $DENV^{WWG}$ mutant NS1, detected by 2B7. **(E)** Schematic diagram of DENV/YFV NS1 chimeras. **(F)** Direct ELISA of WT DENV, YFV, and chimeric DENV/YFV NS1 proteins, detected by 2B7. For (A), data are representative images from n=3 biological replicates. Scale bar, 50 µm. Data are presented as mean ± SEM of n=3 biological replicates for all. ****p<0.001 by unpaired t-test. Part of this figure was published in Biering,* Akey* et al (2021) [29].

Virion binding-deficient DENV^{E343K} NS1 mutant does not affect HPMEC binding or hyperpermeability

One of the ongoing projects in the Harris laboratory studies the capacity of flavivirus NS1 to enhance viral dissemination of flavivirus infections. In this project, NS1 was found to enhance virus crossing through endothelial cell monolayers and infection of monocytes in the basolateral chamber, in part due to NS1-virion interactions (data not shown, manuscript in preparation). Our collaborator Dr. Richard Kuhn at Purdue University identified E343 in the β-ladder of DENV NS1 to be a molecular determinant for NS1 interaction with DENV virion. We cloned and produced the DENV^{E343K} NS1 mutant in the Harris laboratory for further characterizations. We found that in a Transwell setup that models cross-endothelial barrier infection, DENV treatment of apical cells in the presence of DENV^{E343K} NS1 mutant resulted in significantly lower rate of infection of the basolateral monocytic cells compared to DENV treatment in the presence of WT DENV NS1, suggesting that DENV infection of monocytic cells depends on direct NS1-virion interactions.

To investigate whether DENV^{E343K} NS1 has any deficiencies in NS1-EC interactions, we measured NS1-HPMEC binding by IFA, and found that DENV^{E343K} NS1 bound at comparable levels to WT DENV NS1, which were significantly higher than the binding levels of WT WNV NS1 (Fig. 10A, B). We further found that DENV^{E343K} NS1 also results in comparable HPMEC hyperpermeability compared to WT DENV NS1 as measured by TEER. In the TEER assay, WT WNV NS1 was included as a control, which resulted in reduced HPMEC hyperpermeability, alongside endothelial cell dysfunction-deficient DENV^{N207Q} NS1 which showed abrogated hyperpermeability as expected (Fig. 10C). The location of residue E343 was highlighted on a DENV2 NS1 dimer that was resolved in a previous study [29]. E343 was found to be located in the upper part of NS1 dimer (Fig. 10D, E), on the protein face that is hypothesized to be interacting with the DENV virion. Taken together, this suggests that while DENV^{E343K} NS1 is deficient in binding DENV virion, it functions comparably to WT DENV NS1 in binding EC and triggering endothelial hyperpermeability.

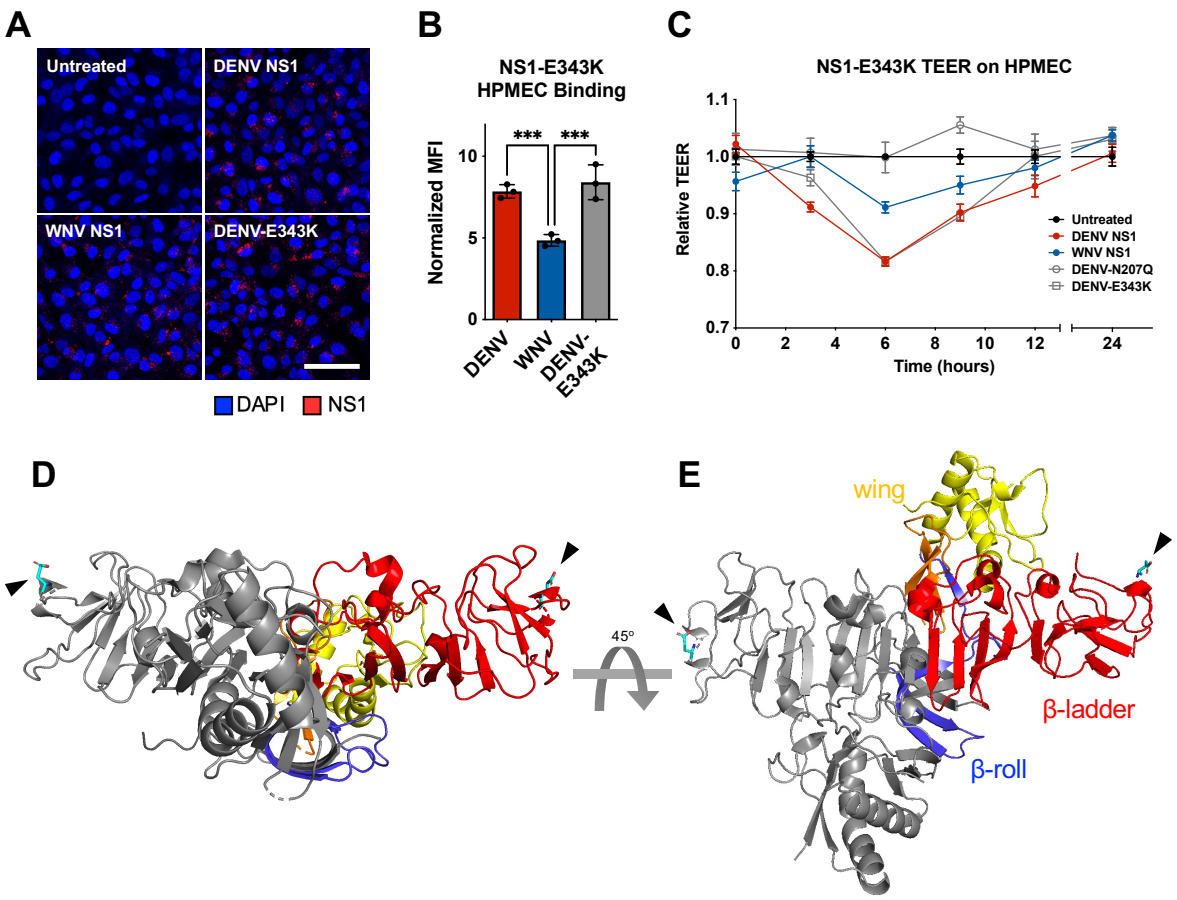

Figure 10. DENV NS1-E343K mutant does not affect binding or TEER on HPMEC.
(A) WT DENV, WNV, or mutant DENV-E343K NS1 proteins were added to HPMEC at 10µg/mL for 2h at 37ºC. NS1 binding was assessed with A684-conjugated anti-His antibody using immunofluorescence microscopy and quantified as mean fluorescence intensity (MFI) in **(B)**. **(C)** WT or mutant NS1 are added to HPMEC seeded on trans-wells. The trans-endothelial electrical resistance (TEER) between the apical and basal chambers are measured over time. **(D, E)** Dimeric DENV2 NS1 structure at 2.89Å (PDB 7K93, [29]) was annotated to show the location of residue E343 in the β-ladder in spatial and structural reference to the rest of NS1. One monomer is coloured grey while the other monomer is coloured as follows: blue for β-roll, yellow for wing, red for β-ladder, and orange for inter-domain connecting regions. E343 is coloured in cyan and indicated with black arrowheads. (D) and (E) are rotated 45º along the X-axis from each other. Data are representative of N=3 biological replicates, plotted as mean ± SEM. Scale bar, 50µm. ***p<0.005 by unpaired t-test.

Table 1. NS1 mutants used in this chapter.

Lab notation	NS1 backbone	Construct chimera/ mutation
C1	DENV-2	WT
C2	WNV	WT
C11	DENV-2	aa 101-135
C14	DENV2	Glycosylation mutant N207Q
C23	ZIKV	WT
C30	DENV2	W115A+W118A+G119A
C32	WNV	DENV2 aa101-135
C35	DENV2	WNV aa110-122
C36	WNV	W115A+W118A+G119A
C37	ZIKV	W115A+W118A+G119A
C41	DENV2	WNV aa101-109
C42	DENV2	WNV aa123-135
C44	YFV	WT
C45	DENV2	YFV aa101-135
C46	DENV2	YFV aa101-119
C47	DENV	YFV NS1 β-ladder
C55	DENV	E343K

Discussion

In this chapter, I laid out a series of investigations supporting my main finding in Chapter 2 that led to defining the wing domain as the driver of NS1-tissue specific interactions with endothelial cells (EC). We first showed that our initial data suggested residues 101-135 to harbour residues important for NS1 tissue specificity, which was subsequently found to be due to protein misfolding. We then attempted to use a high-throughput flow cytometry-based method to evaluate HPMEC binding and discovered that while we could show NS1-HPMEC binding, the tissue-specificity of different flavivirus NS1 was lost. However, by using HEK-293F suspension cells, we could model the EC tissue specificity and showed that residues 123-135 likely did not affect tissue-specific binding. We further showed that the W-W-G motif in the wing domain affects only NS1 binding with HPMEC and to a smaller extent HUVEC, but not HBMEC. Further, we found that the EC entry-deficient N207Q mutant NS1 could cause comparable vascular leak as WT DENV NS1 in a model of localized leak in the mouse dermis. On the host front, we showed that the NS1 wing domain drives binding with the endothelial cell surface-bound glycans. Finally, we examined the virion binding-deficient E343K NS1 mutant and found that it has no defects in binding ECs and causing endothelial hyperpermeability.

Based on the initial binding data of $DENV^{WNV101-135}$, we thought that residues 101-135 might harbour residues involved in determining NS1 tissue-specificity. However, when we analyzed the chimeric protein on native PAGE gel (data not shown) as well as size-exclusion chromatography, we found that $DENV^{WNV101-135}$ was likely misfolded (Fig. 1). Based on the ZIKV NS1 structure, which is the only NS1 structure that has the flexible loop (residues ~108-129) resolved [25], we hypothesize that the chimerization likely disrupted secondary structures to result in protein misfolding. Notably, the DENV NS1 structure we predicted using AlphaFold (Fig. 1E, 4F–G, and 5N–P) suggested an alpha helix at residues 115-122, which was also present in the AlphaFold prediction of ZIKV NS1 (data not shown). However, the alpha helix was not present in the crystallized structure of ZIKV NS1 [25], the only flavivirus NS1 structure that resolved the flexible loop. This caveat points to the limits of protein structure prediction, and highlights the disorderly nature of the flexible loop of the wing domain which requires further structural studies.

Our attempt to evaluate HPMEC binding using flow cytometry did not work as expected, as HPMEC lost the tissue-specific binding capacity and bound all flavivirus NS1 proteins at equal levels (Fig. 2). This methodology was in part adapted from a study demonstrating that DENV NS1 attaches to uninfected cells via interaction with GAGs using flow cytometry, which showed that DENV NS1 bound strongly to dermal and lung ECs, Vero, and CHO cells, among others [17]. As it has been suggested that the GAG components present on EC surfaces play important roles in viral tropism and macrophage localization [33,35,36], it is possible that HPMEC lost its unique GAG composition that determine NS1 tropism after being detached from the adherent surface. In an orthogonal approach, we used flow cytometry to assess NS1 binding to HEK-293F suspension cells, where we found that DENV NS1 but not WNV NS1 bound to 293F cells (Fig. 4). We divided residues 101-135 into three portions, each in a different construct, and found that $DENV^{WNV123-135}$ bound 293F cells comparably to WT whereas $DENV^{WNV101-109}$ had negligible secretion, suggesting that the chimerization of residues 101-135 had disrupted secondary structure within residues 101-109, and that residues 123-135 likely did not harbour the molecular determinants of NS1 tissue-specific interactions.

While different flavivirus NS1 proteins contain residues that mediate tissue-specific binding and interactions with ECs, we hypothesized that certain highly conserved residues might mediate a baseline binding for all flavivirus NS1 proteins with ECs. A group of such residues are W115-

W118-G119 within the NS1 wing domain, which form a motif. The DENV^{WWG} NS1 that mutated this motif to alanines showed reduced HPMEC binding and TEER reduction (Fig. 5). However, WNV^{WWG} and ZIKV^{WWG} NS1 mutants showed reduce binding only on HPMEC but not HUVEC or HBMEC, suggesting that the WWG motif is only a pan-FV NS1 binding motif on HPMEC. One explanation could be that the WWG motif interacts preferentially with the specific GAGs present on the surface of HPMEC, as evident in the predicted DENV NS1 structure which showed the downward orientation of W115 and W118 pointing towards the plasma membrane (Fig. 5N, P). Data from ongoing glycan projects in the Harris laboratory suggest that GAGs on the HPMEC surface are generally less sulfated than on other endothelial cells, where sulfation is known to dictate signaling and trafficking. Indeed, we found that knocking out heparan sulfate on HPMEC reduces overall NS1 binding regardless of its parental viral source (Fig. 7), and that it is the NS1 wing domain that mediates binding to GAG components (Fig. 8). It is no surprise that NS1-GAG binding is also driven by NS1 wing domain, which is consistent with wing-driven EC binding from Chapter 2. The interesting finding is that it is the WNV and not DENV NS1 wing domain that displays higher binding to ECs, and that WNV NS1 bound GAGs at higher levels than DENV NS1. One hypothesis is that the lower DENV NS1-GAG binding levels suggest lower specificity, which would enhance the breadth of GAGs DENV NS1 could in turn bind to, hence explaining the more promiscuous nature of DENV compared to WNV NS1 in interacting with ECs. Overall, the pan-flavivirus NS1 binding data alongside these preliminary glycan data will complement the ongoing glycan and NS1 host receptor projects.

Our previous data from Chapter 2 and other studies [20,29] showed that residues in the NS1 β-ladder domain mediate NS1-induced dysfunction, suggesting that these residues likely also affect NS1-induced vascular leak *in vivo*. In Chapter 2, I found that WNV NS1 containing DENV NS1 molecular determinants for binding were able to cause comparable leak as WT DENV NS1 in our mouse dorsal dermis model, contradicting this reasoning. In this chapter, I find that the N207Q NS1 mutant, which is deficient for cell internalization and NS1-induced EC hyperpermeability [20], caused comparable intradermal leak as WT DENV NS1, at higher levels than WNV NS1 (Fig. 6). This further supports the idea that even though β-ladder residues mediate NS1-induced EC dysfunctions *in vitro*, it is possible that the wing domain remains the dominant determinant pertaining to vascular leak. This then raises the follow-up question as to what the TEER assay is modeling, e.g., mislocalization of TJ/AJ proteins and paracellular transport vs glycocalyx disruption. Alternatively, it is possible that the tissue source plays a role, as the TEER assay was performed on HPMEC (lung origin), while the localized vascular leak model involves the dermal ECs. While it is also possible that vascular leak *in vivo* is driven by cytokine or non-EC intrinsic mechanisms, our data from other projects show negligible NS1-induced secretion of IL-6, IL-8, and TNF-α from human monocytes, making this case less likely. Future experiments would include systemic instead of localized vascular leak, as well as using HMEC for TEER to better model vascular leak *in vitro*. Of course, transferring these and all the aforementioned NS1 mutations into DENV and other flavivirus infectious clones would be the eventual goal, where we could assess the roles of these molecular determinants in the context of viral infections.

Our initial data suggested that the mouse mAb 2B7 may bind to NS1 in the wing domain. As I was unraveling whether the data derived from DENV$^{WNV101-135}$ mutant could be relied on, it was crucial that we know whether 2B7 binds NS1 in the wing or β-ladder domain. We had found that 2B7 recognizes YFV NS1 poorly compared to DENV NS1, and used the DENV/YFV chimeric NS1 to determine that 2B7 binds NS1 in the β-ladder domain. We eventually identified specific residues within the range of 299-340 as the 2B7 epitopes, and showed that 2B7 protects against

vascular leak in lethal DENV challenge by causing steric hindrance with the NS1 wing domain, thus blocking NS1-EC interactions regardless of the oligomeric state of NS1. Data from 2B7 demonstrate a proof-of-concept for an anti-NS1 mAb as an antiviral therapeutic to reduce morbidity and mortality in severe dengue patients.

Overall, this chapter lays out additional structure-function studies conducted on DENV NS1, and provides molecular insights on future studies into pan-flavivirus NS1 molecular determinants, NS1 host factors, as well as flavivirus pathogenesis.

Materials and Methods

Cell lines

FreeStyle 293F suspension cells (Thermo Fisher Scientific) were used for production of recombinant NS1 proteins. 293F cells were cultured in FreeStyle 293 Expression medium (Thermo Fisher Scientific) containing 1% penicillin/streptomycin (P/S) and grown in a CO_2 incubator at 37°C with 8% CO_2 and maintained on a cell shaker at ~130 rpm. HPMEC (HPMEC-ST1.6r) were kindly donated by Dr. J.C. Kirkpatrick at Johannes Gutenberg University, Germany, and were used for NS1 cell binding and TEER assays. HUVEC were received as a kind gift from Dr. Melissa Lodoen at the University of California, Irvine. HUVEC are primary endothelial cells obtained from a single female donor (Lonza). HPMEC and HUVEC cell lines were propagated (passages 5–10) and maintained in endothelial growth medium 2 (EGM-2) using the EGM-2 bullet kit from Lonza following the manufacturer's specifications and grown at 37ºC with 5% CO_2. Human brain microvascular endothelial cells (HBMEC) were kindly donated by Dr. Ana Rodriguez at New York University. HBMECs were maintained in endothelial cell medium supplemented with endothelial growth factors from ScienCell Research Labs and grown at 37°C with 5% CO_2.

NS1 mutagenesis and cloning chimeric NS1 genes

Chimeric NS1 proteins were produced by amplifying fragments of the β-roll, wing, and β-ladder domains from WT DENV2 NS1 (Thailand/16681), WNV NS1 (NY99), or ZIKV NS1 (Uganda MR766), using primers listed in Table 1. The N-terminus of the β-roll and C-terminus of β-ladder primer sequences were flanked with nucleotide bases complementary to the protein expression vector plasmid "pMAB". The pMAB vector encodes a N-terminal CD33 signal sequence and C-terminal 6xHis tag, a kind gift from Dr. Michael Diamond, Washington University at St. Louis. The domain fragments and pMAB vector were fused together using overlap extension PCR. Site-directed NS1 mutants were produced using a site-directed mutagenesis kit (QuikChange XL Site-Directed Mutagenesis Kit, Agilent) following the manufacturer's instructions, with primers listed in Table 1. All mutant NS1 constructs were sequence-verified with 5' and 3' primers that recognize the pMAB vector beyond the mutagenesis insertion region.

NS1 protein production and purification

Plasmids containing WT or mutant NS1 sequences were transfected into FreeStyle 293F cells using polyethylenimine (PEI) (40K) (Sigma) according to the manufacturer's instructions. 48 to 72 hours post-transfection, NS1-containing supernatants were collected, filtered through a 0.45 μm cellulose acetate membrane to remove cell debris, and stored at -80ºC prior to protein purification. The NS1-containing supernatants were thawed, mixed 1:1 with binding buffer (20 mM sodium phosphate, 500 mM sodium chloride, 20 mM imidazole, pH 7.4), and bound to HisPur cobalt resin (Thermo Fisher Scientific) with shaking for 2 hours at room temperature. The NS1-resin mixture was then transferred to a column and washed 5 times in wash buffer (20 mM sodium phosphate, 500 mM sodium chloride, 25 mM imidazole, pH 7.4). NS1 was then eluted from the HisPur cobalt resin with elution buffer (20 mM sodium phosphate, 500 mM sodium chloride, 200 mM imidazole, pH 7.4) over 5 fractions. The purified NS1 stocks were then subjected to dialysis against 1X PBS for 48 hours at 4ºC and concentrated using Amicon filters with 10,000 molecular weight cut-off (Millipore). The Pierce BCA protein quantitation kit (Thermo Fisher Scientific) was used to quantify the purified recombinant proteins according to manufacturer's instructions. These proteins were used for all experiments within this study.

Size-exclusion chromatography
For size-exclusion chromatography, 0.125 mg (500 µL of a 0.25 mg/mL stock) of the indicated purified and dialyzed NS1 proteins was injected into a Superose 6 Increase 10/300 GL column (GE Life Sciences) previously equilibrated with 1X PBS; the eluate was monitored by absorbance at 280 nm. Peak fractions were analyzed by SDS-PAGE (2.5 µL of each 1-mL fraction) and probed with anti-His antibody.

Production of 2B7 antibody and Fab fragment
The 2B7 hybridoma cells were expanded in RPMI media (Gibco) with 10% FBS and 1% P/S (GoldBio). At 800 mL or 1.6 L, the conditioned media was cleared by centrifugation at 1,000 RPM at 4°C for 30 minutes. The cleared media was then mixed with an equal volume of protein G binding buffer (Thermo Scientific). This mixture was then passed over a protein G column (6 mL resin) and washed with binding buffer, and the antibody was eluted with several 5 mL fractions of protein G elution buffer (Thermo Scientific).

The 2B7 Fab fragment was produced by incubation of 600 µL of 2B7 mAb (~12 mg/mL) with immobilized papain at 37°C for 16-18 hours on an orbital rocker, followed by separation on a protein A column (Pierce™ Fab Preparation Kit, ThermoFischer 44985). The protein A flow-through was collected and further purified on a Sephadex 75 (GE) column equilibrated in 50 mM Tris pH 8.5, 50 mM $(NH_4)_2SO_4$ and 10% glycerol.

NS1 adherent cell binding immunofluorescent assay (IFA)
To measure binding of WT and mutant NS1 proteins to HPMEC, HUVEC, and HBMEC, $1x10^5$ cells were seeded on glass coverslips in 24-well plates. Cells were allowed to form a fully confluent monolayer for 3 days, with medium change every other day. On the day of the experiment, 10 µg/mL (3 µg in 300 µL) of NS1 proteins were prepared in 10 µL medium, then added to the cells. Untreated wells were used as negative controls. NS1 and cells were incubated for 1 hour at 37ºC. Mouse anti-6xHis antibody conjugated to Alexa Fluor 647 (Novus Biologicals) was then added at a dilution of 1:200, together with Hoechst 33342 (Immunochemistry) at a 1:2000 dilution for staining of nuclei, for 30 minutes at 37ºC. Cells were then washed twice in 1X PBS followed by fixation in 4% formaldehyde diluted in 1X PBS (Thermo Fisher Scientific).

For heparan sulfate staining, $1x10^5$ HPMEC were seeded on 0.2% gelatin (Sigma)-coated glass coverslips in 24-well plates. Cells were allowed to form a fully confluent monolayer for 3 days, with medium change every other day. On day of experiment, cells were washed 2x with PBS and fixed with 4% formaldehyde in PBS (Thermo Fisher Scientific), followed by another 2x PBS wash. Heparan sulfate was stained with 1:2000 heparan sulfate antibody (Amsbio, clone F58-10E6, 370255-s) overnight at 4ºC. Cells were then washed 2x with PBS and stained with anti-mouse IgM conjugated to Alexa Fluor 488 (Novus Biologicals) together with Hoechst 33342 (Immunochemistry) for 2 hours at RT.

For the 2B7 cell binding assay, 2B7 or an IgG isotype control was added to live cells instead of the fluorophore-treated anti-His antibody and were instead stained with a goat anti-mouse secondary IgG antibody conjugated to Alexa Fluor 647 (Abcam) after fixation to detect 2B7 binding to cells.

For all, coverslips were then mounted onto microscope slides on a drop of ProLong Gold (Thermo Fisher Scientific) and imaged using a Zeiss LSM 710 inverted confocal microscope (CRL Molecular Imaging Center, UC Berkeley). Images were processed using ImageJ software.

NS1 suspension cell binding assay and flow cytometry

To measure binding of WT and mutant NS1 proteins to suspended HPMEC, HPMEC was detached from culture flask using fibronectin-cleaving protease "Dispase" (StemCell Technologies). $1x10^5$ cells/well were used in a 96-well round-bottom plate in FACS buffer (1X PBS + 5% FBS).

To measure binding of WT and mutant NS1 proteins to HEK-293F suspension cells, $1x10^5$ cells/well were seeded into a 96-well round-bottom plate in FACS buffer (1X PBS + 5% FBS).

For 2B7 blocking NS1-EC binding experiments, 2B7 was diluted at indicated concentrations and co-incubated with NS1 for 30 minutes at 37ºC before treatment to cells.

Concurrently, NS1 dilutions were made 1:2 from 10 µg/mL. NS1 ranging from 0.3 to 10 µg/mL was then added to cells and allowed to incubate for 45 minutes at 37°C and was then washed 2x in FACS buffer. A mouse anti-His antibody conjugated to Alexa Fluor 647 (Novus Biologicals) was then added to cells at a dilution of 1:200 and allowed to incubate for 30 minutes at room temperature protected from light. Cells were washed 2x more in FACS buffer, followed by fixation in 4% formaldehyde (Thermo Fisher Scientific) and then resuspension in PBS. Flow cytometry was conducted using an LSR Fortessa Flow Cytometer (UC Berkeley Flow Cytometry Facility) or Intellicyt iQue3 to assess NS1 binding to cells. Flow cytometry profiles were gated on single cells and NS1-positive/negative controls.

Trans-endothelial electrical resistance (TEER)

The trans-endothelial electrical resistance assay was used to measure the functional effect of NS1 on endothelial barrier function in HPMEC as previously described [23]. Briefly, $1x10^5$ cells (HPMEC) were seeded in 300 µL of medium on the polycarbonate membrane insert of a Transwell (Transwell permeable support, 0.4 µm, 6.5 mm insert; Corning Inc.). The Transwell was placed in a well on a 24-well plate, becoming the apical (upper) chamber. 1.5 mL of media was added to the basolateral (lower) chamber. Cells were allowed to form a monolayer for 3 days with media changes in both apical and basolateral chambers every day, until the inter-chamber electrical resistance reached about 60Ω difference between Transwells seeded with (~150Ω) and without cells (~90Ω). On the day of experiment, 2.5 or 5 µg/mL of indicated NS1 proteins (0.75 or 1.5 µg proteins, respectively) were mixed with media up to 10µL, and added to the apical chambers of the Transwells. Electrical resistance between the apical and basolateral chambers was measured in ohms using an Epithelial Volt Ohm Meter (EVOM) with an electrode pair (World Precision Instruments), at the times indicated in the figures. Transwells containing no cells and untreated Transwells containing only cells were used as negative controls to calculate the baseline electrical resistance at each timepoint. Relative TEER was calculated as a ratio of resistance values $((\Omega_{experimental} - \Omega_{media\ only}) / (\Omega_{untreated\ cells} - \Omega_{media\ only}))$. For area under the curve (AUC) analyses, the net AUC was taken from all curves using baseline of Y=1.

Mouse model of localized vascular leak

Five- to eight-week-old WT C57BL/6 male mice were purchased from the Jackson Laboratory (Bar Harbor, ME) and maintained under specific pathogen-free conditions at the University of California, Berkeley, Animal Facility. Mice were housed in a controlled temperature environment on a 12-hour light/dark cycle, with food and water provided *ad libitum*. All experimental procedures involving animals were pre-approved by the Animal Care and Use Committee (ACUC) of the University of California, Berkeley. Three to four days prior to experiment, the dorsal dermises of 6- to 10-week-old WT C57BL/6 female mice (Jackson Laboratory) were shaved using hair clippers, and residual hair was removed using Nair (Church & Dwight). On the day of experiment, 15 μg of WT or mutant NS1 was mixed with PBS in a total volume 50 μL each. NS1 mixtures and PBS were then injected intradermally (ID) into discrete spots in the shaved mouse dermis. Immediately following ID injections, 25 μg of 10-kDa dextran conjugated to Alexa Fluor 680 (1 mg/mL; Sigma) was delivered intravenously (IV) through the retro-orbital route. Two hours post-injection, mice were euthanized, and the dorsal dermis was removed and placed in Petri dishes. The dermis was then placed on a fluorescent scanner (LI-COR Odyssey CLx Imaging System) to visualize the fluorescence signal accumulation at a wavelength of 700 nm. Vascular leak at the ID injection sites was quantified using Image Studio software (LI-COR Biosciences) as described previously [19,20].

Enzyme-linked immunosorbent assay (ELISA)

Enzyme-linked immunosorbent assay (ELISA) Direct NS1 ELISAs were conducted to measure binding of 2B7 to different flavivirus WT and chimeric NS1 proteins. MaxiSorp ELISA plates (Thermo Fisher Scientific/Nunc) were coated with the indicated NS1 protein at a concentration of 0.5 μg/mL in 100 μL 1X PBS and allowed to incubate overnight at 4°C. The next day, plates were blocked in 1X PBS + 1% BSA for 2 hours then washed 3x with 1X PBS. 2B7 was then diluted in blocking buffer, as indicated in the figures, and 100 μL was added to plates. After a 1-hour incubation at 37°C, plates were washed 3x in 1X PBS + 0.1% Tween20. Plates were then incubated for 1 hour at 37°C with an HRP-conjugated secondary antibody diluted at 1:5000 in blocking buffer. Plates were washed 3x in PBS + 0.1% Tween20 and then developed using the 3,3',5,5'-tetramethylbenzidine (TMB) substrate (Sigma). Plates were allowed to develop for ~10 minutes before the addition of 2N H_2SO_4 stop buffer. Absorbance was read at a wavelength of 450 nm using a microplate reader.

For the NS1-BSA-GAG binding ELISA, assay was conducted as above except plates were coated with 200 ng of BSA-GAG, BSA-heparin, and 1% BSA controls diluted in PBS, and allowed to incubate overnight at 4ºC. After the initial blocking step, WT and chimeric NS1 proteins were added to plates at 5 μg/mL for 1 hour at 37ºC, and washed 3x with wash buffer. Bound NS1 was then detected using detected using rabbit anti-His antibody diluted 1:5000 in blocking buffer before being developed as described in the paragraph above.

Statistics

All quantitative analyses were conducted, and all data were plotted, using GraphPad Prism 9 software. Experiments were repeated at least 3 times, to ensure reproducibility. All experiments were designed and performed with both positive and negative controls (indicated in the figures), which were used for inclusion/exclusion determination. For immunofluorescence microscopy experiments, images of random fields were captured. For all experiments with quantitative analysis,

data are displayed as mean ± standard error of the mean (SEM). All cell binding and TEER quantitative data were analyzed using a One-way ANOVA analysis with Tukey's multiple comparisons test. For the localized dermal leak experiments, a non-parametric, unpaired Mann-Whitney U test was used to determine statistical significance between groups. The resulting p-values from the above statistical tests were displayed as n.s., not significant; $p > 0.05$; *$p < 0.05$; **$p < 0.01$; ***$p < 0.001$; ****$p < 0.0001$.

References
Chapter 3

1. Cattarino, L., Rodriguez-Barraquer, I., Imai, N., Cummings, D.A.T., and Ferguson, N.M. (2020). Mapping global variation in dengue transmission intensity. Sci. Transl. Med. *12*, 1–11.
2. Muller, D.A., Depelsenaire, A.C.I., and Young, P.R. (2017). Clinical and Laboratory Diagnosis of Dengue Virus Infection. J. Infect. Dis. *215*, S89–S95.
3. Winkler, G., Maxwell, S., Ruemmler, C., and Stollar, V. (1989). Newly synthesized dengue-2 virus non-structural protein NS1 is a soluble protein but becomes partially hydrophobic and membrane-associated after dimerization. Virology *171*, 302–305.
4. Scaturro, P., Cortese, M., Chatel-Chaix, L., Fischl, W., and Bartenschlager, R. (2015). Dengue Virus Non-structural Protein 1 Modulates Infectious Particle Production via Interaction with the Structural Proteins. PLoS Pathog. *11*, e1005277.
5. Ci, Y., Liu, Z.Y., Zhang, N.N., Niu, Y., Yang, Y., Xu, C., Yang, W., Qin, C.F., and Shi, L. (2020). Zika NS1-induced ER remodeling is essential for viral replication. J. Cell Biol. *219*, e201903062.
6. Płaszczyca, A., Scaturro, P., Neufeldt, C.J., Cortese, M., Cerikan, B., Ferla, S., Brancale, A., Pichlmair, A., and Bartenschlager, R. (2019). A novel interaction between dengue virus non-structural protein 1 and the NS4A-2K-4B precursor is required for viral RNA replication but not for formation of the membranous replication organelle. PLoS Pathog. *15*, e1007736.
7. Flamand, M., Megret, F., Mathieu, M., Lepault, J., Rey, F.A., and Deubel, V. (1999). Dengue Virus Type 1 Non-structural Glycoprotein NS1 Is Secreted from Mammalian Cells as a Soluble Hexamer in a Glycosylation-Dependent Fashion. J. Virol. *73*, 6104–6110.
8. Gutsche, I., Coulibaly, F., Voss, J.E., Salmon, J., D'Alayer, J., Ermonval, M., Larquet, E., Charneau, P., Krey, T., Mégret, F., *et al.* (2011). Secreted dengue virus non-structural protein NS1 is an atypical barrel-shaped high-density lipoprotein. Proc. Natl. Acad. Sci. *108*, 8003–8008.
9. Benfrid, S., Park, K., Dellarole, M., Voss, J.E., Tamietti, C., Pehau-Arnaudet, G., Raynal, B., Brûlé, S., England, P., Zhang, X., *et al.* (2022). Dengue virus NS1 protein conveys pro-inflammatory signals by docking onto high-density lipoproteins. EMBO Rep., 1–14.
10. Shu, B., Ooi, J.S.G., Tan, A.W.K., Ng, T., Dejnirattisai, W., Mongkolsapaya, J., Fibriansah, G., Shi, J., Kostyuchenko, V.A., Screaton, G., *et al.* (2022). CryoEM structures of the multimeric secreted NS1 , a major factor for dengue hemorrhagic fever. bioRxiv, 1–36. doi:https://doi.org/10.1101/2022.04.04.487075
11. Beatty, P.R., Puerta-Guardo, H., Killingbeck, S.S., Glasner, D.R., Hopkins, K., and Harris, E. (2015). Dengue virus NS1 triggers endothelial permeability and vascular leak that is prevented by NS1 vaccination. Sci. Transl. Med. *7*, 304ra141.
12. Modhiran, N., Watterson, D., Muller, D.A., Panetta, A.K., Sester, D.P., Liu, L., Hume, D.A., Stacey, K.J., and Young, P.R. (2015). Dengue virus NS1 protein activates cells via Toll-like receptor 4 and disrupts endothelial cell monolayer integrity. Sci. Transl. Med. *7*, 304ra142.
13. Wessel, A.W., Dowd, K.A., Biering, S.B., Zhang, P., Edeling, M.A., Nelson, C.A., Funk, K.E., DeMaso, C.R., Klein, R.S., Smith, J.L., *et al.* (2021). Levels of Circulating NS1 Impact West Nile Virus Spread to the Brain. J. Virol. *95*, e00844-21.
14. Puerta-Guardo, H., Tabata, T., Petitt, M., Dimitrova, M., Glasner, D.R., Pereira, L., and Harris, E. (2020). Zika Virus Non-structural Protein 1 Disrupts Glycosaminoglycans and Causes Permeability in Developing Human Placentas. J. Infect. Dis. *221*, 313–324.

15. Thiemmeca, S., Tamdet, C., Punyadee, N., Prommool, T., Songjaeng, A., Noisakran, S., Puttikhunt, C., Atkinson, J.P., Diamond, M.S., Ponlawat, A., *et al.* (2016). Secreted NS1 Protects Dengue Virus from Mannose-Binding Lectin–Mediated Neutralization. J. Immunol. *197*, 4053–4065.

16. Avirutnan, P., Hauhart, R.E., Somnuke, P., Blom, A.M., Diamond, M.S., and Atkinson, J.P. (2011). Binding of Flavivirus Non-structural Protein NS1 to C4b Binding Protein Modulates Complement Activation. J. Immunol. *187*, 424–433.

17. Avirutnan, P., Zhang, L., Punyadee, N., Manuyakorn, A., Puttikhunt, C., Kasinrerk, W., Malasit, P., Atkinson, J.P., and Diamond, M.S. (2007). Secreted NS1 of dengue virus attaches to the surface of cells via interactions with heparan sulfate and chondroitin sulfate E. PLoS Pathog. *3*, 1798–1812.

18. Puerta-Guardo, H., Glasner, D.R., and Harris, E. (2016). Dengue Virus NS1 Disrupts the Endothelial Glycocalyx, Leading to Hyperpermeability. PLoS Pathog. *12*, e1005738.

19. Glasner, D.R., Ratnasiri, K., Puerta-Guardo, H., Espinosa, D.A., Beatty, P.R., and Harris, E. (2017). Dengue virus NS1 cytokine-independent vascular leak is dependent on endothelial glycocalyx components. PLoS Pathog. *13*, e1006673.

20. Wang, C., Puerta-Guardo, H., Biering, S.B., Glasner, D.R., Tran, E.B., Patana, M., Gomberg, T.A., Malvar, C., Lo, N.T.N., Espinosa, D.A., *et al.* (2019). Endocytosis of flavivirus NS1 is required for NS1-mediated endothelial hyperpermeability and is abolished by a single N-glycosylation site mutation. PLoS Pathog. *15*, e1007938.

21. Rastogi, M., and Singh, S.K. (2020). Zika virus NS1 affects the junctional integrity of human brain microvascular endothelial cells. Biochimie *176*, 52–61.

22. Barbachano-Guerrero, A., Endy, T.P., and King, C.A. (2020). Dengue virus non-structural protein 1 activates the p38 MAPK pathway to decrease barrier integrity in primary human endothelial cells. J. Gen. Virol. *101*, 484–496.

23. Puerta-Guardo, H., Glasner, D.R., Espinosa, D.A., Biering, S.B., Patana, M., Ratnasiri, K., Wang, C., Beatty, P.R., and Harris, E. (2019). Flavivirus NS1 Triggers Tissue-Specific Vascular Endothelial Dysfunction Reflecting Disease Tropism. Cell Rep. *26*, 1598-1613.e8.

24. Akey, D.L., Brown, W.C., Dutta, S., Konwerski, J., Jose, J., Jurkiw, T.J., DelProposto, J., Ogata, C.M., Skiniotis, G., Kuhn, R.J., *et al.* (2014). Flavivirus NS1 Structures Reveal Surfaces for Associations with Membranes and the Immune System. Science *343*, 881–885.

25. Brown, W.C., Akey, D.L., Konwerski, J.R., Tarrasch, J.T., Skiniotis, G., Kuhn, R.J., and Smith, J.L. (2016). Extended surface for membrane association in Zika virus NS1 structure. Nat. Struct. Mol. Biol. *23*, 865–867.

26. Xu, X., Song, H., Qi, J., Liu, Y., Wang, H., Su, C., Shi, Y., and Gao, G.F. (2016). Contribution of intertwined loop to membrane association revealed by Zika virus full-length NS1 structure. EMBO J. *35*, 2170–2178.

27. Hertz, T., Beatty, P.R., MacMillen, Z., Killingbeck, S.S., Wang, C., and Harris, E. (2017). Antibody Epitopes Identified in Critical Regions of Dengue Virus Non-structural 1 Protein in Mouse Vaccination and Natural Human Infections. J. Immunol. *198*, 4025–4035.

28. Lai, Y.C., Chuang, Y.C., Liu, C.C., Ho, T.S., Lin, Y.S., Anderson, R., and Yeh, T.M. (2017). Antibodies Against Modified NS1 Wing Domain Peptide Protect Against Dengue Virus Infection. Sci. Rep. *7*, 69–75.

29. Biering, S.B., Akey, D.L., Wong, M.P., Brown, W.C., Lo, N.T.N., Puerta-Guardo, H., Tramontini

Gomes de Sousa, F., Wang, C., Konwerski, J.R., Espinosa, D.A., *et al.* (2021). Structural basis for antibody inhibition of flavivirus NS1–triggered endothelial dysfunction. Science *371*, 194–200.

30. Weinbaum, S., Tarbell, J.M., and Damiano, E.R. (2007). The Structure and Function of the Endothelial Glycocalyx Layer. Annu. Rev. Biomed. Eng. *9*, 121–167.

31. Jumper, J., Evans, R., Pritzel, A., Green, T., Figurnov, M., Ronneberger, O., Tunyasuvunakool, K., Bates, R., Žídek, A., Potapenko, A., *et al.* (2021). Highly accurate protein structure prediction with AlphaFold. Nature *596*, 583–589.

32. Glasner, D.R., Puerta-Guardo, H., Beatty, P.R., and Harris, E. (2018). The Good, the Bad, and the Shocking: The Multiple Roles of Dengue Virus Non-structural Protein 1 in Protection and Pathogenesis. Annu. Rev. Virol. *5*, 227–253.

33. Kim, S.Y., Koetzner, C.A., Payne, A.F., Nierode, G.J., Yu, Y., Wang, R., Barr, E., Dordick, J.S., Kramer, L.D., Zhang, F., *et al.* (2019). Glycosaminoglycan Compositional Analysis of Relevant Tissues in Zika Virus Pathogenesis and in Vitro Evaluation of Heparin as an Antiviral against Zika Virus Infection. Biochemistry *58*, 1155–1166.

34. Biering, S.B., de Sousa, F.T.G., Tjang, L. V, Pahmeier, F., Ruan, R., Blanc, S.F., Patel, T.S., Worthington, C.M., Glasner, D.R., Castillo-Rojas, B., *et al.* (2021). SARS-CoV-2 Spike triggers barrier dysfunction and vascular leak via integrins and TGF-β signaling. bioRxiv Prepr. Serv. Biol., 1–49. doi: https://doi.org/10.1101/2022.04.04.487075

35. Feng, T., Zhang, J., Chen, Z., Pan, W., Chen, Z., Yan, Y., and Dai, J. (2022). Glycosylation of viral proteins: Implication in virus–host interaction and virulence. Virulence *13*, 670–683.

36. D'Addio, M., Frey, J., Tacconi, C., Commerford, C.D., Halin, C., Detmar, M., Cummings, R.D., and Otto, V.I. (2021). Sialoglycans on lymphatic endothelial cells augment interactions with Siglec-1 (CD169) of lymph node macrophages. FASEB J. *35*, 1–20.

Chapter 4

Evaluation of iminosugar UV-4B against dengue virus non-structural protein 1

Abstract

The positive-stranded flavivirus DENV causes approximately 100 million symptomatic cases of dengue annually, with half of the global population at risk of infection. While symptomatic DENV infections are mostly asymptomatic or result in mild cases of dengue fever, some develop severe dengue, which is characterized by vascular leak. The current treatment regimen includes only supportive care, with no DENV-specific therapeutics available. The iminosugar UV-4B has previously been shown to demonstrate anti-DENV properties *in vivo* and *in vitro* through inhibiting proper glycosylation processing of viral proteins by host endoplasmic reticulum α-glucosidases, which viruses are reliant on. DENV non-structural protein 1 (NS1) is a secreted glycoprotein with two N-linked glycosylation sites. DENV NS1 has been shown to directly cause vascular leak *in vivo* and endothelial hyperpermeability *in vitro*, independently of the virus. Here, we explored the direct effects of UV-4B against DENV NS1. We found that UV-4B treatment leads to reduced NS1 production of DENV-infected cells but not reduction of NS1 secretion of transfected cells. The NS1 that is secreted under UV-4B treatment exhibits proper glycosylation and pathogenicity. Finally, we showed that UV-4B protects against NS1-induced endothelial dysfunction and hyperpermeability. Taken together, we present the direct effects of UV-4B against DENV NS1.

Introduction

The positive-stranded RNA dengue virus (DENV) of the *Flavivirus* genus causes up to 100 million infections annually with about 4 billion people worldwide at risk of infection [1]. DENV exists as four antigenically distinct serotypes (DENV1-4), each containing multiple genotypes. Symptomatic DENV infection ranges from classic dengue fever to the more severe dengue hemorrhagic fever and dengue shock syndrome [2]. The severe forms of dengue are characterized by vascular leak as a result of endothelial dysfunction and can be fatal [3]. While vaccines have been developed against other flaviviruses such as Japanese encephalitis (JEV) and yellow fever (YFV) viruses, the complexity of DENV immunopathogenesis has impeded the development of a safe and effective vaccine against DENV [4]. Whereas the immune response after primary DENV infection protects against dengue disease with the same serotype, subsequent heterologous infection with different DENV serotypes can increase the risk of severe disease due to antibody-dependent enhancement (ADE) of the infection [5], making DENV vaccine development challenging. Currently, there are no specific treatments for vascular leak besides supportive care. Thus, there is an urgent need for new therapeutics that target severe dengue and its vascular leak pathology.

Enveloped viruses such as DENV rely on the host glycosylation machinery for modifications of virus-encoded glycoproteins. DENV possesses four N-linked glycoproteins: the envelope (E), (pre-)membrane (prM), and non-structural proteins 1 (NS1) and 4B (NS4B) [6]. During DENV replication in the endoplasmic reticulum (ER), precursor oligosaccharides are added to specific asparagine residues ("N-linked") on the DENV glycoproteins [6,7]. The ER-resident enzymes α-glucosidases I and II then trim the glycan groups of the attached oligosaccharides to form glycoproteins with the typical high-mannose, hybrid, and complex types of oligosaccharides [8]. Proper oligosaccharide processing of glycoproteins is crucial for protein folding and progression through the Golgi apparatus and for their eventual transport towards intra- or extra-cellular functions [9]. A recent CRISPR screen for flavivirus host machinery identified ER-resident enzymes as critical host factors for flavivirus replication and infectivity, further supporting its importance [10]. Notably, no virus has been identified to encode the α-glucosidases required for the biosynthesis of N-linked oligosaccharides; thus, these host glycosylation processes are thus vital for the viral life cycle.

Previous studies have identified this host-dependent N-linked oligosaccharide biosynthesis pathway as a potential antiviral target [11,12]. Inhibiting or disrupting the host glycosylation pathways can lead to misfolding and subsequent degradation of the viral glycoproteins, resulting in decreased progeny virions. One such class of antiviral compounds that target the host glycosylation pathways is iminosugars, which are monosaccharide mimics that have demonstrated antiviral properties against DENV and other enveloped viruses such as hepatitis C (HCV) and influenza A (IAV) viruses [13,14], as well as the causative agent SARS-CoV-2 of the ongoing pandemic [15]. In DENV specifically, iminosugars have been shown to inhibit viral assembly and egress [16]. One of the iminosugars, UV-4 (methoxy-*N*-nonyl deoxynojirimycin, M*O*N-DNJ) has been identified as a therapeutic candidate against DENV. UV-4 was shown to protect against lethal DENV infection under ADE conditions, and UV-4-treated mice displayed reductions in viral load and inflammatory cytokine induction [17]. Subsequently, dosing and pharmacokinetics studies of the UV-4 hydrochloride salt UV-4B were conducted in an ADE mouse model of severe DENV infection [18]. In the same study, the mechanistic basis for the antiviral activity of UV-4B was identified to be its inhibition of the ER α-glucosidases and not the glycosphingolipid pathway.

UV-4B has since undergone Phase 1 clinical trials demonstrating safety with no adverse events, and Phase 2 clinical trials have been planned [19].

DENV encodes three structural and seven non-structural (NS) proteins. NS1 participates intracellularly in viral replication and membrane remodeling [20–22] and is also secreted as an oligomeric lipoprotein at levels that correlate with viraemia and disease severity [23–25]. Secreted DENV NS1 plays multiple roles in immune evasion and viral pathogenesis [26–28]. In particular, NS1 has been shown to trigger endothelial hyperpermeability and vascular leak independently of viral infection [29,30], and lethal DENV2 infection can be blocked by anti-NS1 antibodies in mouse models [26,31,32]. NS1-induced pathogenesis occurs in part through the disruption of endothelial glycocalyx layer (EGL) that lines the endothelium, compromising its barrier function [30,33,34], as well as through triggering the release of vasoactive cytokines from immune cells, contributing to endothelial hyperpermeability [28]. Given the multifaceted roles that DENV NS1 plays in DENV pathogenesis and its contribution to severe dengue pathologies, NS1 has been identified as a promising therapeutic target [31,32].

While it has been shown that UV-4B acts against DENV pathogenesis by inhibiting N-linked oligosaccharide processing of viral proteins [18], it remains unclear whether part of UV-4B's antiviral effects is through acting against NS1-induced pathology. NS1 can trigger vascular leak, a hallmark of severe dengue; as such, targeting NS1 is a promising strategy to not only block this critical DENV pathology, but also to inhibit its role in the viral life cycle. An anti-NS1 therapeutic delivered early in DENV infection could reduce the likelihood of developing severe dengue and vascular leak. DENV NS1 contains two N-linked glycosylation sites – Asn-130 and Asn-207 – which are decorated with both complex and high-mannose sugars when produced in mammalian cells [35]. The glycosylation sites are highly conserved across flaviviruses, specifically within NS1 of West Nile (WNV) and Zika (ZIKV) viruses. We previously showed that an N207Q glycosylation mutant of DENV, WNV, and ZIKV NS1 proteins abrogated their respective abilities to trigger EGL disruption and induce endothelial hyperpermeability [36], highlighting the importance of glycosylation for viral proteins and NS1.

In this study, we explored the direct effects of UV-4B against DENV NS1. By treating DENV-infected cells and NS1-transfected cells with UV-4B or control iminosugars, we found that UV-4B leads reduced DENV infection due to improper NS1 glycosylation processing, but had no effects on transfections of cells with NS1 plasmid. However, the NS1 that is secreted under UV-4B treatment exhibits proper glycosylation and functions as wild-type (WT) NS1. We further found that UV-4B treatment of human endothelial cells protects against NS1-induced endothelial dysfunction and hyperpermeability. Taken together, we present the effects of UV-4B against DENV NS1-mediated pathogenesis.

Results

UV-4B treatment of DENV-infected monocytes results in reduced NS1 secretion

UV-4B has been demonstrated to impede DENV infection *in vivo* and *in vitro* as a result of inhibition of ER α-glucosidases [13,18], resulting in mis-folding of essential viral proteins. Given that DENV NS1 has been previously shown to independently cause severe DENV-associated pathologies including endothelial dysfunction *in vitro* and vascular leak *in vivo* [29,30,34], and that NS1 is one of the four proteins encoded by DENV that are glycosylated, we hypothesized that UV-4B could have direct effects on NS1 secretion from DENV-infected cells. To test the capacity of UV-4B to inhibit NS1 secretion, we infected human monocytic U937 cells transduced with dendritic cell-specific intercellular adhesion molecule 3-grabbing non-integrin (DC-SIGN), a known DENV attachment factor, with DENV2 in the presence or absence of UV-4B and its control iminosugar UV-204. We measured the amount of secreted and intracellular NS1 by western blot (Fig. 1A) and enzyme-linked immunosorbent assay (ELISA) (Fig. 1B). We found that U937-DC-SIGN cells treated with UV-4B during DENV infection resulted in dose-dependent reduction of NS1 secretion, beginning at 1 μM of UV-4B, while UV-204-treated DENV infections of U937 exhibited no change in levels of NS1 secretion beyond 10 μM of compounds. While there were no observable differences in levels of intracellular NS1 between UV-204- and UV-4B-treated DENV infections, the intracellular NS1 under UV-4B treatment displayed a higher molecular weight on western blot, indicating an increase in protein size likely due to the impeded glycosylation trimming and processing. These data suggest that UV-4B inhibits glycosylation of NS1, inhibiting NS1 secretion.

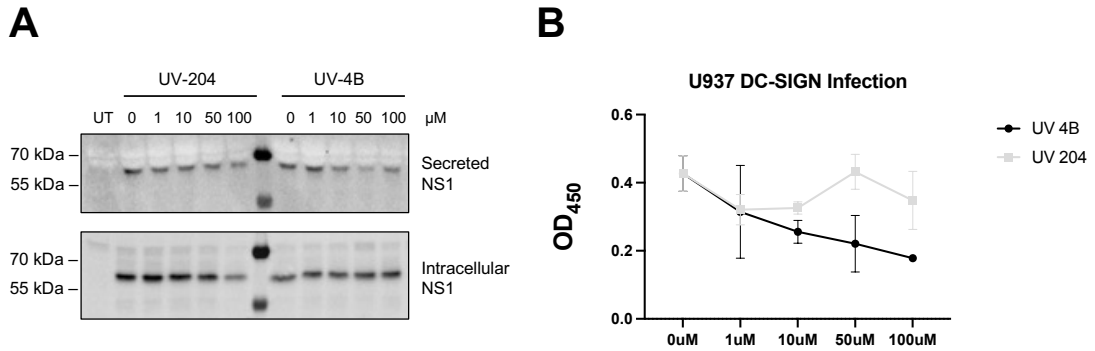

Figure 1. UV-4B reduces NS1 production from DENV-infected monocytes.
U937-DC-SIGN was infected with DENV at an MOI of 0.01 in the presence or absence of UV-4B or the UV-204 iminosugar control. **(A)** Supernatant and cell pellet were collected 24 hpi and analyzed by western blot detecting for NS1. **(B)** Supernatant 24 hpi were separately measured for amounts of NS1 using NS1-capture ELISA. Data plotted from n=3 biological replicates, as mean ± SEM.

UV-4B treatment of transfected cells has no effect on NS1 secretion but affects NS1 glycosylation

The change in molecular weight of intracellular NS1 produced by DENV-infected cells under UV-4B treatment suggests that UV-4B could have a direct effect on NS1. To investigate whether the reduced NS1 secretion observed was due to the overall reduced viral replication or direct effects on NS1 production, we transfected HEK-293T cells with a plasmid encoding DENV NS1 in the presence or absence of UV-4B or its UV-204 control iminosugar (Fig. 2A-C). 24 hours post-transfection, we collected transfected cell supernatants and analyzed by western blot (Fig. 2A and

B), and also quantified NS1 levels using an NS1-capture ELISA (Fig. 2C). We found that UV-4B did not affect either the levels of NS1 production intracellularly or the levels of NS1 secretion. In addition, intracellular NS1 was analyzed by western blot and quantified, with actin normalization. While there was no difference in the amount of intracellular NS1 between UV-4B and UV-204-treated transfections, a gradual dose-dependent increase in the size of the NS1 band in UV-4B-treated cells was observed, indicating the gradual inhibition of glycan processing of NS1 as UV-4B concentration increased (Fig. 2A).

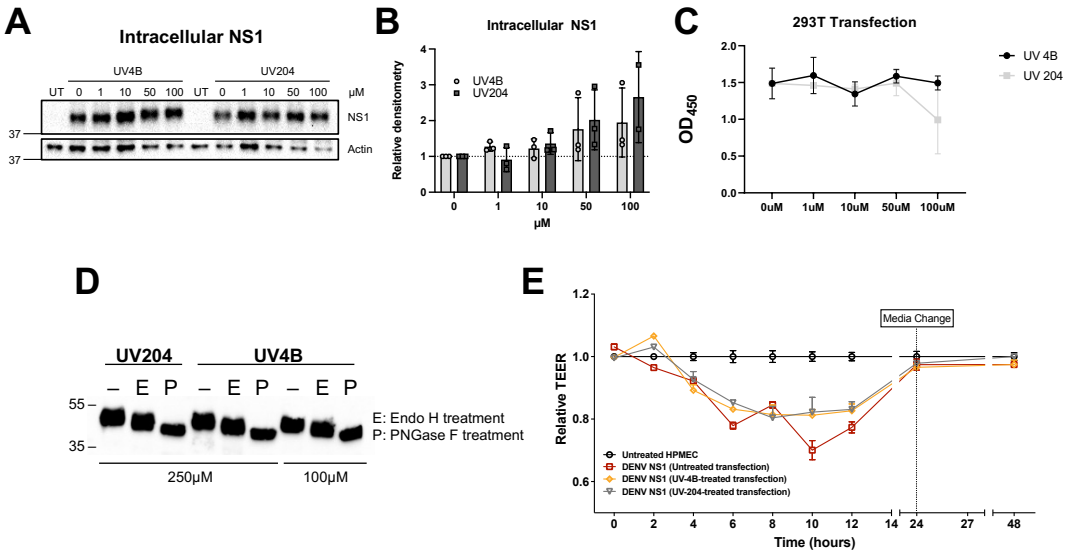

Figure 2. UV-4B altering intracellular NS1 glycosylation, but secreted NS1 behaves normally. HEK-293F cells were lipofectamine-transfected with plasmid containing DENV NS1 with or without indicated UV-4B or control iminosugar UV-204 at indicated concentrations. **(A)** Cells were collected and measured for intracellular NS1 by western blot and quantified by densitometry in **(B)**. **(C)** Supernatants were collected 24hpt and the amount of NS1 is measured by ELISA. **(D)** NS1 produced in the presence or absence of UV-4B and UV-204 were treated with endoglycosidases as indicated, and analyzed on western blot. **(E)** NS1 produced in presence or absence of UV-4B or UV-204 were treated on human pulmonary endothelial cells (HPMEC) seeded on Transwells. Trans-endothelial electrical resistance was measured over time as indicator for HPMEC permeability. UT, untreated. Data plotted from n=3 biological replicates, as mean ± SEM.

Secreted DENV NS1 produced under UV-4B treatment is functionally comparable to WT NS1

It has been previously shown that UV-4B blocks the DENV life cycle by inhibiting ER α-glucosidases. Intracellular NS1 from 293T cells treated with UV-4B during transfection exhibited higher molecular weight, suggesting larger unprocessed glycans. While we found that UV-4B treatment of cells decreased NS1 secretion, it did not completely abrogate protein secretion. To determine if the residual secreted NS1 protein was structurally and functionally comparable to WT NS1, we produced NS1 via 293T transfection in cells treated with either UV-204 or UV-4B. We then purified and concentrated secreted proteins for further downstream analyses. To determine if NS1 secreted in the presence of UV-4B and UV-204 were properly glycosylated, we subjected purified proteins to digestion with endoglycosidases H (Endo H) or peptide:N-glycosidase F (PNGase F). While both endoglycosidases cleave N-linked oligosaccharides from glycoproteins, Endo H can only cleave high-mannose oligosaccharides whereas PNGase F cleaves high-mannose,

hybrid, and complex oligosaccharides, resulting in a deaminated protein. We found that secreted NS1 produced under both iminosugar treatments had the same glycosylation patterns, with no difference even at a higher concentration of UV-4B treatment (Fig. 2G). This suggests that while UV-4B affects proper glycosylation of intracellular NS1, the NS1 proteins that are nonetheless secreted are properly glycosylated. To further determine whether secreted NS1 proteins produced under UV-4B treatment possess functional defects, we tested the capacity of these purified proteins to trigger endothelial hyperpermeability of human pulmonary microvascular endothelial cells (HPMEC) seeded on the apical chamber of a Transwell. We measured the trans-endothelial electrical resistance (TEER) over time to assess the degree of NS1-induced endothelial hyperpermeability, a well-established assay [33,37]. We found that all NS1 proteins tested resulted in comparable endothelial hyperpermeability, suggesting that secreted NS1 produced under UV-4B treatment function normally as WT DENV NS1 (Fig. 2H).

UV-4B blocks NS1-induced endothelial dysfunctions

Next, we tested the impact of UV-4B treatment on NS1-mediated endothelial dysfunction, investigating if UV-4B may block the capacity of soluble hexameric NS1 to trigger pathology. We co-treated HPMEC seeded on Transwells with NS1 and UV-4B or UV-204 as described above and measured TEER over time (Fig. 3A). We found that UV-4B inhibited NS1-mediated endothelial hyperpermeability in a dose-dependent manner, resulting in a partial TEER reduction at 50 and 100 μM. These data indicate a cell-intrinsic property of UV-4B against NS1-induced endothelial dysfunction.

It has previously been shown mechanistically that DENV NS1 triggers endothelial dysfunction by disrupting key endothelial barriers including the endothelial glycocalyx layer (EGL). Major EGL components sialic acid and heparan sulfate have been detected circulating in serum of severe dengue patients experiencing vascular leak [38]. *In vitro*, HPMEC treated with DENV NS1 exhibit decreased levels of sialic acid and heparan sulfate, among other EGL components, on the cell surface [30]. To determine if UV-4B treatment of cells could inhibit NS1-mediated EGL disruption, we treated HPMEC that were pre-treated with UV-4B or the iminosugar control UV-0061 (a compound structurally similar to UV-204) with DENV NS1, and measured sialic acid levels on the surface of HPMEC by immunofluorescence microscopy (IFA) (Fig. 3B). We found that NS1 treatment of UV-0061-treated HPMEC resulted in comparable sialic acid degradation as the controls with no iminosugar treatment, whereas NS1 treatment of UV-4B-treated HPMEC showed partial abrogation of sialic acid degradation at 100 μM, and full abrogation at 500 μM of UV-4B (Fig. 3C). Together, these results demonstrate that UV-4B is able to block NS1-induced EGL degradation, which in turn partially blocks the resulting endothelial hyperpermeability.

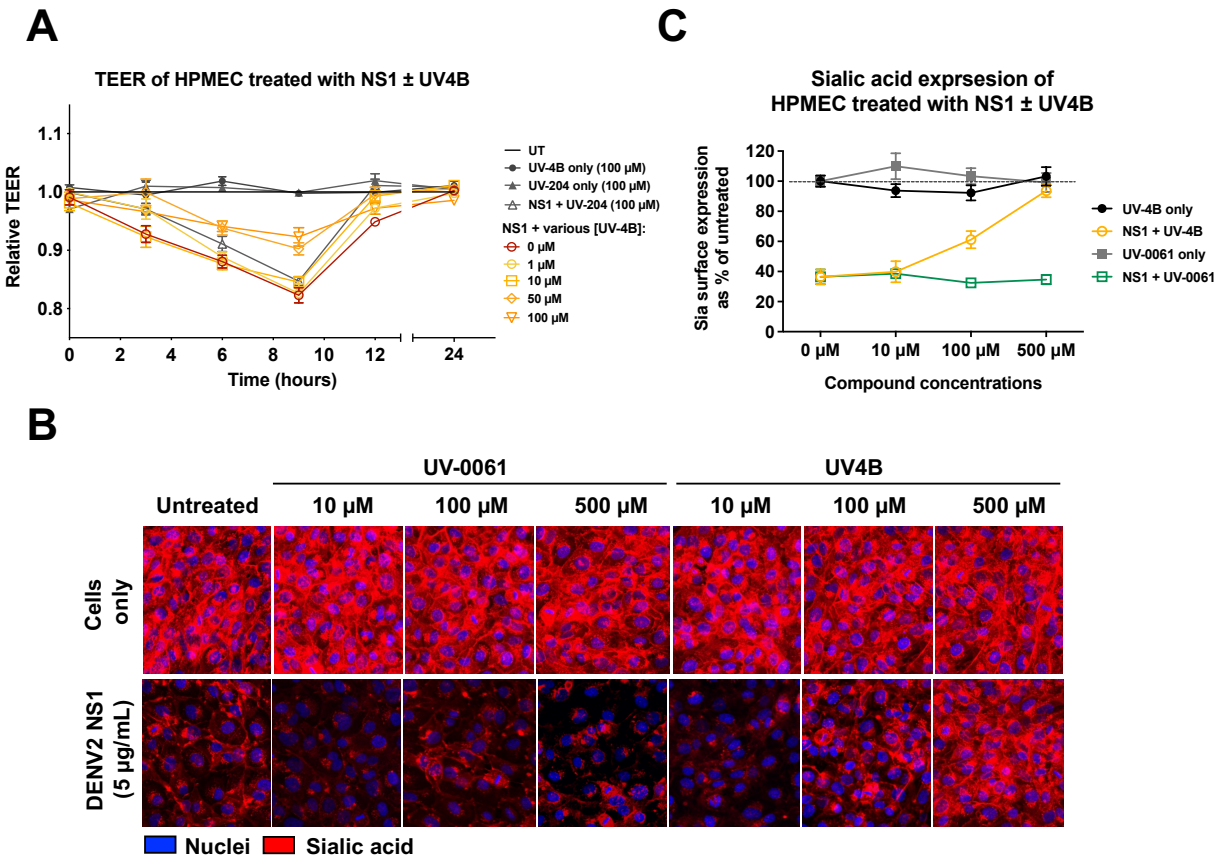

Figure 3. UV-4B blocks NS1-induced endothelial dysfunctions.
(A) NS1 with indicated concentrations of UV-4B or indicated control was treated on human pulmonary microvascular endothelial cells (HPMEC) seeded on Transwells. Trans-endothelial electrical resistance (TEER) between the apical and basolateral chambers were measured over time, as proxy for HPMEC permeability. **(B)** HPMEC pre-treated with UV-4B or control iminosugar UV-0061 at indicated concentrations was treated with 5 µg/mL DENV NS1 and stained for sialic acid, imaged by immunofluorescence microscopy and quantified in **(C)**. Part of this figure is contributed by Dr. Henry Puerta-Guardo. Data plotted from n=3 biological replicates, as mean ± SEM.

Discussion

In this study, we characterized the direct effects of UV-4B against DENV NS1 protein, a viral protein that has been shown to cause endothelial dysfunction and vascular leak independently of the virus. We observed that UV-4B treatment of DENV-infected monocytes resulted in reduced DENV replication as well as NS1 secretion, while UV-4B treatment of NS1-transfected cells did not result in lower NS1 secretion. The NS1 that was secreted under UV-4B treatment exhibited the same glycosylation patterns as control treatments, and induced comparable endothelial dysfunction as WT NS1, as measured by TEER. We further found that UV-4B has cell-intrinsic anti-NS1 effects, as treatment of human endothelial cells with UV-4B was able to block NS1-induced TEER and EGL disruption.

Our observation that UV-4B treatment of DENV-infected U937-DC-SIGN cells resulted in reduced NS1 secretion (Fig. 1) is expected given that UV-4B also blocks viral replication. What was unknown was whether this reduction in NS1 secretion due to improper glycosylation of NS1 directly impacts NS1-modulated endothelial pathologies. Unexpectedly, UV-4B treatment of cells transfected with NS1 plasmid had no effects on either intracellular NS1 production or NS1 secretion. One explanation was that the effects of UV-4B could have been overridden by the robust polyethylenimine (PEI) transfection on HEK-293 cells. UV-4B could potentially still antagonize NS1 secretion, which might be observed by using a cell line that has lower transfection efficiency, or by transfecting using lower levels of NS1 plasmid.

Further, while UV-4B hampered proper intracellular NS1 glycosylation, which was suggested by an apparent upward shift of protein bands in western blots, the proteins that were successfully secreted appeared properly glycosylated and functioned comparably to WT NS1 (Fig. 2). Presumably, NS1 proteins that are improperly glycosylated would be recycled back through the Golgi apparatus and targeted to the proteosome for degradation [8]. An interesting follow-up experiment would be to compare UV-4B blockade of DENV infection by infectious clones containing the $NS1^{N207Q}$ glycosylation mutant. $NS1^{N207Q}$ does not have N-glycosylation at Asn-207 and is unable to be internalized by endothelial cells or cause endothelial dysfunction [36]. Asn-207 is not expected to directly impact viral replication [21], thus it would be interesting to measure the extent to which UV-4B would impact $DENV^{NS1\text{-}N207Q}$ replication and infectivity. Ongoing RNA-seq studies by our group that compared HPMEC transcriptomic profiles between WT NS1 and $NS1^{N207Q}$ mutant treatments have revealed significant differences across multiple signaling pathways, highlighting the importance of glycosylation (S.B. Biering, D.R. Glasner, and E. Harris, unpublished). It remains to be seen what effects UV-4B might have on a DENV strain that already has glycosylation defects in its NS1 protein.

UV-4B treatment of cells can partially block NS1-induced endothelial hyperpermeability and EGL disruption. This is not due to the intrinsic effects on NS1, as we have shown in the present study that NS1 secreted under UV-4B treatment exhibit wild-type properties, and instead points to cell-intrinsic effects. Indeed, NS1 treatment of HPMEC leads to loss of glycocalyx components such as sialic acid and heparan sulfate via the activation of cathepsin L, heparinase, and sialidases, which can be blocked by inhibiting these activated enzymes [30]. Given that UV-4B blocks NS1 cleavage of sialic acid (Fig. 3), the mechanism of UV-4B inhibition of EGL disruption may involve an inhibition of sialidase activations by hindering their glycosylation processing to prevent proper localization to the cell surface. Alternatively, UV-4B could also hinder the disassembly of intercellular junctions, which form the physical endothelial cell-cell barrier that NS1 has also been shown to disrupt [34].

One weakness of the present study is the lack of *in vivo* studies. Several studies have shown the effects of UV-4B against DENV infection [13,17,18], but none have been directly against NS1-mediated dysfunction. Untangling NS1 from DENV effects *in vivo* has been a challenging endeavor, as NS1 itself is intimately involved in multiple steps of the viral life cycle. Performing *in* vivo studies of UV-4B inhibiting EGL disruption would involve *in vivo* imaging of the glycocalyx, which requires advanced techniques and expertise to perform. Alternatively, future *in vivo* studies could assess the extent to which mice treated with UV-4B can be better protected from NS1-induced vascular leak, either in a systemic or localized model of leak [26,29].

Overall, this study examined the relative contribution of anti-NS1 effects of UV-4B as a component of its previously described antiviral activity against DENV. It provides a proof-of-concept for therapeutics that can target the post-translational modifications of viral proteins. Beyond DENV, the cell-intrinsic effects of UV-4B could be expanded against other enveloped RNA viruses such as HCV and SARS-CoV-2, expanding our arsenal of antiviral therapeutics.

Materials and Methods

NS1 protein and UV iminosugars

Recombinant NS1 proteins from DENV-2 (Thailand strain 16681) were obtained from Native Antigen (United Kingdom) and certified to be endotoxin-free and > 95% purity. Recombinant NS1 proteins produced under UV-4B or UV-204 treatment conditions were obtained from KempBio. UV-4B and UV-204 iminosugars were provided by Emergent BioSolutions Inc. (Gaithersburg, MD, USA). Both stocks of 100 mM were reconstituted in sterile molecular grade water. All compounds were stored according to the manufacturers' recommendations.

Cell lines and viruses

Human monocytic U937 cells expressing DC-SIGN (dendritic cell-specific intercellular adhesion molecule3-grabbing nonintegrin), a known DENV attachment factor, kindly provided by Dr. Aravinda de Silva, University of North Carolina (UNC), Chapel Hill, were used for antiviral assays. U937-DC-SIGN were maintained as suspension cell cultures at 37°C with 5% CO 2 in RPMI 1640 (Gibco) supplemented with 1% non-essential amino acids, 1% penicillin and streptomycin, and 5% fetal bovine serum (FBS; HyClone). Human pulmonary microvascular endothelial cells (HPMEC, clone ST1.6R) were a gift from Dr. J.C. Kirkpatrick, Johannes-Gutenberg University, and were used in endothelial barrier dysfunction studies. HPMEC were maintained in endothelial growth medium 2 (EGM-2) using the EGM-2 bullet kit from Lonza following the manufacturer's specifications and grown in a CO_2 incubator at 37ºC with 5% CO_2. HEK-293T cells were obtained from American Type Culture Collection (ATCC) and were expanded and frozen down at early passages upon receipt. HEK-293T cells were maintained with DMEM media (Gibco) supplemented with 1% penicillin and streptomycin, and 5% FBS.

DENV2 mouse-adapted strain D220 was used for U937-DC-SIGN infections, with a titer of $1.7x10^8$ pfu/mL. D220 was generated in Dr. Eva Harris' laboratory from the parental strain DENV PL046 and was propagated in C6/36 cells, tittered via plaque assay in BHK-21 cells as described previously [39]. All viral stocks were confirmed to be *Mycoplasma*-free.

293T transfection of NS1 in presence/ absence of iminosugars

HEK-293T cells were seeded in 24-well plate and allowed to grow to confluency over 2 days. On the day of experiment, media was changed, followed by addition of iminosugars at indicated concentrations, and incubated at 37ºC for 30 minutes. DENV NS1 plasmid was incubated with lipofectamine transfection reagents (Invitrogen) at room temperature for 20 minutes, then added to cells. 6 hours post-transfection, media was replaced with fresh media containing iminosugars at indicated concentrations. 24 hours post-transfection, supernatant was collected. Cell pellets were washed 1x with PBS and permeabilized with RIPA buffer containing protein inhibitor (Roche) by incubating with shaking at 4ºC for 10 minutes, then stored at -80ºC. Cell pellets were analyzed by western blot while supernatant was analyzed by NS1 capture ELISA.

U937-DC-SIGN infection

On the day of experiment, 1 x 10^6 cells were seeded in 24-well plates. Iminosugars were added to cells at indicated concentrations and incubated at 37ºC for 30 minutes. DENV was then added to cells at MOI of 0.01. 24 hours post-infection, the mixture was spun down and the supernatant was collected and analyzed by NS1 capture ELISA. Cell pellet was washed 1x with PBS and permeabilized with RIPA buffer containing protein inhibitor (Roche) by incubating with shaking

at 4ºC for 10 minutes, then stored at -80ºC. Cell pellets were subsequently analyzed by western blot.

Western blot

Recombinant proteins or cell pellets were collected in protein sample buffer (0.1 M Tris pH 6.8, 4% SDS, 4 mM EDTA, 286 mM 2-mercaptoethanol, 3.2 M glycerol, 0.05% bromophenol blue) and then resolved by SDS-PAGE. Proteins were then transferred onto nitrocellulose membranes and probed with primary antibodies diluted in Tris-buffered saline with 0.1% Tween20 (TBST) containing 5% nonfat dry milk. Membranes and antibodies were incubated overnight rocking at 4°C. The next day, membranes were washed three times with TBST before being probed with anti-mouse HRP secondary antibodies diluted in 5% milk in TBST at a dilution of 1:5,000 at room temperature for 1 hour. Afterwards, membranes were washed with TBST three more times before being developed with ECL reagents and imaged on a ChemiDoc system with Image Lab software (Bio-Rad). The following antibodies were used: mouse anti-DENV NS1 (2B7, Harris lab; 7E11, Walter Reed Military Medical Center), mouse anti-His (MA1-21315, Thermo Scientific), goat anti-mouse HRP (405306, Biolegend).

Enzyme-linked immunosorbent assay (ELISA)

NS1 detection ELISAs were conducted to measure the amounts of NS1 in the supernatant of cells transfected with NS1, or infected with DENV. MaxiSorp ELISA plates (Thermo Fisher Scientific/Nunc) were coated with mouse anti-NS1 mAb at a concentration of 2.5 µg/mL in 100 µL PBS and incubated overnight at 4ºC. The next day, plates were blocked in 1X PBS + 1% BSA for 2 hours then washed 3x with PBS. 200 µL of cell supernatant from either NS1 transfection or DENV infection was added to the plate and incubated at for 1h at 37ºC. Plates were then washed 3x in PBS + 0.1% Tween20. NS1 was detected using biotin-conjugated 2B7 mouse mAb for 1h at 37ºC. Plates were then washed 3x in PBS + 0.1% Tween20, and then developed using the 3,3',5,5'-tetramethylbenzidine (TMB) substrate (Sigma). Plates were allowed to develop for ~10 minutes before the addition of 2N H_2SO_4 stop buffer. Absorbance was read at a wavelength of 450 nm using a microplate reader.

Endoglycosidase treatment

1 µg of WT NS1 or NS1 produced under either UV-4B or UV-204 conditions were treated with either Endo H or PNGase F (New England BioLabs) under denaturing conditions, following manufacturers' recommendations. NS1 samples were boiled in glycoprotein denaturing buffer at 100ºC for 10 minutes, chilled on ice and centrifuged for 10 seconds, followed by addition of either 1.5 µl of Endo H or 1 µL of PNGase F (in 20 µL total volume) and incubated at 37ºC for 1 hour. For PNGase F treatment, NP-40 compound was additionally added into the mixture. Samples were then analyzed by western blot.

Trans-endothelial electrical resistance

The trans-endothelial electrical resistance assay was used to measure the functional effect of NS1 on endothelial barrier function in HPMEC as previously described [33]. Briefly, $1x10^5$ cells (HPMEC) were seeded in 300 µL of medium on the polycarbonate membrane insert of a Transwell (Transwell permeable support, 0.4 µm, 6.5 mm insert; Corning Inc.). The Transwell is placed in a well on a 24-well plate, becoming the apical (upper) chamber. 1.5 mL of media was added to the basolateral (lower) chamber. HPMEC were allowed to form a monolayer for 3 days with media

changes in both apical and basolateral chambers every day, until the inter-chamber electrical resistance reached approximately 60Ω difference between Transwells seeded with (~150Ω) and without cells (~90Ω). On the day of experiment, 5 μg/mL of indicated NS1 proteins (1.5 μg proteins) and indicated amounts of UV-4B as described in figure legends were mixed with media up to 20μL total volume, and added to the apical chambers of the Transwells. Electrical resistance between the apical and basolateral chambers is measured in ohms using an Epithelial Volt Ohm Meter (EVOM) with an electrode pair (World Precision Instruments), at the times indicated in the figures. Transwells containing no cells and untreated Transwells containing only cells were used as negative controls to calculate the baseline electrical resistance at each timepoint. Relative TEER is calculated as a ratio of resistance values $((\Omega_{experimental} - \Omega_{media\ only}) / (\Omega_{untreated\ cells} - \Omega_{media\ only}))$. For area under the curve (AUC) analyses, the net AUC was calculated as the area between the curves and Y=1.

Sialic acid binding

To measure the capacity of flavivirus NS1 proteins to degrade sialic acid, $6x10^4$ HPMECs were seeded on 0.2% gelatin (Sigma)-coated glass coverslips in 24-well plates. Cells were allowed to form a fully confluent monolayer for three days, with media change every other day. On the day of the experiment, cells were either pre-incubated with UV-4B or UV-0061 as indicated in the figures at 37ºC for 30 minutes, and 5 μg/mL of DENV NS1 was added directly to the wells. NS1, iminosugars, and cells were allowed to incubate for 6 hours. Sialic acid was detected using sialic acid-specific lectin, wheat germ agglutinin (WGA), conjugated to Alexa Fluor 647 (Thermo Fisher Scientific). A 1 mg/mL stock of WGA-647 was diluted 1:100 in the media of live cells 5.5 hours post-NS1 treatment (30 minutes pre-fixation). Nuclei were stained using Hoechst 33342 (Immunochemistry) at a dilution of 1:200 alongside WGA treatment. Cells were then washed twice in 1X PBS followed by fixation in 4% formaldehyde (Thermo Fisher Scientific). Coverslips were mounted onto microscope slides on a drop of ProLong Gold (Thermo Fisher Scientific) and imaged using a Zeiss LSM 710 inverted confocal microscope (CRL Molecular Imaging Center, UC Berkeley).

Statistics

All quantitative analyses were conducted, and all data were plotted, using GraphPad Prism 9 software. Experiments were repeated at least 3 times, to ensure reproducibility. All experiments were designed and performed with both positive and negative controls (indicated in the figures), which were used for inclusion/exclusion determination. For immunofluorescence microscopy experiments, images of random fields were captured. For all experiments with quantitative analysis, data are displayed as mean ± standard error of the mean (SEM). All cell binding and TEER quantitative data were analyzed using a one-way ANOVA analysis with Tukey's multiple comparisons test. The resulting p-values from the above statistical tests were displayed as n.s., not significant; $p > 0.05$; *$p < 0.05$; **$p < 0.01$; ***$p < 0.001$; ****$p < 0.0001$.

References
Chapter 4

1. Cattarino, L., Rodriguez-Barraquer, I., Imai, N., Cummings, D.A.T., and Ferguson, N.M. (2020). Mapping global variation in dengue transmission intensity. Sci. Transl. Med. *12*, 1–11.
2. Guzman, M., and Harris, E. (2015). Dengue. Lancet *385*, 453–65.
3. Simmons, C.P., Farrar, J.J., van Vinh Chau, N., and Wills, B. (2012). Dengue. N. Engl. J. Med. *366*, 1423–1432.
4. Chong, H.Y., Leow, C.Y., Abdul Majeed, A.B., and Leow, C.H. (2019). Flavivirus infection—A review of immunopathogenesis, immunological response, and immunodiagnosis. Virus Res. *274*, 197770.
5. Katzelnick, L.C., Gresh, L., Halloran, M.E., Mercado, J.C., Kuan, G., Gordon, A., Balmaseda, A., and Harris, E. (2017). Antibody-dependent enhancement of severe dengue disease in humans. Science *358*, 929–932.
6. Miller, J.L., Tyrrell, B.E., and Zitzmann, N. (2018). Dengue and Zika: Control and Antiviral Treatment Strategies R. Hilgenfeld and S. G. Vasudevan, eds. (Singapore: Springer Singapore).
7. Aebi, M. (2013). N-linked protein glycosylation in the ER. Biochim. Biophys. Acta - Mol. Cell Res. *1833*, 2430–2437.
8. Stanley, P., Moreman, K.W., Lewis, N.E., Taniguchi, N., and Aebi, M. (2022). N-Glycans. In Essentials of Glycobiology, A. Varki, R. D. Cummings, J. D. Esko, J. J. Prestegard, R. L. Schnaar, P. H. Seeberger, G. W. Hart, M. Aebi, D. Mohnen, T. Kinoshita, et al., eds. (Cold Spring Harbor (NY): Cold Spring Harbor Laboratory Press).
9. Roth, J., Zuber, C., Park, S., Jang, I., Lee, Y., Kysela, K.G., Fourn, V., Santimaria, R., Guhl, B., and Cho, J.W. (2010). Protein N-glycosylation, protein folding, and protein quality control. Mol. Cells *30*, 497–506.
10. Zhang, R., Miner, J.J., Gorman, M.J., Rausch, K., Ramage, H., White, J.P., Zuiani, A., Zhang, P., Fernandez, E., Zhang, Q., *et al.* (2016). A CRISPR screen defines a signal peptide processing pathway required by flaviviruses. Nature *535*, 164–168.
11. Tripathi, N., Goel, B., Bhardwaj, N., Vishwakarma, R.A., and Jain, S.K. (2022). Exploring the Potential of Chemical Inhibitors for Targeting Post-translational Glycosylation of Coronavirus (SARS-CoV-2). ACS Omega *7*, 27038–27051.
12. Sobala, Ł.F., Fernandes, P.Z., Hakki, Z., Thompson, A.J., Howe, J.D., Hill, M., Zitzmann, N., Davies, S., Stamataki, Z., Butters, T.D., *et al.* (2020). Structure of human endo-α-1,2-mannosidase (MANEA), an antiviral host-glycosylation target. Proc. Natl. Acad. Sci. *117*, 29595–29601.
13. Warfield, K.L., Alonzi, D.S., Hill, J.C., Caputo, A.T., Roversi, P., Kiappes, J.L., Sheets, N., Duchars, M., Dwek, R.A., Biggins, J., *et al.* (2020). Targeting Endoplasmic Reticulum α-Glucosidase i with a Single-Dose Iminosugar Treatment Protects against Lethal Influenza and Dengue Virus Infections. J. Med. Chem. *63*, 4205–4214.
14. Qu, X., Pan, X., Weidner, J., Yu, W., Alonzi, D., Xu, X., Butters, T., Block, T., Guo, J.T., and Chang, J. (2011). Inhibitors of endoplasmic reticulum α-glucosidases potently suppress hepatitis C virus virion assembly and release. Antimicrob. Agents Chemother. *55*, 1036–1044.
15. Franco, E.J., Warfield, K.L., and Brown, A.N. (2022). UV-4B potently inhibits replication of multiple SARS-CoV-2 strains in clinically relevant human cell lines. Front. Biosci. *27*, 1.

16. Courageot, M.-P., Frenkiel, M.-P., Duarte Dos Santos, C., Deubel, V., and Desprès, P. (2000). α-Glucosidase Inhibitors Reduce Dengue Virus Production by Affecting the Initial Steps of Virion Morphogenesis in the Endoplasmic Reticulum. J. Virol. *74*, 564–572.

17. Perry, S.T., Buck, M.D., Plummer, E.M., Penmasta, R.A., Batra, H., Stavale, E.J., Warfield, K.L., Dwek, R.A., Butters, T.D., Alonzi, D.S., *et al.* (2013). An iminosugar with potent inhibition of dengue virus infection in vivo. Antiviral Res. *98*, 35–43.

18. Warfield, K.L., Plummer, E.M., Sayce, A.C., Alonzi, D.S., Tang, W., Tyrrell, B.E., Hill, M.L., Caputo, A.T., Killingbeck, S.S., Beatty, P.R., *et al.* (2016). Inhibition of endoplasmic reticulum glucosidases is required for in vitro and in vivo dengue antiviral activity by the iminosugar UV-4. Antiviral Res. *129*, 93–98.

19. U.S. National Institutes of Health (2016). NCT02061358: Randomized, Double-Blind, Placebo-Controlled, Parallel Group, Single-Ascending Dose Study to Determine the Safety, Tolerability and Pharmacokinetics of UV-4B Solution Administered Orally in Healthy Subjects.

20. Płaszczyca, A., Scaturro, P., Neufeldt, C.J., Cortese, M., Cerikan, B., Ferla, S., Brancale, A., Pichlmair, A., and Bartenschlager, R. (2019). A novel interaction between dengue virus nonstructural protein 1 and the NS4A-2K-4B precursor is required for viral RNA replication but not for formation of the membranous replication organelle. PLoS Pathog. *15*, e1007736.

21. Scaturro, P., Cortese, M., Chatel-Chaix, L., Fischl, W., and Bartenschlager, R. (2015). Dengue Virus Non-structural Protein 1 Modulates Infectious Particle Production via Interaction with the Structural Proteins. PLoS Pathog. *11*, e1005277.

22. Glasner, D.R., Puerta-Guardo, H., Beatty, P.R., and Harris, E. (2018). The Good, the Bad, and the Shocking: The Multiple Roles of Dengue Virus Nonstructural Protein 1 in Protection and Pathogenesis. Annu. Rev. Virol. *5*, 227–253.

23. Flamand, M., Megret, F., Mathieu, M., Lepault, J., Rey, F.A., and Deubel, V. (1999). Dengue Virus Type 1 Nonstructural Glycoprotein NS1 Is Secreted from Mammalian Cells as a Soluble Hexamer in a Glycosylation-Dependent Fashion. J. Virol. *73*, 6104–6110.

24. Muller, D.A., and Young, P.R. (2013). The flavivirus NS1 protein: Molecular and structural biology, immunology, role inpathogenesis and application asadiagnostic biomarker. Antiviral Res. *98*, 192–208.

25. Libraty, D.H., Young, P.R., Pickering, D., Endy, T.P., Kalayanarooj, S., Green, S., Vaughn, D.W., Nisalak, A., Ennis, F.A., and Rothman, A.L. (2002). High Circulating Levels of the Dengue Virus Nonstructural Protein NS1 Early in Dengue Illness Correlate with the Development of Dengue Hemorrhagic Fever. J. Infect. Dis. *186*, 1165–1168.

26. Beatty, P.R., Puerta-Guardo, H., Killingbeck, S.S., Glasner, D.R., Hopkins, K., and Harris, E. (2015). Dengue virus NS1 triggers endothelial permeability and vascular leak that is prevented by NS1 vaccination. Sci. Transl. Med. *7*, 304ra141.

27. Avirutnan, P., Hauhart, R.E., Somnuke, P., Blom, A.M., Diamond, M.S., and Atkinson, J.P. (2011). Binding of Flavivirus Nonstructural Protein NS1 to C4b Binding Protein Modulates Complement Activation. J. Immunol. *187*, 424–433.

28. Modhiran, N., Watterson, D., Muller, D.A., Panetta, A.K., Sester, D.P., Liu, L., Hume, D.A., Stacey, K.J., and Young, P.R. (2015). Dengue virus NS1 protein activates cells via Toll-like receptor 4 and disrupts endothelial cell monolayer integrity. Sci. Transl. Med. *7*, 304ra142.

29. Glasner, D.R., Ratnasiri, K., Puerta-Guardo, H., Espinosa, D.A., Beatty, P.R., and Harris, E. (2017). Dengue virus NS1 cytokine-independent vascular leak is dependent on endothelial glycocalyx components. PLoS Pathog. *13*, e1006673.

30. Puerta-Guardo, H., Glasner, D.R., and Harris, E. (2016). Dengue Virus NS1 Disrupts the Endothelial Glycocalyx, Leading to Hyperpermeability. PLoS Pathog. *12*, e1005738.

31. Biering, S.B., Akey, D.L., Wong, M.P., Brown, W.C., Lo, N.T.N., Puerta-Guardo, H., Tramontini Gomes de Sousa, F., Wang, C., Konwerski, J.R., Espinosa, D.A., *et al.* (2021). Structural basis for antibody inhibition of flavivirus NS1–triggered endothelial dysfunction. Science *371*, 194–200.

32. Modhiran, N., Song, H., Liu, L., Bletchly, C., Brillault, L., Amarilla, A.A., Xu, X., Qi, J., Chai, Y., Cheung, S.T.M., *et al.* (2021). A broadly protective antibody that targets the flavivirus NS1 protein. Science *371*, 190–194.

33. Puerta-Guardo, H., Glasner, D.R., Espinosa, D.A., Biering, S.B., Patana, M., Ratnasiri, K., Wang, C., Beatty, P.R., and Harris, E. (2019). Flavivirus NS1 Triggers Tissue-Specific Vascular Endothelial Dysfunction Reflecting Disease Tropism. Cell Rep. *26*, 1598-1613.e8.

34. Puerta-Guardo, H., Biering, S.B., de Sousa, F.T.G., Shu, J., Glasner, D.R., Li, J., Blanc, S.F., Beatty, P.R., and Harris, E. (2022). Flavivirus NS1 Triggers Tissue-Specific Disassembly of Intercellular Junctions Leading to Barrier Dysfunction and Vascular Leak in a GSK-3β-Dependent Manner. Pathogens *11*, 615.

35. Thiemmeca, S., Tamdet, C., Punyadee, N., Prommool, T., Songjaeng, A., Noisakran, S., Puttikhunt, C., Atkinson, J.P., Diamond, M.S., Ponlawat, A., *et al.* (2016). Secreted NS1 Protects Dengue Virus from Mannose-Binding Lectin–Mediated Neutralization. J. Immunol. *197*, 4053–4065.

36. Wang, C., Puerta-Guardo, H., Biering, S.B., Glasner, D.R., Tran, E.B., Patana, M., Gomberg, T.A., Malvar, C., Lo, N.T.N., Espinosa, D.A., *et al.* (2019). Endocytosis of flavivirus NS1 is required for NS1-mediated endothelial hyperpermeability and is abolished by a single N-glycosylation site mutation. PLoS Pathog. *15*, e1007938.

37. Chao, C.-H., Wu, W.-C., Lai, Y.-C., Tsai, P.-J., Perng, G.-C., Lin, Y.-S., and Yeh, T.-M. (2019). Dengue virus nonstructural protein 1 activates platelets via Toll-like receptor 4, leading to thrombocytopenia and hemorrhage. PLoS Pathog. *15*, e1007625.

38. Suwarto, S., Sasmono, R.T., Sinto, R., Ibrahim, E., and Suryamin, M. (2017). Association of endothelial glycocalyx and tight and adherens junctions with severity of plasma leakage in dengue infection. J. Infect. Dis. *215*, 992–999.

39. Orozco, S., Schmid, M.A., Parameswaran, P., Lachica, R., Henn, M.R., Beatty, R., and Harris, E. (2012). Characterization of a model of lethal dengue virus 2 infection in C57BL/6 mice deficient in the alpha/beta interferon receptor. J. Gen. Virol. *93*, 2152–2157.

Chapter 5

Conclusion

Summary

This dissertation aimed to unravel the molecular determinants of flavivirus NS1 protein, a multifaceted viral protein with roles in pathogenesis, immune evasion, viral replication, and viral dissemination. Following the observation that NS1 proteins from different flaviviruses interact with endothelial cells in a tissue-specific manner, further work was undertaken to determine the specific roles of individual domains or amino acid residues or motifs within distinct NS1 domains.

In Chapter 2, I identified the wing domain to be driving tissue-specific NS1-endothelial cell (EC) interactions for DENV, WNV, and ZIKV NS1. I further pinpointed a 3-residue motif of Gly-Asp-Ile as a molecular determinant for DENV NS1-EC binding, endothelial hyperpermeability, and vascular leak. In Chapter 3, I laid out the additional data that set the foundation for this dissertation. Focusing on the structure-function relationship of DENV NS1 and EC interaction, I identified further molecular determinants. I found that the cell entry-deficient glycosylation N207Q NS1 mutant was still able to cause vascular leak *in vivo*; that the virion binding-deficient E343K NS1 mutant maintained WT-equivalent functions; that the highly conserved W-W-G motif in the NS1 wing domain mediated pan-flavivirus NS1 binding with pulmonary ECs; and that the mouse anti-NS1 mAb 2B7 definitively bound the β-ladder domain of DENV NS1. These findings had helped inform the strategy of domain-swapping to map NS1 residues in Chapter 2. In Chapter 4, I explored the anti-NS1 capacity of an iminosugar "UV-4B", a known anti-DENV antiviral that acts by disrupting the post-translational glycan-processing modification of proteins. I showed that UV-4B treatment resulted in reduced DENV infection of human monocytes as well as reduced NS1 production in transfected cells. In addition, I found that UV-4B exhibits cell-intrinsic properties that reduce NS1-induced endothelial barrier dysfunction. These results demonstrate a proof-of-concept for anti-NS1 compounds as a viable therapeutic class against NS1-induced severe dengue pathologies of endothelial dysfunction, in contrast to existing antiviral compounds.

Future Directions

NS1 is a multifaceted protein intimately involved in the major steps of the flavivirus life cycle. With key functions in viral replication, immune evasion, and pathogenesis, it is arguably the most important protein for DENV and flaviviruses. Significant research advances have been made in the field since our group first connected NS1 to DENV pathogenesis by directly triggering endothelial hyperpermeability in 2015 [1]. While this dissertation contributes to further elucidation of the residues and motifs on NS1 as they pertain to NS1-induced endothelial dysfunction, intriguing open questions remain – particularly surrounding the mechanism, interaction partners, and structure.

One of the most obvious open questions is the apparent disconnect between the NS1-induced TEER phenotype and that of binding and vascular leak in the dorsal dermis mouse model. In Chapter 2, I found that while the wing domain drives NS1-EC binding and localized vascular leak *in vivo*, it is the β-ladder that drives the TEER phenotype at higher concentrations of 5 and 10 μg/mL. The β-ladder domain driving NS1-induced *functional* outcome is supported by alanine point mutations of other β-ladder residues, where these NS1 mutants retained their ability to bind EC, but displayed abrogated TEER and EGL disruption phenotypes [2]. However, none of the β-ladder NS1 mutants had been tested in *in vivo* experiments until the glycosylation mutant $NS1^{N207Q}$, as elaborated in Chapter 3. We have shown that $NS1^{N207Q}$ is deficient for endocytosis and TEER [3], and it was hypothesized that the *in vivo* outcome would follow the *in vitro* endothelial dysfunction data. Surprisingly, $NS1^{N207Q}$ (which contains an intact DENV wing domain) was still able to cause vascular leak, which supports the data from Chapter 2 that pointed to the wing domain

and the 3-residue motif within, GDI, to be the molecular determinants of DENV NS1 functions. As the EC binding and localized vascular leak data are consistent with each other across multiple NS1 chimeras and point mutants, further study is required to better understand how TEER is modeling vascular leak. For instance, EGL disruption and transcytosis of solutes and fluids is distinct from intercellular junction disruption and paracellular transport, and it is likely that the distinct *in vitro* and *in vivo* assays model these processes differently. In addition, it would be interesting to investigate whether systemic leak data using these NS1 mutants corroborate data obtained using the localized leak model.

Flavivirus infectious clones are infamously challenging to work with, as the toxicity and instability of the flavivirus genome in bacterial hosts often necessitates piecemeal genomic assembly using several sub-genomic cDNA segments [4]. Nevertheless, it remains to be seen what effects the residues highlighted in this dissertation across the NS1 protein would have on flavivirus (and specifically DENV) replication, pathogenesis, and tissue-specific tropism. The residues 91-93, as well as β-ladder residues identified herein are not among residues known to interfere with viral replication [5–7], thus reducing the risk of recovering replication-dead DENV mutants.

The mechanisms and molecular determinants underlying NS1-induced endothelial hyperpermeability in this dissertation are only part of a bigger story. The other aspect of NS1-induced pathology is the interaction with immune cells – however, NS1 induction of cytokine production by immune cells remains to be further investigated [8,9]. For instance, data from our laboratory (not shown) has indicated that the DENV/WNV chimeric NS1 proteins that induced localized vascular leak in the murine dorsal dermis (Chapter 2) did not induce production of inflammatory cytokines such as IL-6 and IL-8 in THP-1 cells, consistent with previous observations [8]. In the context of the virus, DENV infection of immune cells as well as antibody-dependent enhancement in heterologous secondary infections add to the complexity of the role that immune factors play in both DENV- and NS1-induced pathogenesis, which remains to be further elucidated.

On the host perspective, the roles of EGL on the EC surface and the proteinaceous receptor(s) of NS1 are important paths to follow up with. Data from Chapter 3 of this dissertation identified the NS1 wing domain to be conferring NS1 binding to different GAG species, albeit in an unexpected manner where the wing domain of WNV NS1 instead of DENV NS1 conferred GAG binding. One explanation for this could be that the DENV NS1-GAG interaction is less specific, hence binding at lower levels, which in turn could broaden the diversity of GAGs to which DENV NS1 could bind, accounting for the more promiscuous nature of DENV compared to WNV NS1 in EC interactions. The specific types of glycans that confer flavivirus NS1-EC binding specificity, the levels of sulfation, and the species composition remain to be further studied.

NS1 carries a lipid cargo within its oligomeric barrel that has recently been linked to interactions with HDL, with possible roles in inducing vascular dysfunction having been proposed [10–15]. Emerging evidence points to differences in the structure of flavivirus NS1 proteins (e.g., DENV, WNV, and ZIKV NS1), and it could be hypothesized that these different structures could have an impact on the lipid cargo NS1 harbours. Moreover, it is possible that structural differences among flavivirus NS1 proteins could have an effect on tissue-specific interactions with endothelial and other cell types, and the molecular determinants identified herein and others could affect tissue specificity by altering NS1 structure. Structural studies of the chimeric NS1 proteins and NS1 point mutants would yield further insights with regards to specific structure-function relationships, as well as the lipid cargos these NS1 proteins might contain, and their collective roles in NS1-induced endothelial dysfunction. Given data from our group and others showing that NS1 may be used as

a viral toxin by flaviviruses during infection to gain access to the underlying tissues beyond endothelial barriers, answers to these questions will illuminate the fate of NS1 during human disease and contribute to our overall understanding of its role in infection.

As far as dengue vaccines and therapeutics are concerned, the field still has a long journey ahead. Any E protein-based vaccines will have to resolve potential ADE issues, making NS1 an attractive vaccine target. However, NS1-based vaccines will need to elicit sufficient, long-lasting immunity and would only protect against (severe) disease and not infection. On the therapeutics front, NS1 is a viable candidate to target against severe dengue, either using antibodies that do not pose ADE risks, or small molecule compounds. The anti-NS1 mAb 2B7 and the iminosugars highlighted in this dissertation are some of many molecules that have shown promise towards protection against severe dengue and other flaviviral diseases. Putting NS1 on the horizon of future anti-flavivirus efforts would expand the breadth of candidate molecules that can protect against these diseases.

With accelerating climate change and increased connectivity of humans and goods, we will witness an increase in diseases caused by arboviruses such as flavivirus, alphavirus, bunyaviruses and others in time to come. Work in this dissertation represents advances in understanding the molecular determinants that make a particular flavivirus NS1 unique from another distinct flavivirus NS1 in its interactions with host cells. NS1 remains a fascinating topic in the flavivirus field; inclusion of the insights from this dissertation into studies of different viruses in the future will broaden our understanding of both NS1 and flaviviruses.

References
Chapter 5

1. Beatty, P.R., Puerta-Guardo, H., Killingbeck, S.S., Glasner, D.R., Hopkins, K., and Harris, E. (2015). Dengue virus NS1 triggers endothelial permeability and vascular leak that is prevented by NS1 vaccination. Sci. Transl. Med. *7*, 304ra141.

2. Biering, S.B., Akey, D.L., Wong, M.P., Brown, W.C., Lo, N.T.N., Puerta-Guardo, H., Tramontini Gomes de Sousa, F., Wang, C., Konwerski, J.R., Espinosa, D.A., *et al.* (2021). Structural basis for antibody inhibition of flavivirus NS1–triggered endothelial dysfunction. Science *371*, 194–200.

3. Wang, C., Puerta-Guardo, H., Biering, S.B., Glasner, D.R., Tran, E.B., Patana, M., Gomberg, T.A., Malvar, C., Lo, N.T.N., Espinosa, D.A., *et al.* (2019). Endocytosis of flavivirus NS1 is required for NS1-mediated endothelial hyperpermeability and is abolished by a single N-glycosylation site mutation. PLoS Pathog. *15*, e1007938.

4. Aubry, F., Nougairède, A., Gould, E.A., and De Lamballerie, X. (2015). Flavivirus reverse genetic systems, construction techniques and applications: A historical perspective. Antiviral Res. *114*, 67–85.

5. Scaturro, P., Cortese, M., Chatel-Chaix, L., Fischl, W., and Bartenschlager, R. (2015). Dengue Virus Non-structural Protein 1 Modulates Infectious Particle Production via Interaction with the Structural Proteins. PLoS Pathog. *11*, e1005277.

6. Ci, Y., Liu, Z.Y., Zhang, N.N., Niu, Y., Yang, Y., Xu, C., Yang, W., Qin, C.F., and Shi, L. (2020). Zika NS1-induced ER remodeling is essential for viral replication. J. Cell Biol. *219*, e201903062.

7. Płaszczyca, A., Scaturro, P., Neufeldt, C.J., Cortese, M., Cerikan, B., Ferla, S., Brancale, A., Pichlmair, A., and Bartenschlager, R. (2019). A novel interaction between dengue virus nonstructural protein 1 and the NS4A-2K-4B precursor is required for viral RNA replication but not for formation of the membranous replication organelle. PLoS Pathog. *15*, e1007736.

8. Glasner, D.R., Ratnasiri, K., Puerta-Guardo, H., Espinosa, D.A., Beatty, P.R., and Harris, E. (2017). Dengue virus NS1 cytokine-independent vascular leak is dependent on endothelial glycocalyx components. PLoS Pathog. *13*, e1006673.

9. Modhiran, N., Watterson, D., Blumenthal, A., Baxter, A.G., Young, P.R., and Stacey, K.J. (2017). Dengue virus NS1 protein activates immune cells via TLR4 but not TLR2 or TLR6. Immunol. Cell Biol. *95*, 491–495.

10. Säemann, M.D., Poglitsch, M., Kopecky, C., Haidinger, M., Hörl, W.H., and Weichhart, T. (2010). The versatility of HDL: a crucial anti-inflammatory regulator. Eur. J. Clin. Invest. *40*, 1131–1143.

11. Birner-Gruenberger, R., Schittmayer, M., Holzer, M., and Marsche, G. (2014). Understanding high-density lipoprotein function in disease: Recent advances in proteomics unravel the complexity of its composition and biology. Prog. Lipid Res. *56*, 36–46.

12. Benfrid, S., Park, K., Dellarole, M., Voss, J.E., Tamietti, C., Pehau-Arnaudet, G., Raynal, B., Brûlé, S., England, P., Zhang, X., *et al.* (2022). Dengue virus NS1 protein conveys pro-inflammatory signals by docking onto high-density lipoproteins. EMBO Rep., 1–14.

13. Coelho, D.R., Carneiro, P.H., Mendes-Monteiro, L., Conde, J.N., Andrade, I., Cao, T., Allonso, D., White-Dibiasio, M., Kuhn, R.J., and Mohana-Borges, R. (2021). ApoA1 Neutralizes Proinflammatory Effects of Dengue Virus NS1 Protein and Modulates Viral Immune Evasion. J. Virol. *95*, e01974-20.

14. Flamand, M., Megret, F., Mathieu, M., Lepault, J., Rey, F.A., and Deubel, V. (1999). Dengue Virus Type 1 Nonstructural Glycoprotein NS1 Is Secreted from Mammalian Cells as a Soluble Hexamer in a Glycosylation-Dependent Fashion. J. Virol. *73*, 6104–6110.

15. Gutsche, I., Coulibaly, F., Voss, J.E., Salmon, J., D'Alayer, J., Ermonval, M., Larquet, E., Charneau, P., Krey, T., Mégret, F., *et al.* (2011). Secreted dengue virus nonstructural protein NS1 is an atypical barrel-shaped high-density lipoprotein. Proc. Natl. Acad. Sci. *108*, 8003–8008.